

Scientific report of the Structural Materials Group (SMA) in the period 2013-2014

Collection of extended abstracts of peer review papers

Compiled by M. Konstantinovic

August, 2015

SCK•CEN
Boeretang 200
BE-2400 Mol
Belgium

SMA group

Scientific report of the Structural Materials Group (SMA) in the period 2013-2014

Collection of extended abstracts of peer review papers

Compiled by M. Konstantinovic

A, 2015
Status: Unclassified
ISSN 1379-2407

SCK•CEN
Boeretang 200
BE-2400 Mol
Belgium

SMA group

© SCK•CEN
Studiecentrum voor Kernenergie
Centre d'étude de l'énergie Nucléaire
Boeretang 200
BE-2400 Mol
Belgium

Phone +32 14 33 21 11
Fax +32 14 31 50 21

<http://www.sckcen.be>

Contact:
Knowledge Centre
library@sckcen.be

RESTRICTED

All property rights and copyright are reserved. Any communication or reproduction of this document, and any communication or use of its content without explicit authorization is prohibited. Any infringement to this rule is illegal and entitles to claim damages from the infringer, without prejudice to any other right in case of granting a patent or registration in the field of intellectual property.

SCK•CEN, Studiecentrum voor Kernenergie/Centre d'Etude de l'Energie Nucléaire
Stichting van Openbaar Nut – Fondation d'Utilité Publique - Foundation of Public Utility
Registered Office: Avenue Herrmann Debroux 40 – BE-1160 BRUSSEL
Operational Office: Boeretang 200 – BE-2400 MOL



Foreword

This report presents the collection of extended abstracts from scientific articles which are published in international journals with impact factors (and as such appear in web-of-knowledge database; <http://webofknowledge.com>). The purpose of this document is to provide a brief overview of the two year scientific activity of the SMA group. In this way the summary of achieved results and topics of research are easily assessible to both internal and external collaborators.

The reports which are part of the service to industry and/or other R&D international and national projects/programs are not included in this document. It is possible though, that a lot of such reports contain similar data (especially those which are not ranked as restricted reports, e.g. for European projects).

The extended abstracts are listed and grouped around research topics, since their organization per unit or per SCK.CEN strategic R&D line would be not very efficient as a consequence to variety of crosslinking. Still, an indication is given for every article under which strategic R&D topic can be listed (one or more), namely:

NSMA1A: Reactor pressure vessel materials for Generation II and III reactors

NMSA1B: Internals for Generation II and III reactors

NSMA2A: Materials for advanced Generation IV reactors and accelerator driven system

NSMA2B: Materials for fusion reactors and systems

This document is prepared in collaboration with all members of the SMA group.

Konstantinovic Milan

*Gavrilov Serguei
Bakaeva Anastasiia
Bosch Rik-Wouter
Chaouadi Rachid
Charalampopoulou
Evangelia
Ersoy Feyzan Ozgun
Gong Xing
Lambrinou
Konstantza*

*Marmy Pierre
Stergar Erich
Vankeerberghen
Marc
Bakaeva Anastasiia

Lambrecht Marlies
Bens Luc
Berkmans Geert*

*Djikanovic Tamara
Eysermans Ludo
Joris Jasper
Knaeps Jan
Puzzolante Luigi
Vanuytven Roel
Wouters Paul

Malerba Lorenzo
Bakaev Alexander*

*Bonny Giovanni
Chiapetto Monica
Grigorev Petr
Terentyev Dmitry

Uytendhouwen Inge
Schuurmans Johan*

TABLE OF CONTENT

<i>Studies of Fe and Fe-C.....</i>	<i>7</i>
<i>Ferritic/martensitic steels and model alloys</i>	<i>22</i>
<i>Reactor pressure vessel steels and model alloys</i>	<i>37</i>
<i>Austenitic steels and alloys</i>	<i>44</i>
<i>Tungsten.....</i>	<i>55</i>
<i>Other works</i>	<i>77</i>

Fe and Fe-C

Transfer of molecular dynamics data to dislocation dynamics to assess dislocation–dislocation loop interaction in iron

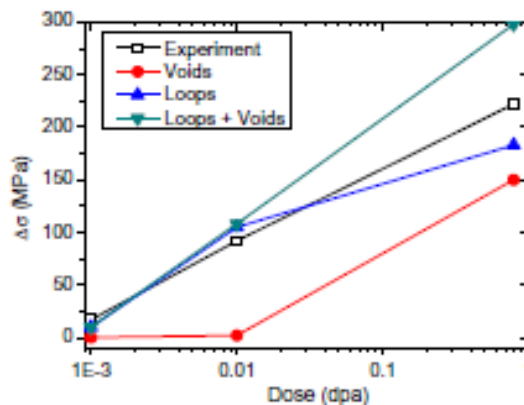
V D. Terentyev^a, G. Monnet^b and P. Grigorev^a

^aSCK-CEN, Nuclear Material Science Institute, Boeretang 200, B-2400 Mol, Belgium

^bDepartment MMC, EDF R&D, Moret-sur-Loing, France

Introduction: We propose a computationally fast and physically justifiable method to treat dislocation loops as stochastic thermally activated finite-size obstacles in discrete dislocation dynamics simulations. The method was parameterized using molecular dynamics data for the interaction of dislocations with $a_0/2(111)$ dislocation loops. As demonstration, the method is applied to rationalize experimental hardening of neutron-irradiated iron. The obtained results show good agreement with experimental data.

Main results: We have discussed a general mechanism of DL–dislocation interaction, studied earlier by MD, and proposed a simple way to transfer it to DD models. MD results show that junction glide is a thermally activated process, hence a stress-dependent activation energy determining the probability of the activation of the junction is required for its application in DD at finite temperature. The $\Delta G(\tau_c)$ for $a_0/2(111)$ loop–dislocation interaction was determined using the stochastic analysis of loading histories from MD simulations, implemented in “microMegas” DD code and benchmarked, showing good agreement in a wide temperature interval. Furthermore a reasonable agreement between the predicted increase in the flow stress, assessed by DD, and experimental data is found for low doses, which induce homogeneous distribution of dislocation loops in neutron irradiated Fe at 300°C.



Strengthening computed from DD simulations and experimental

Conclusions: Consideration of small but resolvable and numerous dislocation loops as stochastic thermally activated obstacles can be done in a simple, fast and reliable way. The proposed methodology can be applied to other types of dislocation-like objects, e.g. $\langle 100 \rangle$ loops and stacking fault tetrahedra, as long as the interaction mechanism is determined by the properties of junctions. Hence, the presented treatment opens a new way to evaluate the strengthening and evolution of complex microstructure upon deformation of irradiated Fe and its alloys.

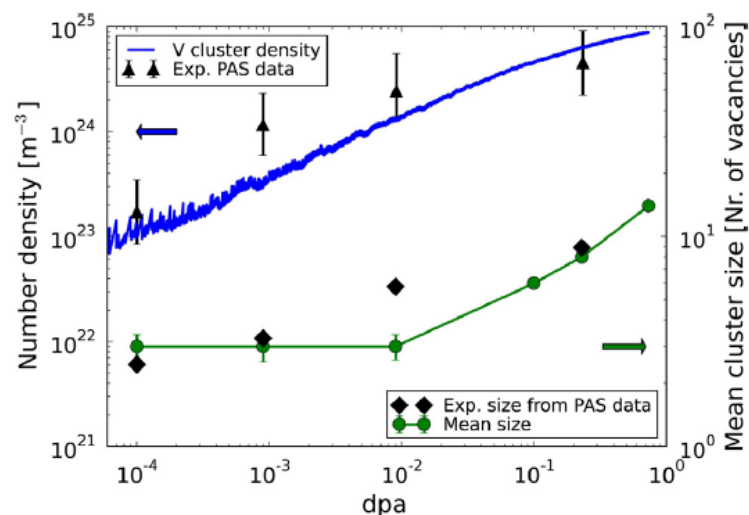
Published in: D. Terentyev, G. Monnet and P. Grigorev Scripta Materialia. 69(8): p. 578-581.

Simulation of the nanostructure evolution in irradiated Fe-C alloys

Ville Jansson¹ and Lorenzo Malerba, SCK·CEN, The Belgian Nuclear Energy Research Centre, Institute for Nuclear Materials Science, Structural Materials Group, Boeretang 200, B-2400 Mol, Belgium

Introduction: Neutron irradiation induces in steels nanostructural changes, which are at the origin of the mechanical degradation that these materials experience during operation in nuclear power plants. Some of these effects can be studied by using as model alloy the iron-carbon system. The Object Kinetic Monte Carlo technique has proven capable of simulating in a realistic and quantitatively reliable way a whole irradiation process. We have developed a model for simulating Fe-C systems using a physical description of the properties of vacancy and self-interstitial atom (SIA) clusters, based on a selection of the latest data from atomistic studies and other available experimental and theoretical work from the literature.

Main results: The model proved suitable to reproduce the results of low (<350 K) temperature neutron irradiation experiments, as well as the corresponding post-irradiation annealing up to 700 K, both in terms of defect cluster densities and size distribution, when compared to available experimental data from the literature. As an example, the Figure shows the results of the model in comparison with experimental data for vacancy clusters.



The vacancy cluster number density and mean size evolution versus dpa according to model and experiments.

Conclusions: The effect of carbon on radiation defect evolution can be largely understood in terms of formation of immobile complexes with vacancies that in turn act as traps for SIA clusters. This effect can be introduced using generic traps for SIA and vacancy clusters, with a binding energy that depends on the size of the clusters, also chosen on the basis of previously performed atomistic studies. The use of traps correctly parameterized based on atomistic studies was in fact instrumental for the validity of the model.

¹ Currently at Accelerator Laboratory, [Helsinki Institute of Physics](#), P.O.Box 43 (Pietari Kalmink. 2) 00014 [University of Helsinki](#)

Future work: This work was seminal in that it provided the starting point for the development of successful models valid not only at higher temperature for Fe-C, but also for more complex alloys, such as Fe-C-Cr and Fe-C-Mn-Ni.

Acknowledgment: This work was supported within by the 7th Framework Programme Project PERFORM60 under Grant Agreement No. FP7-232612..

Published in: V. Jansson and L. Malerba, Journal of Nuclear Materials 443 (2013) 274-285.

The nanostructure evolution in Fe-C systems under irradiation at 560 K

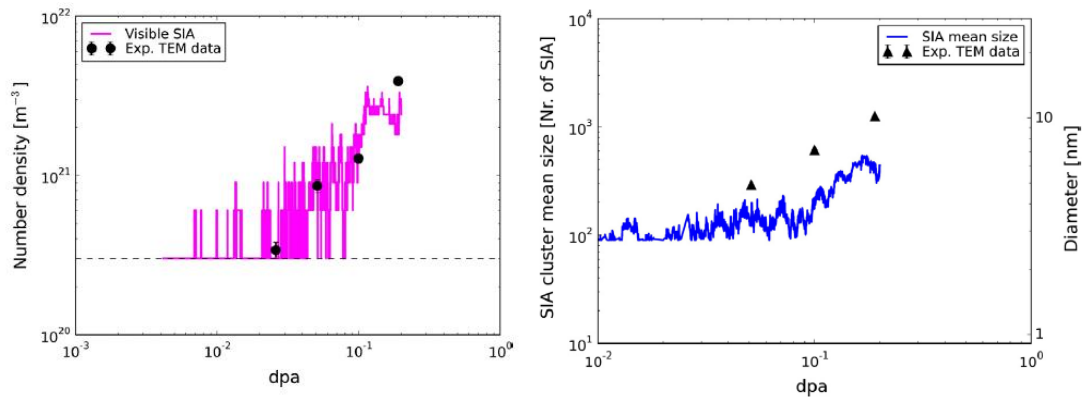
Ville Jansson², Monica Chiapetto and Lorenzo Malerba, SCK-CEN, The Belgian Nuclear Energy Research Centre, Institute for Nuclear Materials Science, Structural Materials Group, Boeretang 200, B-2400 Mol, Belgium

Introduction: Neutron irradiation induces in steels nanostructural changes, which are at the origin of the mechanical degradation that these materials experience during operation in nuclear power plants. Some of these effects can be studied by using as model alloy the iron-carbon system. The Object Kinetic Monte Carlo (OKMC) technique has proven capable of simulating in a realistic and quantitatively reliable way a whole irradiation process. This work extends our OKMC model for neutron irradiation-induced nanostructure evolution in Fe-C alloys to consider higher irradiation temperatures. The previous study concentrated on irradiation temperatures <370 K. Here we study the evolution of vacancy and self-interstitial atom (SIA) cluster populations at the operational temperature of light water reactors, by simulating specific reference irradiation experiments.

Following our previous study, the effect of carbon on radiation defect evolution can be described in terms of formation of immobile complexes with vacancies, that in turn act as traps for SIA clusters. This dynamics is simulated using generic traps for SIA and vacancy clusters. The traps have a binding energy that depends on the size and type of the clusters and is also chosen on the basis of previously performed atomistic studies. The model had to be adapted to account for the existence of two kinds of SIA clusters, $\frac{1}{2}\langle 111 \rangle$ and $\langle 100 \rangle$, as observed in electron microscopy examinations of Fe alloys neutron irradiated at the temperatures of technological interest.

Main results: The model, which is fully based on physical considerations and only uses a few parameters for calibration, is found to be capable of reproducing the experimental trends, thereby providing insight into the physical mechanisms of importance to determine the type of nanostructural evolution undergone by the material during irradiation. As an example, the Figure shows the results of the model in comparison with experimental data for SIA clusters.

² Currently at Accelerator Laboratory, [Helsinki Institute of Physics](#), P.O.Box 43 (Pietari Kalmink. 2) 00014 [University of Helsinki](#)



The SIA cluster number density (left) and mean size (right) evolution versus dpa according to model and experiments.

Conclusions: The following two assumptions, namely:

1. C atoms and complexes involving C atoms and vacancies, mainly C2V, act as traps for SIA clusters and their effect can be described in first approximation as immobile traps to which a given trapping energy is associated that depends on the size of the trapped cluster.
2. While visible SIA loops have $\langle 100 \rangle$ Burgers vector, those invisible to the electronic microscope include loops of both $\langle 100 \rangle$ and $\frac{1}{2}\langle 111 \rangle$ type, and this fact can be taken into account by using effective migration parameters for invisible clusters.

Lead to the construction of a model that proved able to predict correctly reference data from the especially complete microstructural examination of neutron irradiated Fe-C alloys.

Future work: The work continued with the development of models for Fe-C-Cr and Fe-C-Mn-Ni alloys. Next step will be the inclusion in the model of the transport of solute atoms.

Acknowledgment: This work was supported within the 7th Framework Programme by the Project PERFORM60 under Grant Agreement No. FP7-232612.

Published in: V. Jansson, M. Chiapetto and L. Malerba, Journal of Nuclear Materials 442 (2013) 341-349.

Effect of carbon decoration on the absorption of $\langle 100 \rangle$ dislocation loops by dislocations in iron

D Terentyev¹, A Bakaev^{1,2,3} and E E Zhurkin³

¹ SCK•CEN, Nuclear Materials Science Institute, Boeretang 200, Mol, B2400, Belgium

² Center for Molecular Modeling, Department of Physics and Astronomy, Ghent University, Technologiepark 903, 9052 Zwijnaarde, Belgium

³ Department of Experimental Nuclear Physics, Institute of Physics, Nanotechnologies and Telecommunications, St Petersburg State Polytechnical University, 29 Polytekhnicheskaya str., 195251, St Petersburg, Russia

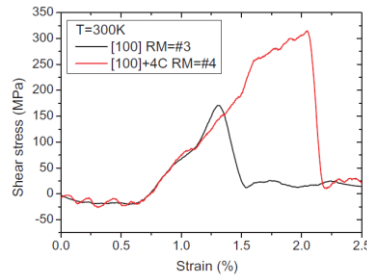
Introduction: Body-centred cubic iron (bcc Fe) is one of the most important technological metals especially for structural applications, including nuclear sector. Fe–chromium–carbon-based ferritic and ferritic/martensitic (F/M) steels are promising candidate structural materials

for Fusion and GEN IV nuclear reactors. Nevertheless they suffer from severe degradation of mechanical properties when exposed to neutron irradiation at reactor operation temperature in terms of hardening, loss of ductility and finally embrittlement. Moreover, once a relatively high level of radiation-induced hardening is reached, the work hardening measured in uniaxial tensile tests becomes either strongly reduced or even inexistent. The latter phenomenon is called plastic-induced softening or instability and it is considered as a potentially serious problem in the assessment of the integrity of components made with steels and subjected to high neutron dose.

The physical origin of the hardening and change of plastic behaviour of neutron irradiated Fe (and metals in general) lays in the formation of nano-scale agglomerates being clusters of point defects which obstruct dislocation movement. Agglomeration of vacancies results in the formation of nanovoids, while gathering of self-interstitial atoms (SIAs) leads to the formation of platelet clusters known as dislocation loops. Self-interstitials and vacancies are produced in neutron-induced collision cascades in equal amounts. However, the growth of voids and SIA clusters occurs at different rates, depending on irradiation conditions and material. In the case of bcc Fe and Fe-based ferritic steels, the dislocation loops are recognized as the primary neutron-induced nano-structural defects. Hence, the degradation of the mechanical response is primarily related to the accumulation and growth of dislocation loops. This is why the complete understanding of the interaction of dislocations with dislocation loops, i.e. reaction mechanism and unpinning stress, is an important subject. Moreover, the plastic instability phenomenon, mentioned earlier, is currently understood to be a consequence of the removal of the dislocation loops by moving dislocation lines. This process can explain the formation of clear bands or dislocation channels, seen by transmission electron microscopy, that make the material locally inhomogeneous and unstable upon load.

Real F/M steels contain a set of alloying elements among which the most important are substitutional chromium (Cr) and interstitial carbon (C). Two types of interstitial dislocation loops with Burgers vector (BV) $\frac{1}{2}\langle 111 \rangle$ and $\langle 100 \rangle$ are known to form in high Cr steels, with the fraction being dependent on Cr content and irradiation temperature. More recently, fine atom probe and transmission electron microscopy (TEM) experiments unambiguously revealed Cr and C segregation to dislocation loops in model Fe–Cr alloys as well as in commercial F/M steels. Taking into account this evidence, recent MD studies have addressed the effect of Cr and C segregation on $\frac{1}{2}\langle 111 \rangle$ loops and $\langle 100 \rangle$ loops. In the case of $\frac{1}{2}\langle 111 \rangle$ loops, it was demonstrated that Cr or C segregation modifies the interaction mechanism and increases the unpinning stress depending on ambient temperature and loop size. However, the effect of carbon decoration on the resistance of $\langle 100 \rangle$ loops, observed in bcc Fe, Fe–C and Fe–Cr alloys, as well as in F/M steels, upon irradiation at elevated temperature, has not been studied so far, while there is evidence of strong interaction of C with $\langle 100 \rangle$ loops.

Main results: It was considered the interaction of $\langle 100 \rangle$ interstitial dislocation loops decorated by different numbers of carbon atoms in a wide temperature range. The results reveal clearly that the decoration affects the reaction mechanism and increases the unpinning stress, in general. The most pronounced and reproducible increase of the unpinning stress is found in the intermediate temperature range from 300 up to 600 K.



τ - ϵ plots of reactions with undecorated and decorated (by 4 C atoms) [100] loop simulated at T=300 K

Conclusions: The carbon-decoration effect is seen as an increase of the unpinning stress and is related to the modification of the loop–dislocation reaction and it is very important at the technologically relevant neutron irradiation conditions.

Future work: Further research can be performed on the study of how the ‘pipe migration’ of carbon would influence reaction mechanism and unpinning stress.

Acknowledgment: This work, supported by the European Commission under the Contract of Association between EURATOM/SCK-CEN, was carried out within the framework of the European Fusion Development Agreement. Partial support was also received from the EURATOM 7th framework programme, under Perform 60 project. DT thanks his colleague Dr. L. Malerba for the useful remarks and proofreading.

Published in: D Terentyev, A. Bakaev, E.E Zhurkin / J. Phys.: Condens. Matter 26 (2014) 165402

Interaction of dislocations with carbides in BCC Fe studied by molecular dynamics

F. Granberg^a, D. Terentyev^b, K. Nordlund^a

^a Department of Physics, P.O. Box 43, FIN-00014 University of Helsinki, Finland

^b Nuclear Materials Science Institute, SCK-CEN, Boeretang 200, B-2400 Mol, Belgium

Introduction: In this study, the atomic processes involving the interaction of an edge dislocation with carbide precipitates in an iron matrix are investigated by molecular dynamics, utilizing two interatomic potentials (Hepburn, 2008 and Henriksson, 2013). The carbides investigated were Fe₃C and M₂₃C₆, where M was either Fe or Cr..

Main results:

The results from spherical precipitates were compared with rod shaped obstacles, to investigate the effect of climb in the unpinning process and the stress related to this process. The rod simulations showed a higher unpinning stress for all investigated sizes and temperatures, which indicates that climb will play a role in the unpinning phenomenon. The results showed, as previous studies, a decrease of the unpinning stress with increasing temperature and that a larger obstacle yields a higher unpinning stress. The Orowan process of dislocation unpinning was observed with both potentials as an increase in the needed unpinning stress in consecutive interactions with the same obstacle.

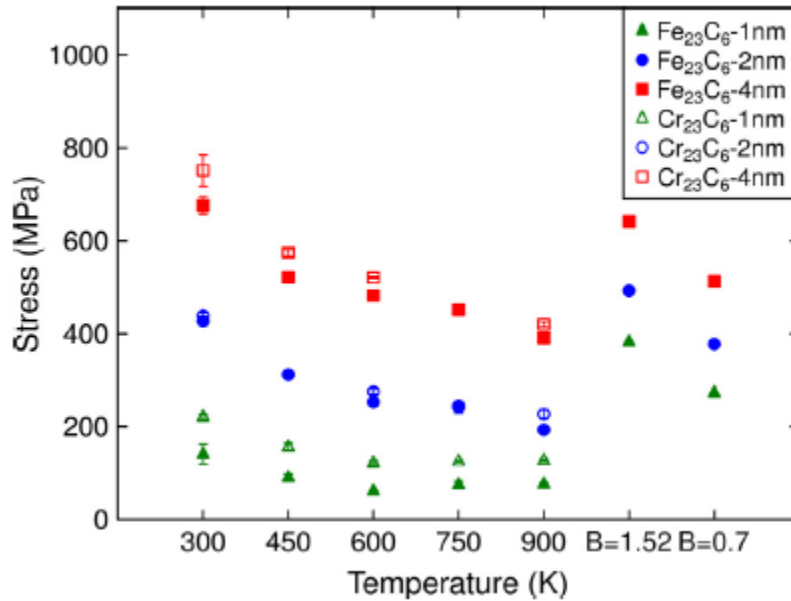


Fig.1. Comparison of the critical unpinning stress for the spherical Cr₂₃C₆ and Fe₂₃C₆ carbides.

Conclusions:

The results showed that the structure of the obstacle does not affect the unpinning stress, as much as temperature, for obstacles P 2 nm. Comparison of obstacles with the same structure but with different composition, Fe₂₃C₆ and Cr₂₃C₆, showed that the small shearable chromium carbides were stronger than the corresponding iron carbides, pointing to the importance of the chemical composition of the carbide.

Future work: Perform the same assessment for the screw dislocation

Acknowledgment: This research was funded by the Academy of Finland project SIRDAME (Grant No. 259886). We thank the IT Center for Science, CSC, for granted computational resources. The authors acknowledges the support of the EUROfusion programme

Published in: F. Granberg, D. Terentyev, K. Nordlund / Journal of Nuclear Materials 460 (2015) 23–29

Interaction of carbon-vacancy complex with minor alloying elements of ferritic steels

A. Bakaev^{1,2,3}, D. Terentyev¹, X. He⁴, E.E. Zhurkin³ and D. Van Neck²

¹ SCK•CEN, Nuclear Materials Science Institute, Boeretang 200, Mol, B2400, Belgium

² Center for Molecular Modeling, Department of Physics and Astronomy, Ghent University, Technologiepark 903, 9052 Zwijnaarde, Belgium

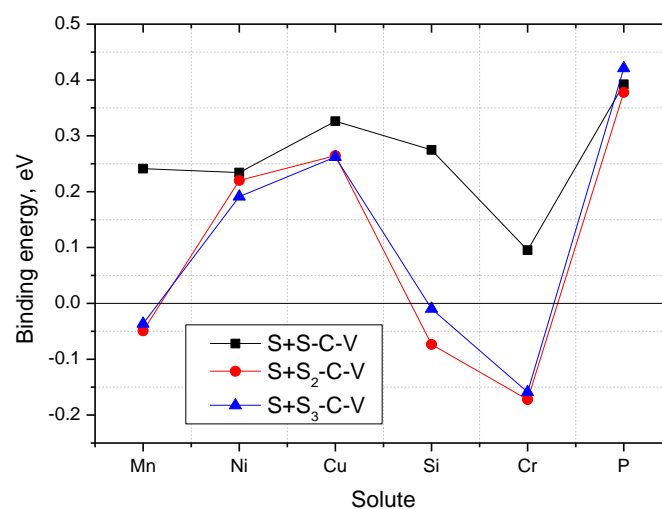
³ Department of Experimental Nuclear Physics K-89, Institute of Physics, nanotechnology and telecommunications, St.Petersburg State Polytechnical University, 29 Polytekhnicheskaya str., 195251, St.Petersburg, Russia

⁴ China Institute of Atomic Energy, P.O.Box:275-51, 102413, Beijing, China

Introduction: Fe-based steels with body centered cubic (BCC) structure such as bainitic or high-Cr ferritic-martensitic ones are the common structural materials for nuclear applications. During operation the steels undergo degradation due to the harsh exploitation conditions. Radiation-induced embrittlement is one of the limiting factors determining safety and effective exploitation of a nuclear setup. The embrittlement is conventionally attributed to the obstruction of dislocation movement by nanometric lattice defects formed as a result of radiation-induced/enhanced segregation and accumulation of point defect clusters growing to the dislocation loops and nano-voids. Recent experimental studies involving several high resolution techniques including atom probe tomography (APT) emphasize the presence of solute-rich clusters (SRC), composed of major alloying elements, revealed in different types of commercial steels. Remarkably, all the mentioned experimental works report extremely high density of SRC (up to 10^{24} m^{-3}). Due to their small size, these clusters are invisible to transmission electron microscopy (TEM).

The APT techniques, however, cant not determine the full structure of the SRCs and therefore their possible association with radiation-induced lattice defects remains unknown. Specially dedicated atomistic study addressing segregation in Fe-Mn-Ni-Cu alloys – a model for reactor pressure vessels (RPV) steel, has suggested that non-equilibrium formation of SRCs can be explained by their association with in-cascade created dislocation loops. In line with that, the association of Mn and Si (important solutes entering RPV steels) with self-interstitial atoms resulting in highly stable configurations was also recently proven by *ab initio* calculations. However, a combination of APT and positron annihilation spectroscopy (PAS) analysis also revealed the presence of vacancy-rich SRC complexes in both western and Russian types of RPV steels. Hence, the mechanism of nucleation of SRCs on vacancies also needs to be clarified.

Main results: It was performed a parametric *ab initio* study to investigate thermal stability of S-C-V complexes and consider a main set of alloying elements entering the composition of RPV steels, namely: Mn, Ni, Cu, Si, Cr and P. The S-C-V structures with the lowest energy were identified, the corresponding binding and dissociation energy of such complexes were computed, and the evolution of the incremental binding energy by addition of extra solutes to stable S-C-V clusters was examined.



The incremental binding energy of the nth solute to $S_{(n-1)}$ -C-V cluster.

Conclusions: It is found that all the considered solutes (Mn, Ni, Cu, Si, Cr and P) form stable triple clusters resulting in the increase of the total binding energy by 0.2-0.3 eV. As a result of the formation of energetically favourable solute-carbon-vacancy triplets, the dissociation energy for vacancy/carbon emission is also increased by ~0.2-0.3 eV, suggesting that the solutes enhance thermal stability of carbon-vacancy complex. Association of carbon-vacancy pairs with multiple solute clusters is found to be favorable for Ni, Cu and P. The energetic stability of solute(s)-carbon-vacancy complexes was rationalized on the basis of pairwise interaction data and by analyzing the variation of local magnetic moments on atoms constituting the clusters.

Acknowledgment: This work, supported by the European Commission under the Contract of Association between EURATOM/SCK-CEN, was carried out within the framework of the European Fusion Development Agreement. We are grateful to the ICT Department of Ghent University for partial support of this work. Part of calculations has been performed at HPC Julich within the 'SORT' project. The research was partly supported by the FWO grant.

Published in: A. Bakaev, D. Terentyev, X. He, E.E. Zhurkin and D. Van Neck / Journal of Nuclear Materials 451 (2014) 82–87

Carbon–vacancy interaction controls lattice damage recovery in iron

D. Terentyev^a, K. Heinola^b, A. Bakaev^c and E.E. Zhurkin^d

^a SCK-CEN, Nuclear Materials Science Institute, Boeretang 200, Mol B2400, Belgium

^b Department of Physics, University of Helsinki, PO Box 43, FIN-00014 Helsinki, Finland

^c Center for Molecular Modeling, Department of Physics and Astronomy, Ghent University, Technologiepark 903, 9052 Zwijnaarde, Belgium

^d Department of Experimental Nuclear Physics K-89, Institute of Physics, Nanotechnology and Telecommunications, St Petersburg State Polytechnical University, 29 Polytekhnicheskaya Str., 195251 St Petersburg, Russia

Introduction: The radiation resistance of crystalline materials is determined by their ability to recover lattice defects produced by energetic particles. The addition of impurities is crucial from the metallurgical viewpoint, while their presence usually has a tremendous effect on the recovery of lattice defects. The most common example is iron–carbon (Fe–C) solid solution representing the matrix for steels currently operating and being proposed for future nuclear concepts. C atoms affect mechanical properties before and after irradiation, implying their interaction with both dislocations and radiation-induced lattice defects. In-depth experimental investigations discovered that C atoms strongly bind to vacancies (V) and weakly with self-interstitial atoms (SIAs). C atoms therefore glue vacancies in clusters and hinder their migration, provoking nucleation of nanovoids. Consequently, carbon–vacancy (C–V) interaction plays a crucial role in the process of accumulation and recovery of radiation damage macroscopically seen as hardening, swelling and creep under prolonged irradiation.

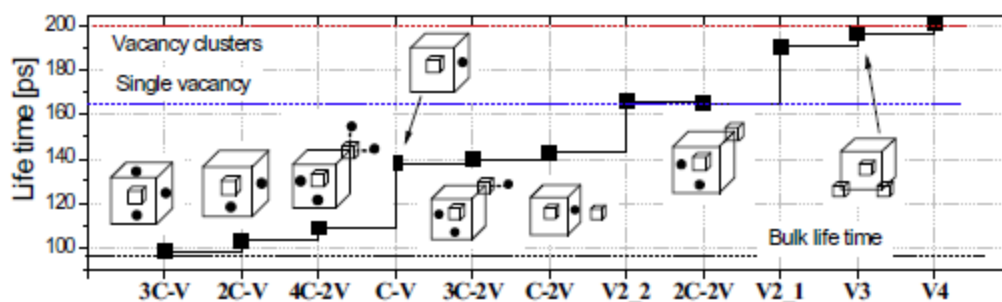
Although significant experimental and theoretical efforts have been dedicated to unravelling the interaction of C with radiation defects, the annealing of irradiated Fe–C alloys in the technological temperature range is not yet completely understood. A combination of resistivity measurements (RMs) and positron annihilation spectroscopy (PAS) is the standard way to investigate the elementary recovery processes driven by the migration of radiation-induced defects. Both RM and PAS techniques reveal that complete recovery of vacancies in Fe–C alloys

occurs around 600 K. This temperature corresponds to the energetic stability of double carbon–vacancy (2CV) clusters, whose dissociation energy is ~ 1.8 eV.

If the initial concentration of vacancies, C_V , exceeds the amount of dissolved C atoms, C_C , then damage annealing is controlled by clustering of vacancies and their subsequent evaporation. In the opposite case (i.e. $C_C > C_V$), the formation of C–V clusters leads to a complex positron annihilation spectrum, revealing both isolated and clustered vacancies at 450–600 K.

A recent analysis employing *ab initio* data on the stability of C–V complexes and kinetic Monte Carlo (kMC) simulations reported disagreement with experimental data in the temperature range 450–600 K. While vacancy clustering took place experimentally, it could not be reproduced in the simulations. Moreover, even the interpretation of PAS data and direct comparison with kMC calculations is challenging since carbon significantly alters the lifetime of a positron trapped by C–V complexes. Although several PAS studies have been performed on electron- and neutron-irradiated Fe and Fe–C alloys, the lifetime of multiple C–V complexes cannot be decomposed from the experimental spectra. Consequently, information on the structure of C–V complexes appearing in the technological temperature range remains unknown, while this is a crucial input for coarse-grain models dealing with the evolution of radiation damage and its recovery in Fe–C alloys.

Main results: It was employed the density functional theory (DFT) to assess the thermal stability and positron lifetime of C–V complexes in body-centered cubic (bcc) Fe. Confronting the obtained lifetime against the experimental data allowed physically plausible assumption on mobility of the 2CV cluster to be made, which is necessary to complete the formulation of a self-consistent model describing the evolution of both isolated and clustered vacancies upon irradiation and subsequent annealing. As proof, we employed kinetic rate theory calculations to model annealing of electron-irradiated Fe–C alloys using the DFT-established library of binding and dissociation energies for C–V clusters. The migration energy of the 2CV complex, 1.1 eV, was deduced by fitting the model to the experimental data.



Lifetime of C–V clusters and their structures corresponding to the lowest formation enthalpy. An empty square and filled circle denote a vacancy and a C atom, respectively. Configurations marked “V2_1” and “V2_2” are the di-vacancies representing, respectively, first and second nearest neighbours.

Conclusions: The study has revealed that positron lifetime is extremely sensitive to C–V arrangement and multiplicity. Following the *ab initio* lifetime data, a C–V complex can be detected as a single or clustered vacancy, or remain indistinguishable from bulk. Combining *ab initio* data with kinetic rate theory, we modelled annealing of irradiated Fe–C alloys and performed one-to-one comparison with experiment, which revealed a good agreement.

OKMC simulations of Fe-C systems under irradiation: Sensitivity studies

Ville Jansson³ and Lorenzo Malerba, SCKCEN, The Belgian Nuclear Energy Research Centre, Institute for Nuclear Materials Science, Structural Materials Group, Boeretang 200, B-2400 Mol, Belgium

Introduction: This is the continuation of our previous work on a nanostructural evolution model for Fe-C alloys under irradiation, using Object Kinetic Monte Carlo modeling techniques. A number of sensitivity studies on the effect of parameters of the model have been performed, mainly evaluating the effect of the carbon content in the material, represented by generic traps for point defects, and thus the importance of traps, their size dependence, and the effect of the dose rate.

Main results: The effect of the trap concentration, which translates the C content, on the evolution of the density of both vacancy and visible SIA clusters, is found to be moderate. An increase of two orders of magnitude in the trap density, from 1 appm to 100 appm, only increases the vacancy cluster density by less than one order of magnitude after 0.2 dpa. So, at least at this irradiation temperature, variations in the actual C content (in the matrix) are not expected to have any strong influence, so long as the concentration is sufficiently high. Our results also show that, in order to remove the effect of C, it is necessary to reduce its concentration very significantly, down to a level of purity rarely reached in iron. The results show that there is a clear dose rate effect on both the vacancy and the visible SIA cluster density evolution, at least at the temperature considered here (much lower than the operation temperature of RPV steels). However, a change of the dose rate by eight orders of magnitude only gives a difference of one order of magnitude for both the vacancy and the visible SIA densities, so the effect can be considered limited. It can be summarized by saying that, the lower the dose rate, the more time defects have to cluster, also by coalescence, before new defects are nucleated; or to disappear at sinks before new defects come to make them grow. The overall effect is that the density decreases, while the size increases. The gap to decide whether this will have or not an effect also on mechanical property changes is wide. However, one can speculate that the effect on radiation hardening of the increased size with lower dose rate might be offset by decreased density of obstacles to dislocation motion, with overall limited effect on not only hardening, but also embrittlement.

Conclusions: The sensitivity study performed here shows that a model for nanostructural evolution under irradiation in iron based on traps translating the effect of C is effective and physically solid, as the variation of the key parameters lends itself to physically consistent interpretations

Future work: The work on this subject continues with models that address more complex alloys (FeCrC, FeMnNiC, ...), in a "grey alloy" approach.

³ Currently at Accelerator Laboratory, [Helsinki Institute of Physics](#), P.O.Box 43 (Pietari Kalmink. 2) 00014 [University of Helsinki](#)

Acknowledgment: This work was supported within by the 7th Framework Programme Project PERFORM60 under Grant Agreement No. FP7-232612..

Published in: V. Jansson and L. Malerba, Journal of Nuclear Materials 452 (2014) 118-124.

Dislocation glide in Fe–carbon solid solution: From atomistic to continuum level description

H.A. Khater ^{a,d}, G. Monnet ^b, D. Terentyev ^c, A. Serra ^d

^a Physics Department, Faculty of Science, Assiut University, Assiut 71516, Egypt

^b EDF-R&D, MMC, Avenue des Renardières, 77818 Moret sur Loing, France

^c SCKCEN, Structural Materials Modelling and Microstructure Unit, SMA/NMS, Boeretang 200, 2400 Mol, Belgium

^d Universitat Politècnica Catalunya, Jordi Girona 1-3, 08034 Barcelona, Spain

Introduction: The role of interstitial carbon impurities on the dislocation glide in bcc iron is investigated by means of molecular dynamics simulations. The local stress induced by carbon atoms, interaction energy map for the $a_0/2\langle 111 \rangle\{110\}$ and $a_0/2\langle 111 \rangle\{112\}$ edge dislocations and the dynamics of dislocation–carbon interaction is assessed. The local stress exerted on the dislocation due to the carbon atoms and computed by atomistic simulations is used to describe the interaction strength on the continuum level. The derived here analysis of the atomistic data enabled the determination of the activation enthalpy and volume as a function of stress. Having that information, a comparative study demonstrates that at finite temperature, the resistance to the dislocation glide induced by the carbon atoms is lower in $\{112\}$ than in $\{110\}$ slip systems.

Main results:

Examination of the carbon–dislocation interaction energy reveals a clear difference between the edge dislocations with $\{110\}$ and $\{112\}$ slip planes. Profiles in Fig. 1 are symmetrical for the TDA[001] and anti-symmetrical for the others. No symmetry is observed for the $\{112\}$ dislocation slip plane, as expected due to the asymmetry of the dislocation core structure (Monnet and Terentyev, 2009). This feature is important and must be taken into account in investigations of the asymmetry of glide in BCC materials (see for ex. Wang and Beyerlein, 2011). Consequently, the unpinning stress upon the interaction with a carbon atom should be different for the twinning and antitwinning glide direction, as confirmed by the results. Importantly, the interaction is stronger for the antitwinning glide direction, implying that carbon solution intensifies the twinning-antitwinning asymmetry as compared to pure Iron. Investigation of the lattice distortion induced by a C atom near the dislocation cores reveals a good qualitative agreement with previous works, in terms of the interaction energy (Tapasa et al., 2007; De Hosson, 1975; Shu and Wang, 2007) and unpinning stress (Clouet et al., 2008). The results of the atomistic calculations also closely match the prediction of the anisotropic elasticity theory (Tapasa et al., 2007). In all cases, an increase of the interaction energy is consistent with the increase of the unpinning stress. Another important information obtained by the MS calculations is the dependence of the interaction strength on the distance between a C atom and glide plane. Irrespective of the TDA orientation, the interaction strength monotonically decreases as the C atom distance from the glide plane increases. This aspect may lead to simplify the modeling of dislocation–carbon interaction in random solid solution **at**

dislocation dynamics scale, as it allows to disregard the actual TDA orientation and use an effective approach.

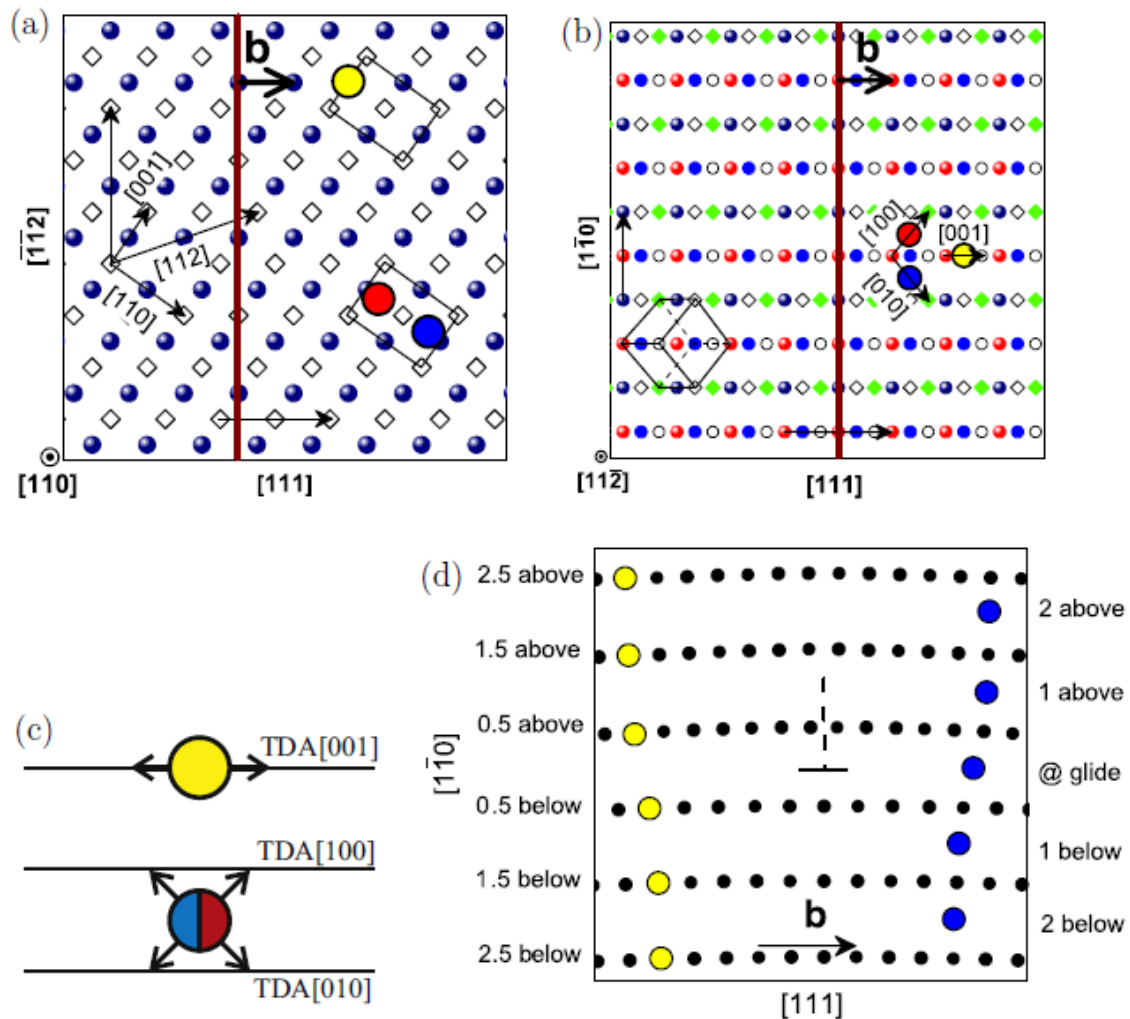


Fig.1. Possible octahedral positions together with the orientation of the Burgers vector and dislocation line in the slip systems. (a) and (b) top view of the models and (c) side view showing traces of atomic planes parallel to the glide plane and positions of C atoms with respect to them. (d) Projection along dislocation line with the positions of the C atoms relative to each plane. In-plane octahedral positions are shown by circles at left and inter-plane octahedral positions are at right. Yellow shaded circles demonstrate in-plane C atoms, TDA[001], blue and red shaded circles demonstrate between planes C atoms, TDA[100] and TDA[010].

Conclusions:

Statics simulations of edge dislocations moving in a Fe–C solution containing 400 ppm of carbon have shown that collective effect of C atoms coupled with the residual lattice friction is rather complex. Certain TDA configurations cause a strong modification in the local lattice friction so that a weak softening effect (as compared to pure Fe) takes place as a net result.

Future work: Perform the same assessment for the screw dislocation

Acknowledgment: The authors express their thanks to Prof. David J. Bacon for his advice and helpful discussions. This research has been funded by the EC under the FP7 EURATOM Project

PERFORM60 (232612), the Spanish Ministry of Science and Innovation (FIS2012-39443-C02-02) and the Catalan Government (CIRIT 2009SGR 1003). This work also contributes to the Joint Programme on Nuclear Materials (JPNM) of the European Energy Research Alliance (EERA).
Published in: H.A. Khater, G. Monnet, D. Terentyev, A. Serra / International Journal of Plasticity 62 (2014) 34–49

F/M steels and model alloys

On the radiation-induced segregation: Contribution of interstitial mechanism in Fe–Cr alloys

V.A. Pechenkin ^a, V.L. Molodtsov ^a, V.A. Ryabov ^a, D. Terentyev

a a Institute of Physics and Power Engineering, 249033 Obninsk, Russia

b SCK-CEN, Nuclear Materials Science Institute, Boeretang 200, B-2400 Mol, Belgium

Introduction:

In this work, we perform molecular dynamics simulations to study the diffusion characteristics of a self-interstitial atom (SIA) in BCC Fe-Cr alloys and corresponding mass transport of Fe and Cr atoms via SIA migration mechanism. The calculations have been performed in the temperature range 600-1000 K in the alloys with Cr content 5-25 at.%, which is relevant for ferritic/martensitic steels.

Main results:

The results of atomistic simulations have been applied to evaluate the contribution of SIA diffusion mechanism to radiation - induced segregation (RIS) phenomenon. An original treatment is proposed in this work to account for the contribution from both vacancy and SIA mechanisms to RIS at sinks for point defects in multi-component system. By combining available experimental data on diffusion of Fe and Cr via vacancy mechanism with the results of MD simulations for SIAs, we demonstrate that enrichment of sinks by Cr atoms is possible in the Fe-Cr alloys containing less than 13% Cr. This result is discussed in the light of available experimental data on the RIS in Fe-Cr alloys and ferritic/martensitic steels. It is predicted that the degree of the Cr enrichment goes up with decreasing Cr content in the alloy and irradiation temperature.

Conclusions:

we proposed the way to study the contribution to radiation - induced segregation in binary alloys coming from the self-interstitial migration mechanism based on molecular dynamics simulations. The latter were used to characterize the diffusivity of self-interstitial defects, Fe and Cr atoms and corresponding correlation factors in random Fe – (5 – 25 at.%) Cr alloys at temperature varied from 600 up to 1000 K. By combining available experimental data and the results of atomistic simulations we demonstrate that enrichment of Cr near sinks for mobile point defects is possible due to the competition between interstitial and vacancy migration mechanisms in the alloys containing less than ~ 13-15 %at. Cr. It is predicted that the degree of enrichment goes up with decreasing Cr content and irradiation temperature. A scheme to generalize the applied approach for multi-component system accounting for both vacancy and SIA diffusion is also presented in this work.

Future work: Not foreseen.

Acknowledgment: This work was partially supported by the Russian Foundation for Basic Research under the Project No. 12-02-97526. It was also partially supported by the EURATOM seventh Framework Programme, under Grant Agreement No. 212175 (GetMat Project).

Published in: V.A. Pechenkin, V.L. Molodtsov, V.A. Ryabov, D. Terentyev / Journal of Nuclear Materials 433 (2013) 372–377

Cr segregation on dislocation loops enhances hardening in ferritic Fe–Cr alloys

D. Terentyev^a, F. Bergner^b, Y. Osetsky^c

a SCK-CEN, Nuclear Material Science Institute, Boeretang 200, B-2400 Mol, Belgium

b Helmholtz-Zentrum Dresden-Rossendorf, PO Box 510119, 01314 Dresden, Germany

c Materials Science and Technology Division, ORNL, Oak Ridge, TN 37831, USA

Introduction:

To clarify the possibility of Cr segregation on dislocation loops and its impact on obstacle strength we performed a dedicated atomistic study. The Monte Carlo technique was first applied to study Cr arrangement near interstitial dislocation loops as a function of loop size and temperature in a Fe–10Cr alloy. The equilibrium configurations of dislocation loops surrounded by Cr atoms obtained from these calculations were used in large-scale molecular dynamics (MD) modeling to study the interaction of Cr-decorated loops with gliding dislocations. In this work we primarily address $\frac{1}{2}\langle 111 \rangle$ interstitial dislocation loops, as these are known to form under irradiation at low temperature, while $\langle 100 \rangle$ loops are predominant at high temperature [7]. Secondly, $\frac{1}{2}\langle 111 \rangle$ loops are known to glide easily and thus under the action of a stress field of moving dislocations they enter direct dislocation reactions.

Main results:

The effect of chromium on iron hardening via segregation on dislocation loops was studied by atomic scale computer modeling. A combination of Monte Carlo and molecular dynamics techniques together with the recently determined Fe–Cr interatomic potentials fitted to ab initio data was used to investigate Cr segregation on $\frac{1}{2}\langle 111 \rangle$ interstitial dislocation loops and its impact on the interaction with moving dislocations. The Monte Carlo results reveal that Cr atoms segregate to the loop tensile strain region and dissolve well above the temperature corresponding to the solubility limit. The molecular dynamics results demonstrated that local micro-chemical changes near the loop reduce its mobility and increase the strength. The stress to move dislocation through the array of Cr “decorated” loops increases due to modification of the dislocation–loop interaction mechanism. A possible explanation for a number of experimental observations being dependent on the radiation dose and for Cr concentration effects on the yield stress is given on the basis of the modeling results.

Conclusions:

Cr enrichment modifies the properties of $\frac{1}{2}\langle 111 \rangle$ dislocation loops, particularly their mobility and the mechanism of interaction with moving edge dislocations. The mechanism changes from complete absorption to Orowan-like, controlled by the closure of a screw dipole, and therefore requires a much higher unpinning stress. In practice such a change in mechanism is equivalent to an increase in the effective obstacle strength. The test temperature and number of segregated Cr atoms determine one of the two possible reaction pathways.

Future work: Not foreseen.

Acknowledgment: The research was partially supported by the EURATOM Seventh Framework Programme, under Grant Agreement No. 212175 (GetMat Project). This work was also partially supported by the European Commission under the contract of Association between Euratom and the Belgian State, and was carried out within the framework of the European Fusion Development Agreement, and by the US Department of Energy, Office of Basic

Energy Sciences, Materials Sciences and Engineering Division, Center for Defect Physics, an Energy Frontier Research Center. The authors greatly acknowledge the assistance of Prof. D.J. Bacon (Liverpool University). Calculations were performed by the Juelich supercomputer cluster within the EMAC Project.

Published in: D. Terentyev, F. Bergner, Y. Osetsky / Nuclear Instruments and Methods in Physics Research B 303 (2013) 33–36

Radiation-induced strengthening and absorption of dislocation loops in ferritic Fe-Cr alloys: the role of Cr segregation

D. Terentyev¹ and A. Bakaev^{1,2}

¹ *SCK-CEN, Nuclear Material Science Institute, Boeretang 200, B-2400 Mol, Belgium*

² *Centre for Molecular Modelling, Ghent University, Technologiepark 903, B-9052 Zwijnaarde, Belgium*

Introduction: Dislocation loops are the primary signature of radiation damage in commercial ferritic–martensitic and austenitic steels and model alloys at temperature $\sim(0.3–0.6)T_M$, where T_M is the melting point. These defects cause strengthening by obstructing dislocation motion, if the deformation is mediated by dislocation glide. In turn, the obstruction of dislocation motion (strengthening) leads to embrittlement, while the ability of dislocations to absorb dislocation loops when unpinning is believed to be the reason for the formation of clear channels, as suggested by post-deformation investigations. The presence of clear bands, on the other hand, is known to cause plastic flow localization and non-homogeneous deformation, and lead to loss of ductility as a result.

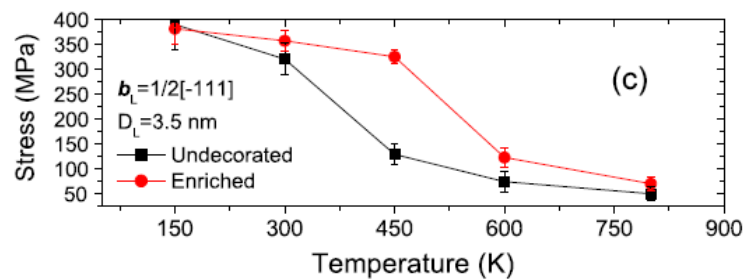
For the above reasons, the dislocation–loop interaction is being intensively studied both experimentally and theoretically. In particular, recently the numerical modelling of this interaction has become a very active field, where two major complementing techniques are applied, namely the discrete dislocation dynamics (DDD) and classical molecular dynamics (MD) techniques. The direct dislocation–loop interaction involves the atomic rearrangement of dislocation cores and other atomic-scale processes, like the formation of new junctions, their movement and their unzipping. MD simulations, being inherently atomistic, are especially efficient to use to study dislocation-core effects and defects of nanometric sizes, which are hardly or not at all resolvable in transmission electron microscopy (TEM).

Real materials (even pure ones) always contain a certain amount of impurities, while alloys contain alloying elements expressly introduced to provide specific properties. These, under irradiation, a priori may segregate to lattice imperfections, e.g. dislocation loops, and form so-called ‘decorated’ loops. By ‘decoration’, we mean the presence of high concentrations of interstitial impurities or substitutional solute atoms in the strained region around the loop.

Unlike for pure metals, for concentrated model alloys as well as ferritic–martensitic and austenitic steels, beside the possible decoration with interstitial impurities like C, the segregation of Cr, Ni and other alloying elements is known to occur under irradiation. In particular, the segregation of Cr on both $\langle 100 \rangle$ and $1/2\langle 111 \rangle$ dislocation loops is a well-established phenomenon, which has been reported by different independent researchers for different grades of Fe–Cr steels and model alloys. Recently, an indisputable proof of the

segregation of Cr to dislocation lines and dislocation loops was obtained using tomography atom probe (TAP) techniques applied to examine an irradiated high-Cr ferritic–martensitic steel. Hence, it is important to assess the influence of Cr enrichment on the pinning strength of loops and on their ability to be absorbed by moving dislocations.

Main results: It was performed an atomistic study to investigate the impact of Cr segregation at loops on the interaction with dislocations. In particular, two kinds of interstitial dislocation loops: $1/2\langle 111 \rangle$ and $\langle 100 \rangle$ were considered, which are typically observed under neutron irradiation at elevated temperature in the high-Cr steels and other Fe–Cr model alloys. The emphasis was put on the interaction with edge dislocations, since they are known to be more efficient means for loop absorption and removal as compared to screw dislocations. In addition, the contribution to the plastic flow is comparable for edge and screw dislocations at room temperature and above it. It was shown that Cr enrichment modifies the interaction mechanism for both $1/2\langle 111 \rangle$ and $\langle 100 \rangle$ loops. The effect of loop size, test temperature and dislocation velocity on the extra strengthening caused by solute segregation was explored.



Average unpinning stress calculated in the reactions with $1/2[-111]$ loops, $D_L = 3.5$ nm, $v_D = 10$ m s⁻¹

Conclusions: The overall effect of Cr enrichment is to penalize the mobility of intrinsically glissile $1/2\langle 111 \rangle$ loops, modifying the reaction mechanisms as a result. The following three most important effects associated with Cr enrichment have been revealed: (i) absence of dynamic drag; (ii) suppression of complete absorption; (iii) enhanced strength of small dislocation loops (2 nm and smaller). Overall the effect of the Cr enrichment is therefore to increase the unpinning stress, so experimentally ‘invisible’ nanostructural features may also contribute to radiation-induced strengthening.

Future work: Further research can be performed on the effect of strain rate in the reactions involving the emergence and movement of screw dislocations.

Acknowledgment: This research was partially supported by the EURATOM seventh Framework Programme, under Grant Agreement No. 212175 (GetMat Project). This work was also partially supported by the European Commission under the Contract of Association between Euratom and the Belgian State, and carried out within the framework of the European Fusion Development Agreement. The authors acknowledge Dr L Malerba for discussion and proofreading. AB acknowledges an FWO grant for financial support.

Published in: D. Terentyev and A. Bakaev / J. Phys.: Condens. Matter 25 (2013) 265702

On the Mobility of Vacancy Clusters in Reduced Activation Steels: An Atomistic Study in the FeCrW Model Alloy

G. Bonny¹, N. Castin¹, J. Bullens^{1,2}, A. Bakaev^{1,3}, T.C.P. Klaver⁴ and D. Terentyev¹

¹ SCK•CEN, Nuclear Materials Science Institute, Boeretang 200, B-2400 Mol, Belgium.

² Université Libre de Bruxelles, Physics Department, CP 238, Boulevard du Triomphe, 1050 Bruxelles, Belgium.

³ Ghent University, Center for Molecular Modeling, Technologiepark 903, B-9052 Zwijnaarde, Belgium.

⁴ Delft University of Technology, Department of Materials Science and Engineering, Mekelweg 2, 2628 CD Delft, the Netherlands.

Introduction:

We performed a multi-scale study addressing the mobility and life time of vacancy clusters in bcc FeCr, FeW and FeCrW alloys. We performed DFT calculations and used them to fit and validate the developed interatomic potential (IAP). In turn, the latter was used to derive an artificial neural network (ANN) regression to predict the migration barrier of vacancies as a function of local atomic environment in bcc FeCrW alloy. Based on the obtained regression, atomistic kinetic Monte Carlo (AKMC) simulations were executed to characterize the mobility, life time and free path (until the break event) of small vacancy clusters (containing up to six vacancies), known to be as mobile as a single vacancy. As a result, we provide the database of the properties of small vacancy clusters to be applied in rate theory or object kinetic Monte Carlo (OKMC) models.

Main results:

The DFT data shows that W is a slow diffuser and Cr a fast diffuser compared to Fe. We also conclude that fast vacancy migration paths exist in dilute FeCr and FeW alloys.

The developed IAP provides good qualitative agreement with the DFT data although it was only fitted to a limited number of configurations. Therefore the IAP provides good transferability and can be used in other atomistic studies, e.g., molecular dynamics studies in the FeCrW system. As also mentioned in [44], we emphasize that the present potential was fitted to the ferro-magnetic alloy and its application should be limited to temperatures well below the Curie temperature.

The ANN regression trained on random examples of vacancy migration barriers in the ternary alloy using the IAP proves an accurate and fast method for on-the-fly migration barriers calculation.

Within the limitation of transferrability of the fitted potentials, the AKMC results show that for a single vacancy the addition of W or Cr enhances diffusivity by a factor of 2-4. The increase of 9Cr is equivalent to that of Fe-(1-2)W. The enhancement of diffusivity is due to Cr-vacancy exchange (occurring with a lower energy barrier), since the geometric correlation factor indicates no correlated movement. For Fe-W, on the other hand, the enhanced diffusion is due to some correlated movement.

For vacancy clusters, the amplification of cluster diffusivity increases for larger vacancy clusters (starting from size 4). At the same time, the lifetime monotonically decreases with W concentration. The larger the cluster size, the larger the decrease of the lifetime is. We note that in Fe-9Cr, both the lifetime decrease and diffusivity enhancement does not depend on the size of a vacancy cluster. For the ternary alloy, no synergetic effects are observed, and the alloy

behaves as the superposition of the Fe9Cr and FeW alloys. We also note that W atoms remain immobile in all simulations and solely act as 'break up' centres for vacancy clusters.

Conclusions:

We conclude that the presence of W in concentrations of 1-2% has a huge impact on the stability of migrating vacancy clusters, i.e., they do breakup as soon as a W atom is met. This result implies that W should effectively suppress the growth of in-cascade formed vacancy clusters. Hence, we conclude that one of the effects of W in the microstructural evolution under irradiation is to suppress the nucleation of stable vacancy clusters, which may grow to voids. The validity of the latter statement is to be validated using object kinetic Monte Carlo simulations in our future work.

Future work:

The developed potential is used to model AKMC and MD simulations within the SMM group.

Acknowledgment:

EFDA / HPC Julich / HELIOS HPC Japan

Published as: G. Bonny et al., Journal of Physics Condensed Matter 26 (2013) 315401.

Microchemical effects in irradiated Fe-Cr alloys as revealed by atomistic simulation

Lorenzo Malerba, Giovanni Bonny and Dmitry Terentyev, SCK-CEN, The Belgian Nuclear Energy Research Centre, Institute for Nuclear Materials Science, Structural Materials Group, Boeretang 200, B-2400 Mol, Belgium

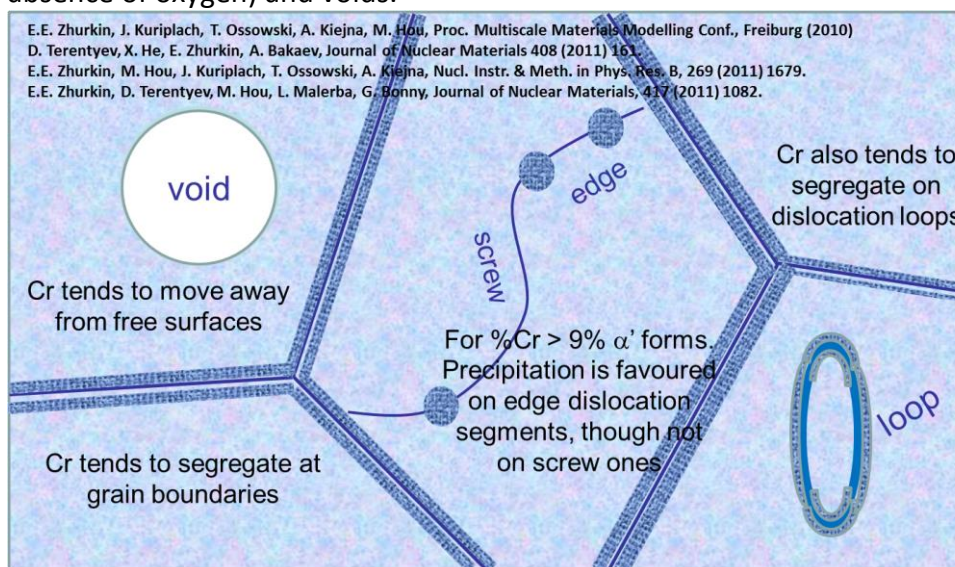
Evgeny E. Zhurkin, Experimental Nuclear Physics Department, K-89, Faculty of Physics and Mechanics, Saint-Petersburg State Polytechnical University, 29 Polytekhnicheskaya Str., 195251 St. Petersburg, Russia

Marc Hou, Physique des Solides Irradiés et des Nanostructures CP234, Faculté des Sciences, Université Libre de Bruxelles, Bd du Triomphe, B-1050 Bruxelles, Belgium

Katharina Vörtler and Kai Nordlund, Association EURATOM-Tekes, Department of Physics, P.O. Box 43, FI-00014, University of Helsinki, Finland

Introduction: Neutron irradiation produces evolving nanostructural defects in materials, that affect their macroscopic properties. Defect production and evolution is expected to be influenced by the chemical composition of the material. In turn, the accumulation of defects in the material results in microchemical changes, which may induce further changes in macroscopic properties. In this work we review the results of recent atomic-level simulations conducted in Fe-Cr alloys, as model materials for high-Cr ferritic-martensitic steels, to address the following questions: 1. Is the primary damage produced in displacement cascades influenced by the Cr content? If so, how? 2. Does Cr change the stability of radiation-produced defects? 3. Is the diffusivity of cascade-produced defects changed by Cr content? 4. How do Cr atoms redistribute under irradiation inside the material under the action of thermodynamic driving forces and radiation-defect fluxes?

Main results: It is found that the presence of Cr does not influence the type of damage created by displacement cascades, as compared to pure Fe, while cascades do contribute to redistributing Cr, in the same direction as thermodynamic driving forces. The presence of Cr does change the stability of point-defects: the effect is weak in the case of vacancies, stronger in the case of self-interstitials. In the latter case, Cr increases the stability of self-interstitial clusters, especially those so small to be invisible to the electron microscope. Cr reduces also significantly the diffusivity of self-interstitials and their clusters, in a way that depends in a non-monotonic way on Cr content, as well as on cluster size and temperature; however, the effect is negligible on the mobility of self-interstitial clusters large enough to become visible dislocation loops. Finally, Cr-rich precipitate formation is favoured in the tensile region of edge dislocations, while it appears not to be influenced by screw dislocations; prismatic dislocation loops (typically produced under irradiation) tend to be decorated by Cr. Cr has also tendency to accumulate at grain boundaries, while it tends to deplete in the proximity of free surfaces (at least in the absence of oxygen) and voids.



Pictorial illustration of the tendencies governing Cr redistribution under irradiation.

Conclusions: The analysis of a wide range of atomistic simulation results, specifically density functional theory (DFT) calculations, as well as DFT-based interatomic potential studies, e.g. by Metropolis Monte Carlo techniques, allowed a fairly complete description of how Cr redistribute under irradiation in Fe-Cr alloys to be obtained, that agrees with experimental observations or explains them.

Future work: The work on this subject continues by looking at more complex alloys as well as at the effect of C on nanostructural and microchemical evolution under irradiation, for example within the FP7/MatISSE project, but also as part of the IREMEV task in EUROfusion.

Acknowledgment: The research was partially supported by the EC within the 7th Framework Programme Project GETMAT under Grant Agreement No. 212175.

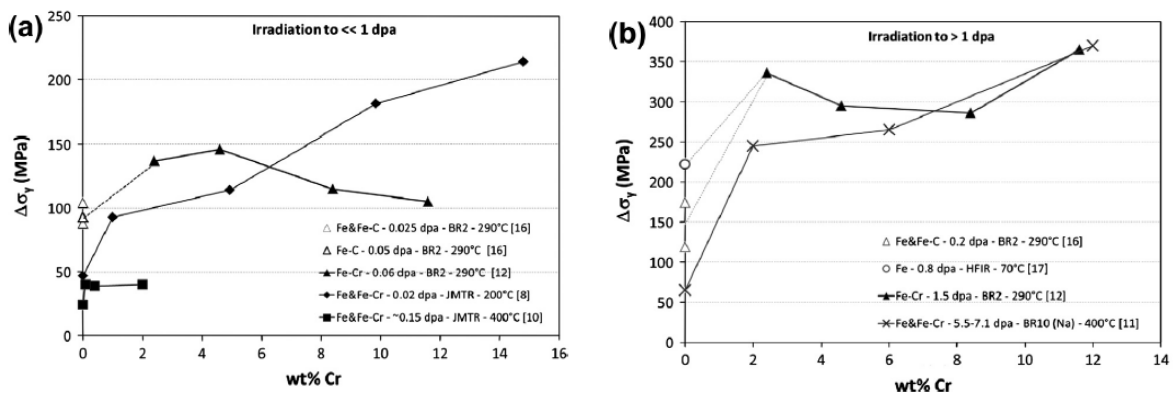
Published in: L. Malerba, G. Bonny, D. Terentyev, E.E. Zhurkin, M. Hou, K. Vörtler, K. Nordlund, Journal of Nuclear Materials 442 (2013) 486-498.

Mechanisms of radiation strengthening in Fe-Cr alloys as revealed by atomistic studies

Dmitry Terentyev, Giovanni Bonny and Lorenzo Malerba, SCK•CEN, The Belgian Nuclear Energy Research Centre, Institute for Nuclear Materials Science, Structural Materials Group, Boeretang 200, B-2400 Mol, Belgium

Christophe Domain and Ghiath Monnet, EDF-R&D, Département MMC, Les Renardières, 77818 Moret sur Loing Cedex, France

Introduction: A review of experimental results shows that the dependence on Cr content of radiation-induced strengthening in Fe-Cr alloys and ferritic/martensitic steels is peculiar, exhibiting an increase as soon as Cr is added, followed by a local maximum and then a local minimum (see Figure). This dependence is to date unexplained. In this work we try to rationalise it, by reviewing recent (published and unpublished) molecular dynamics simulations work, devoted to the investigation of several possible mechanisms of radiation strengthening in Fe-Cr. In particular, the following questions are addressed quantitatively: (i) Does Cr influence the glide of dislocations? If so, how? (ii) Does Cr influence the interaction between dislocations and radiation-produced defects? If so, why? The latter question involves also a study of the interaction of moving dislocations with experimentally observed Cr-enriched loops.



Experimental data on radiation hardening as a function of Cr content in Fe-Cr alloys according to literature.

Main results: We find that the fact of shifting from a loop-absorption (pure Fe) to a loop-non-absorption (Fe-Cr) regime, because of the Cr-enrichment of loops, contributes to explaining why Fe-Cr alloys harden more under irradiation than Fe. If, in addition, the existence of a large density of invisible and Cr-enriched loops is postulated, the origin of the effect becomes even more clear. Moreover, the different strength of $\frac{1}{2}\langle 111 \rangle$ and $\langle 100 \rangle$ loops as obstacles to dislocations movement, depending on whether or not loop absorption can occur, might explain why radiation strengthening decreases between 2 and 9 %Cr. The formation of α' precipitates, finally, explains why radiation strengthening increases again above 9%Cr. Altogether, these effects might explain the origin of the minimum of radiation-induced embrittlement at 9%Cr, as correlated to strengthening.

Conclusions: The analysis of a wide range of atomistic simulation results, specifically molecular dynamics simulations of the interaction between dislocations and defects, especially interstitial dislocation loops, Cr-decorated and not, allowed a quantitative rationalisation of the peculiar

experimentally observed dependence on Cr content of radiation-hardening in Fe-Cr alloys to be provided.

Future work: The work on this subject continues by looking at more complex alloys as well as at the effect of C on loop strength as obstacles for dislocations, for example within the FP7/MaTISSE project, but also as part of the IREMEV task in EUROfusion.

Acknowledgment: The research was partially supported by the EC within the 7th Framework Programme Project GETMAT under Grant Agreement No. 212175.

Published in: D. Terentyev, G. Bonny, C. Domain, G. Monnet, L. Malerba, Journal of Nuclear Materials 442 (2013) 470-485.

Critical assessment of Cr-rich precipitates in neutron-irradiated Fe-12 at%Cr: Comparison of SANS and APT

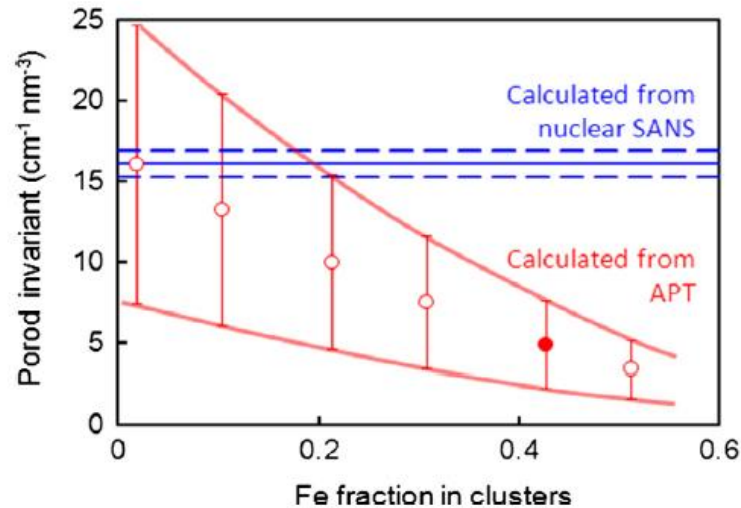
*Frank Bergner, Andreas Ulbricht and Arne Wagner, Helmholtz-Zentrum Dresden-Rossendorf,
POB 510119, 01314 Dresden, Germany*

Cristelle Pareige, Vladimir Kuksenko and Philippe Pareige, Groupe de Physique des Matériaux, Université et INSA de Rouen, UMR 6634 CNRS, Avenue de l'Université, BP 12, 76801 Saint Etienne du Rouvray, France

*Lorenzo Malerba, SCK-CEN, The Belgian Nuclear Energy Research Centre, Institute for Nuclear
Materials Science, Structural Materials Group, Boeretang 200, B-2400 Mol, Belgium*

Introduction: Neutron irradiation at 300°C up to 0.6 dpa of an industrial purity Fe-12at%Cr alloy gives rise to the formation of Cr-rich precipitates of radii of about 1 nm. Small-angle neutron scattering (SANS) and atom probe tomography (APT) applied to the same material should reveal consistent characteristics of the irradiation-induced features. They roughly do so with respect to size and volume fraction, but they do not with respect to the composition of the precipitates or clusters. Namely, APT reveals an Fe content as high as 40%, which would suggest that thermodynamic equilibrium is far from being reached, if one assumes that the composition of α' should be less than 5% Fe at the temperature considered here, according to the accepted phase diagram. The equilibrium concentration, on the other hand, is assumed in SANS for the analysis of the data. In this work the possible origins of this discrepancy are systematically analysed, in order to learn how to improve the interpretation of both APT and SANS results concerning precipitates.

Main results: The discrepancy between APT and SANS was expressed in terms of the Porod invariant of nuclear SANS. This quantity can be determined directly by integrating the measured nuclear difference scattering cross section or, alternatively, estimated from the APT results. Both estimates were compared taking into account all potential sources of deviation including error propagation. We have found that the deviation is significant and can be progressively removed by artificially reducing the Fe fraction in the Cr-rich clusters with respect to the APT measured value, as illustrated in the Figure. A well-known effect of this kind is the different evaporation fields of Cr-rich clusters and the Fe-rich matrix and resulting ion trajectory overlaps in APT. State-of-the-art consideration of this effect indicates, however, that it is not sufficient to remove the observed discrepancy.



Comparison of the Porod invariant calculated from data measured in APT and derived from SANS. The full symbol corresponds to the measured Fe-fraction of clusters, the open symbols were obtained for various assumed offsets of the Fe-fraction

Conclusions: The maximum Fe concentration that remains, within uncertainties, consistent with the SANS data is 20%. The main uncertainty, when assessing the composition of clusters from APT, concerns the way in which the evaporation field is simulated. The present analysis suggests that the origin of the enduring discrepancy between APT and SANS might be possibly found by revisiting in detail the hypothesis made in the simulation of the evaporation field in APT

Future work: The investigation of the origin of the differences between SANS and APT studies on the same materials are a key point in order to be confident about the information deduced from these experiments on precipitates, thus for sure this investigation will continue, although in fact it is not openly part of any funded project.

Acknowledgment: The research was partially supported by the EC within the 7th Framework Programme Project GETMAT under Grant Agreement No. 212175.

Published in: F. Bergner, C. Pareige, V. Kuksenko, L. Malerba, P. Pareige, A. Ulbricht, A. Wagner, *Journal of Nuclear Materials* 442 (2013) 463-469.

Interaction of minor alloying elements of high-Cr ferritic steels with lattice defects: An ab initio study

A. Bakaev¹²³, D. Terentyev¹, G. Bonny¹, T.P.C. Klaver⁴, P. Olsson⁵ and D. Van Neck²

¹ SCK•CEN, Nuclear Materials Science Institute, Boeretang 200, Mol, B2400, Belgium

² Center for Molecular Modeling, Department of Physics and Astronomy, Ghent University, Technologiepark 903, 9052 Zwijnaarde, Belgium

³ Department of Experimental Nuclear Physics K-89, Faculty of Physics and Mechanics, St.Petersburg State Polytechnical University, 29 Polytekhnicheskaya str., 195251, St.Petersburg, Russia

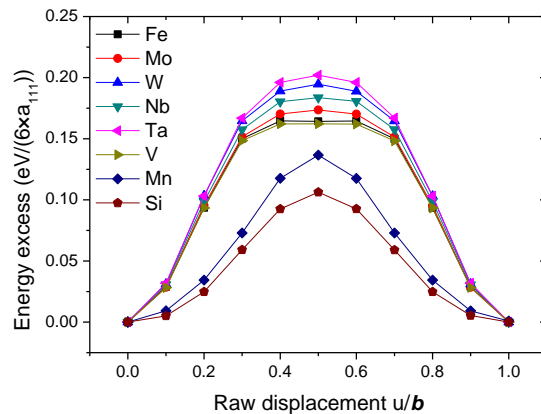
⁴ Department of Materials Science and Engineering, Faculty of 3mE, TU Delft, Mekelweg 2, 2628 CD Delft, The Netherlands

Introduction: Because of its low price and superior mechanical properties, Fe-based alloys are one of the most important and widely used metallic materials. One of the fields of application for ferritic steels is the nuclear sector, which due to large safety margins poses special requirements such as good corrosion resistance, low creep rate, high mechanical yield stress and ductility. It is important that these properties must be preserved upon exploitation in a radiation environment, which is known to cause the degradation of the desired materials properties. The irradiation-induced degradation originates from out-of-equilibrium atomic rearrangement processes that occur by means of radiation induced defects, whose density is much higher than the thermal equilibrium vacancy concentration. Moreover, some of the lattice defects such as self-interstitial atoms and dislocation loops cannot be generated under thermal ageing conditions due to their very high formation energy.

Interstitial impurities and alloying elements (AEs) play a key role in the development of the materials with designed properties. Consequently, the interaction of the steel's alloying elements with radiation defects, efficiency of their mass transport, affinity of the alloying elements to different microstructural units (e.g. grain boundary, free surface, dislocations, etc.) determines their rearrangement in the course of the irradiation process. For example, non-equilibrium segregation of solutes may lead to the formation of unwanted secondary phases or reduce the strength of grain boundaries. Thus, the preservation of the optimum microstructure during high temperature irradiation is essential for the resistance against the degradation of the material's mechanical properties.

In an effort to study the properties of lattice defects at the atomic scale, a few density functional theory (DFT) works have already been devoted to characterize the interaction of the most important elements of ferritic-martensitic steels, i.e. C and Cr. In particular, DFT methods were applied to investigate the properties of point, linear and some planar defects in bcc Fe, FeC and FeCr systems. However, for the other minor alloying elements typically entering high-Cr commercial steels no extended study has been performed yet.

Main results: Electronic structure calculations were performed to consider the interaction of these minor AEs with a number of important and well defined lattice structures, such as point defects, the core structure of a $\frac{1}{2}\langle 111 \rangle$ screw dislocation, high angle symmetric grain boundaries and free surfaces. As the first step, the calculations in pure Fe matrix were performed and Cr was introduced in the dilute limit with the purpose to distinguish and separate contributions of AEs to different radiation-related degradation mechanisms. Additionally, it was provided a full and consistent set of ab initio data to be used for the parameterization and validation of upper-scale atomistic cohesive models for large scale simulations. The correspondence between the obtained DFT data and available experimental data was also discussed.



The variation of the excess energy (normalized over a length of the displaced row and the amount of nearest-neighbor atomic rows (six rows)) versus atomic row displacement (u/b) for a single row of solutes in the Fe matrix.

Conclusions: It was concluded that the refractory alloying elements (Mo, W, Ta and Nb) follow the same trend whereas Mn and Si exhibit peculiar behaviour with respect to the interaction with both point and extended lattice defects.

Future work: Further research can be performed on the rationalization and understanding of the observed systematic trends and some off-trend results (specifically of Mn and Si).

Acknowledgment: This work was performed in the framework of the EFDA project, under grant agreement. We are grateful to the ICT Department of Ghent University for partial support of this work. Part of calculations has been performed at HPC Julich within the 'SORT' project. The research was partly supported by the FWO grant.

Published in: A. Bakaev, D. Terentyev, G. Bonny, T.P.C. Klaver, P. Olsson and D. Van Neck / Journal of Nuclear Materials 444 (2014) 237–246

Application of a three-feature dispersed-barrier hardening model to neutron-irradiated Fe-Cr model alloys

Frank Bergner and Cornelia Heintze, Helmholtz-Zentrum Dresden-Rossendorf, POB 510119, 01314 Dresden, Germany

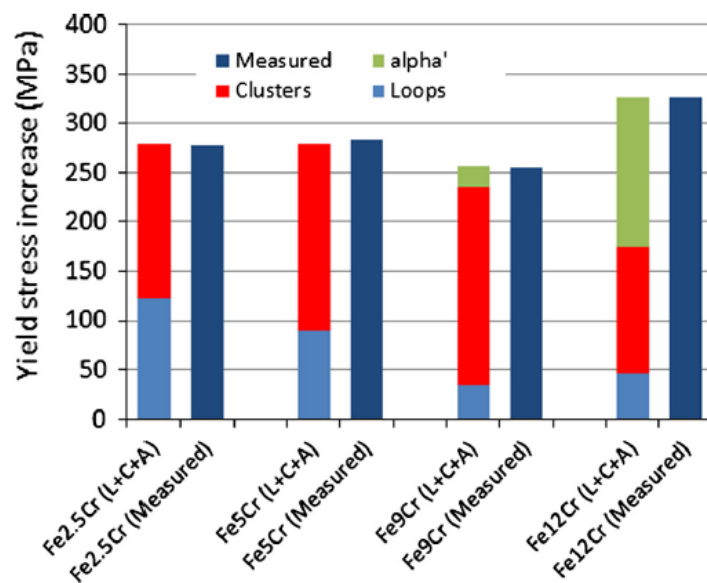
Cristelle Pareige, Groupe de Physique des Matériaux, Université et INSA de Rouen, UMR 6634 CNRS, Avenue de l'Université, BP 12, 76801 Saint Etienne du Rouvray, France

Mercedes Hernández Mayoral, Division of Materials, CIEMAT, Avenida Complutense 22, 28040 Madrid, Spain

Lorenzo Malerba, SCK•CEN, The Belgian Nuclear Energy Research Centre, Institute for Nuclear Materials Science, Structural Materials Group, Boeretang 200, B-2400 Mol, Belgium

Introduction: Industrial-purity Fe-Cr model alloys with nominal Cr contents of 2.5, 5, 9 and 12 wt.% Cr have been neutron irradiated in the BR2 at ~300°C up to 0.06 dpa and subsequently examined by means of transmission electron microscopy (TEM), atom probe tomography (APT), and small-angle neutron scattering (SANS). The former technique revealed a radiation-induced nanostructure characterized by moderate densities of heterogeneously distributed interstitial-type dislocation loops (with the exception of the 2.5 %Cr alloy, where loops were uniformly distributed). The latter techniques revealed the formation of high densities of nanometric NiSiPCr-enriched clusters in all alloys, as well as α' -phase particles in the alloys with highest Cr content (Ni, Si and P were present at the level of impurities). All these features act as obstacles to dislocation glide, leading to an increase of the yield strength measured in tensile tests. Here an attempt is made to quantify the contributions of the different types of features to the total irradiation-induced yield stress.

Main results: The values of the dimensionless obstacle strength are estimated in the framework of a three-feature dispersed-barrier hardening model, according to the Bacon-Kocks-Scattergood (BKS) expression for the yield strength increase due to a dislocation passing through an array of randomly distributed obstacles and using linear superposition for the different classes of obstacles. The results are well summarised in the Figure, which shows that the high density of NiSiPCr clusters can be overall considered the principal contributor to the irradiation hardening in these Fe-Cr alloys, especially for the 9 %Cr alloy.



Decomposition of the measured total yield stress increase (denoted “Measured”) into three individual components.

Conclusions: The three families of obstacles detected by microstructural examination and the hardening model are well capable of reproducing the observed yield stress increase as a function of Cr content, suggesting that the nanostructural features identified experimentally are the main, and probably the only, causes of irradiation hardening in these model alloys. Out of the three features, the contribution to irradiation hardening of the CrNiSiP clusters is prominent.

Future work: The importance of nanometric NiSiPCr clusters invisible to TEM in determining yield strength increase in irradiated Fe-Cr alloys lead both modelling and experimental effort to

focus on the mechanisms leading to their formation, with a view to being able to assess more precisely their effect on dislocation motion. This research is done in the framework of the Mefisto pilot project of the Joint Programme on Nuclear Materials of the European Energy Research Alliance, which is funded by the currently ongoing FP7/MatISSE project

Acknowledgment: The research was partially supported by the EC within the 7th Framework Programme Project GETMAT under Grant Agreement No. 212175.

Published in: F. Bergner, C. Pareige, M. Hernández-Mayoral, L. Malerba, C. Heintze, Journal of Nuclear Materials 448 (2014) 96-102.

RPV steels and model alloys

On the thermal stability of late blooming phases in reactor pressure vessel steels: An atomistic study

G. Bonny¹, D. Terentyev¹, A. Bakaev^{1,2,3}, E.E. Zhurkin³, M. Hou⁴ and L. Malerba¹

¹ SCK•CEN, Nuclear Materials Science Institute, Boeretang 200, B-2400 Mol, Belgium.

² Ghent University, Center for Molecular Modeling, Technologiepark 903, B-9052 Zwijnaarde, Belgium.

³ Saint-Petersburg State Polytechnical University, Experimental Nuclear Physics Department, K-89, Faculty of Physics and Mechanics, 29 Polytekhnicheskaya Str., 195252, St. Petersburg, Russia.

⁴ Université Libre de Bruxelles, Physique des Solides Irradiés et des Nanostructures CP234, Faculté des Sciences, Bd du Triomphe, B-1050 Bruxelles, Belgium.

Introduction:

Radiation-induced embrittlement of bainitic steels is the lifetime limiting factor of reactor pressure vessels in existing nuclear light water reactors. The primary mechanism of embrittlement is the obstruction of dislocation motion produced by nanometric defect structures that develop in the bulk of the material due to irradiation. In view of improving the predictive capability of existing models it is necessary to understand better the mechanisms leading to the formation of these defects, amongst which the so-called "late blooming phases". In this work we study the stability of the latter by means of density functional theory (DFT) calculations and Monte Carlo simulations based on a here developed quaternary FeCuNiMn interatomic potential. The potential is based on extensive DFT and experimental data. The reference DFT data on solute-solute interaction reveal that, while Mn-Ni pairs and triplets are unstable, larger clusters are kept together by attractive binding energy.

Main results:

We developed an interatomic potential for the FeCuNiMn quaternary alloy based on extensive DFT data on solute-solute and solute-point defect interaction, as well as on experimental data, always privileging experimental consistency within the unavoidable series of compromises that have to be made in the fitting process.

The reference DFT data on solute-solute interaction reveal that, while Mn-Ni pairs and triplets are unstable, larger clusters are actually kept together by attractive binding energy. Thus, the formation of thermodynamically stable Mn-Ni-rich phases in Fe is actually possible and this fact is accounted for by the potential, in agreement with Calphad predictions, thereby removing the apparent discrepancy of the latter with DFT, if only pairs and triplets are considered.

The Ni-Mn synergy increases significantly the temperature range of stability of solute atom precipitates in Fe as compared to binary alloys. Cu is found to extend the range of thermodynamic stability of the precipitates even further, thereby explaining the observations of MNPs, and making their appearance possible in RPV steels, even under thermal ageing and in the absence of Si. Nevertheless, under reactor conditions (temperature, composition...), the system will be barely inside the miscibility gap: small variations in temperature and composition will determine significantly different thermodynamic conditions in terms of precipitate stability, making the production of sufficient volume fractions of these phases to observe a late blooming effect rather elusive. It is therefore speculated that the appearance of Mn-Ni-rich precipitates under irradiation, irrespective of their thermodynamic stability, is actually made

kinetically possible by the massive fluxes of point-defects and by point-defect cluster formation, that are strictly the consequence of irradiation.

The mechanism leading to the formation of the so-called late blooming phases, or more correctly Mn-Ni-rich clusters (with inclusion or not of point-defects), as well as their actual thermodynamic stability under reactor conditions, are assumed to influence their strength as obstacles to dislocation motion, thereby determining (or not) a visible change in the mechanical response of the material after their appearance. The interatomic potential presently developed is expected to contribute significantly to unravel these still open issues.

Conclusions:

The NiMnCu synergy is found to increase the temperature range of stability of solute atom precipitates in Fe significantly as compared to binary FeNi and FeMn alloys. This allows for thermodynamically stable phases close to reactor temperature, the range of stability being very sensitive to composition.

Future work:

The developed potential is used to model AKMC and MD simulations within the SMM group.

Acknowledgment:

PERFORM60 / HELIOS HPC Japan

Published as: G. Bonny et al., Journal of Nuclear Materials 442 (2013) 282.

Monte Carlo study of decorated dislocation loops in FeNiMnCu model alloys

G. Bonny¹, D. Terentyev¹, E.E. Zhurkin² and L. Malerba¹

¹ *SCK•CEN, Nuclear Materials Science Institute, Boeretang 200, B-2400 Mol, Belgium*

² *Saint-Petersburg State Polytechnical University, Experimental Nuclear Physics Department, K-89, Faculty of Physics and Mechanics, 29 Polytekhnicheskaya Str., 195252, St. Petersburg, Russia*

Introduction:

Radiation-induced embrittlement of bainitic steels is the lifetime limiting factor of reactor pressure vessels in existing nuclear light water reactors. The primary mechanism of embrittlement is the obstruction of dislocation motion by nano-metric defects in the bulk of the material due to irradiation. Such features are known to be solute clusters that may be attached to point defect clusters. In this work we study the thermal stability of solute clusters near edge dislocation lines and loops with Burgers vector $b=\frac{1}{2} [111]$ and $b=[100]$ in FeNiMnCu model alloys by means of Metropolis Monte Carlo simulations.

Main results:

In this work we studied the thermal stability of solute clusters near edge dislocation lines and loops in FeMn, FeNi, FeCu, FeNiMn and FeNiMnCu alloys. We found that the solutes precipitate as bcc Mn, B2 FeNi, bcc Cu, B2 MnNi and bcc random NiMnCu solid solutions in the respective alloys. All phases precipitate in the compressed region of the lattice defects, except for Cu, which precipitates in the tensile region.

All precipitated phases, except for Mn and Cu, show affinity towards the dislocation-type defects, in terms of a strong decrease in the solubility limit compared to the situation without

defect. Small (2 nm) loops yield a stronger affinity than the edge dipoles, and defects with $b=[100]$ a stronger affinity than those with $b=\frac{1}{2}[111]$.

Conclusions:

It is concluded that small dislocation loops may indeed act as points for heterogeneous nucleation of solute precipitates in reactor pressure vessel steels and increase their thermodynamic stability up to and above normal reactor operating temperatures. We also found that, in the presence of dislocation-type defects, the Ni content determines the thermodynamic driving force for precipitation, rather than the Mn content.

Future work:

The present results are used to study the hardening by decorated loops by means of MD within the SMM group.

Acknowledgment:

PERFORM60 / JPNM / EERA

Published as: G. Bonny et al., Journal of Nuclear Materials 452 (2014) 486.

Post-irradiation annealing behavior of neutron-irradiated FeCu, FeMnNi and FeMnNiCu model alloys investigated by means of small-angle neutron scattering

Frank Bergner and Andreas Ulbricht, Helmholtz-Zentrum Dresden-Rossendorf, POB 510119, 01314 Dresden, Germany

P. Lindner, Institut Laue-Langevin Grenoble, BP 156, 38042 Grenoble Cedex 9, France

U. Keiderling, Helmholtz-Zentrum Berlin, Hahn-Meitner-Platz 1, 14109 Berlin, Germany

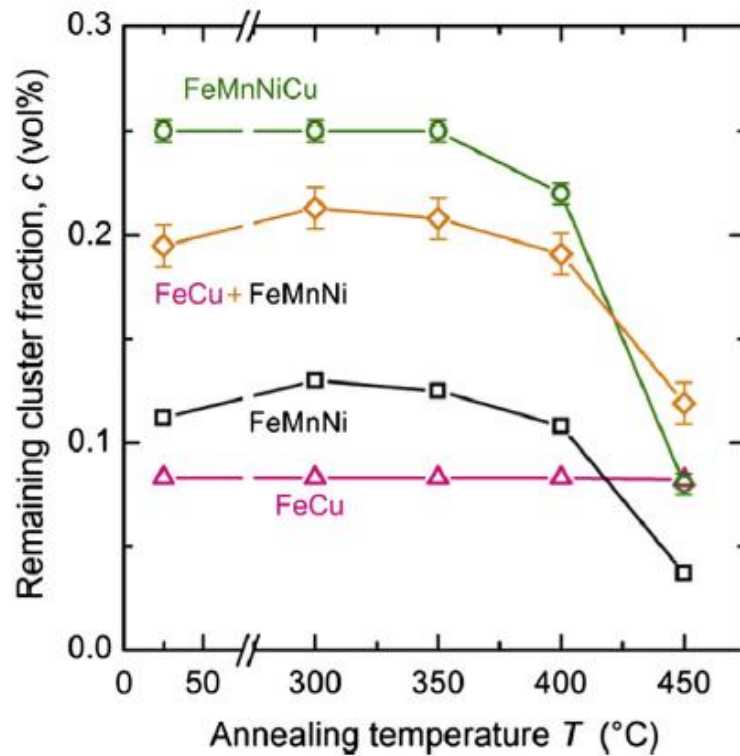
Lorenzo Malerba, SCKCEN, The Belgian Nuclear Energy Research Centre, Institute for Nuclear Materials Science, Structural Materials Group, Boeretang 200, B-2400 Mol, Belgium

Introduction: Neutron irradiation of reactor pressure vessel steels gives rise to the formation of thermodynamically stable and unstable nano-features. The present work is focused on the stability of Cu-, Mn- and Ni-containing solute clusters in model alloys exposed to post-irradiation annealing. Fe_{0.1}Cu, Fe_{1.2}Mn_{0.7}Ni and Fe_{1.2}Mn_{0.7}Ni_{0.1}Cu (wt%) model alloys irradiated up to neutron exposures of 0.1 and 0.19 dpa (displacements per atom) were annealed at stepwise increasing temperatures in the range from 300 degrees C (i.e. near irradiation temperature) to 500 degrees C and characterized by means of small-angle neutron scattering (SANS).

Main results: While the volume fraction of Cu precipitates produced under irradiation remains unaffected by annealing up to 450°C, the neutron scatterers produced by irradiation in presence of Mn and Ni, most likely Mn-Ni-rich clusters, show a clear trend to disappearance between 400 and 450°C. An analysis of the size distribution reveals a weak tendency to coarsening during dissolution. It is noteworthy that the volume fraction of scatterers in FeCuMnNi is higher than the sum of the volume fractions in FeCu and in FeMnNi, pointing to clear synergistic effects, namely to the fact that the presence of Cu enhances also the precipitation of Ni-Mn (and/or viceversa). This is illustrated in the figure, that refers to the annealing of specimens irradiated to 0.1 dpa.

Conclusions: The study revealed that the variety of defect-solute clusters formed in Fe-based model alloys upon irradiation mostly dissolve upon annealing at increasing temperatures

according to their thermodynamic stability. Mn–Ni-enriched clusters dissolve completely between 400 and 500 °C. In the same temperature range, the Ni-rich shells of Ni–Cu-rich clusters are removed from the Cu-rich cores, whereas the latter behave like Cu-rich clusters in binary Fe–Cu alloys with the options to dissolve or coarsen... ..



Cluster fraction in vol% as a function of the annealing temperature for the 0.1-dpa irradiations in the different alloys.

Future work: At the moment there are no plans to extend this work, especially because there are no more specimens available.

Acknowledgment: This work was supported within by the 7th Framework Programme Project PERFORM60 under Grant Agreement No. FP7-232612..

Published in: F. Bergner *et al.*, Journal of Nuclear Materials 454 (2014) 22-27.

Synergetic effects of Mn and Si in the interaction with point defects in bcc Fe

A. Bakaev^{abcd}, D. Terentyev^a, X.He^d, D. Van Neck^b

^a SCK-CEN, Nuclear Materials Science Institute, Boeretang 200, Mol B2400, Belgium

^b Center for Molecular Modeling, Department of Physics and Astronomy, Ghent University, Technologiepark 903, 9052 Zwijnaarde, Belgium

^c Department of Experimental Nuclear Physics, Institute of Physics, Nanotechnologies and Telecommunications, St. Petersburg State Polytechnical University, 29 Polytekhnicheskaya Str., 195251 St. Petersburg, Russia

^d China Institute of Atomic Energy, PO Box 275-51, 102413 Beijing, China

Introduction: Fe-Cr-based ferritic steels are considered as candidate materials for Generation IV and fusion installations. Radiation induced degradation of high-Cr ferritic steels is an important factor limiting the temperature window for applications and the operational time span. A series of recent works, where the post irradiation experimental analysis of several Fe-Cr model alloys has been performed, reveal the numerous formation of Cr-Si clusters (also containing Ni and P but in less quantities than Cr and Si) with a number density of 10^{23} m^{-3} and mean radius of $\sim (1.5-2.5) \text{ nm}$, which can not be classified as α' precipitates because of too low Cr content in them. Radiation induced segregation is most likely to be responsible for their formation as the composition of Si in the considered alloys is less than 0.5 at.% i.e. far below its solubility limit in Fe at 300 °C of 10 at.%.

Although the content of Mn (well below the solubility limit in α -Fe at 300°C) and Si in high-Cr steels is rather low (up to 0.5 wt.%), atom probe studies performed in irradiated commercial ferritic-martensitic steels revealed formation of Mn-Si clusters (also containing Ni) with a similar density and size. The scenario by which these clusters are formed and how they contribute to hardening in high-Cr steels is so far unclear. Assuming that radiation induced/enhanced segregation is responsible for the occurrence of the above discussed solute-rich clusters, investigation of the interaction of these solutes with point defects (PDs) is the first step.

The interaction of multiple solute-PD clusters involving Mn, Si and Cr (the latter being the major alloying element in high-Cr steels) has not been studied so far. Here, we perform a dedicated *ab initio* study looking for a possible synergy between Mn, Si and Cr simultaneously interacting with PDs attempting to provide some evidence of the enhanced Mn-Si or Cr-Si binding, following the evidence from the above mentioned experiments. Given that in Fe-Cr-Mn-Si alloys the formation of mixed Fe-Cr and Fe-Mn dumbbells is energetically favourable, the interaction of the mixed SIAs with an isolated Mn or Si atom and with Mn-Si pairs is also addressed to highlight the possible trapping effect originating from the multiple solute-PD interaction.

Main results: It was performed a dedicated *ab initio* study looking for a possible synergy between Mn, Si and Cr simultaneously interacting with PDs attempting to provide some evidence of the enhanced Mn-Si or Cr-Si binding, following the evidence from the above mentioned experiments. Given that in Fe-Cr-Mn-Si alloys the formation of mixed Fe-Cr and Fe-Mn dumbbells is energetically favourable, the interaction of the mixed SIAs with an isolated Mn or Si atom and with Mn-Si pairs is also addressed to highlight the possible trapping effect originating from the multiple solute-PD interaction.



Distribution of charge density around a $\langle 110 \rangle$ split dumbbell in a eight atom bcc cell. Isosurfaces of $0.55 \text{ e}^-/\text{\AA}^3$ are shown. The color of the atom refers to its type: red-Fe, black-Mn, white-Si. (a) and (b) figures correspond to FeMn($\langle 110 \rangle$ dumbbell) and FeMn($\langle 110 \rangle$ dumbbell)+Si(C2) complexes.

Conclusions: The study has revealed that the interaction energy for a self-interaction with the Mn-Si pair varies from ~ 0.1 - 0.8 eV and strongly depends on the local solute arrangement. The strongest binding was observed between an FeFe dumbbell and the 1st Mn-Si pair, which amounted to 0.78 eV. Based on the analysis of the charge density maps and local magnetic moments, the origin of the strong Mn-Si-self interstitial interaction is attributed to the compensation of the magnetic moments of Fe atoms surrounding the dumbbell, occurring due to the perturbation caused by the insertion of diamagnetic Si in ferromagnetic Fe matrix. It was also concluded that the synergetic interaction of Mn-Si with point defects (not involving Cr), might be responsible for the nucleation of radiation-induced solute-rich complexes associated with growing clusters of point defects.

Future work: Further research can be performed on the identification of the role of interstitial carbon and other solutes such as e.g. Ni and P to complete a complex picture on the elementary interaction of point defects with solutes in Fe-based ferritic steels.

Acknowledgment: This work, supported by the European Commission under the Contract of Association between EURATOM/SCK-CEN, was carried out within the framework of the European Fusion Development Agreement. We are grateful to the ICT Department of Ghent University for partial support of this work. Part of calculations has been performed at HPC Julich within the 'SORT' project. The research was partly supported by the FWO grant.

Published in: A. Bakaev, D. Terentyev, X.He, D. Van Neck / Journal of Nuclear Materials 455 (2014) 5–9

Austenitic steel and alloys

Effect of liquid metal embrittlement on low cycle fatigue properties and fatigue crack propagation behavior of a modified 9Cr-1Mo ferritic-martensitic steel in an oxygen-controlled lead-bismuth eutectic environment at 350°C

Xing Gong^{1,2}, Pierre Marmy¹, Ling Qin², Bert Verlinden², Martine Wevers², Marc Seefeldt²
¹ SCK•CEN (Belgian Nuclear Research Centre), Boeretang 200, B-2400 Mol, Belgium
² KU Leuven, Department of Metallurgy and Materials Engineering, Kasteelpark Arenberg 44, Box 2450, B-3001 Heverlee, Belgium

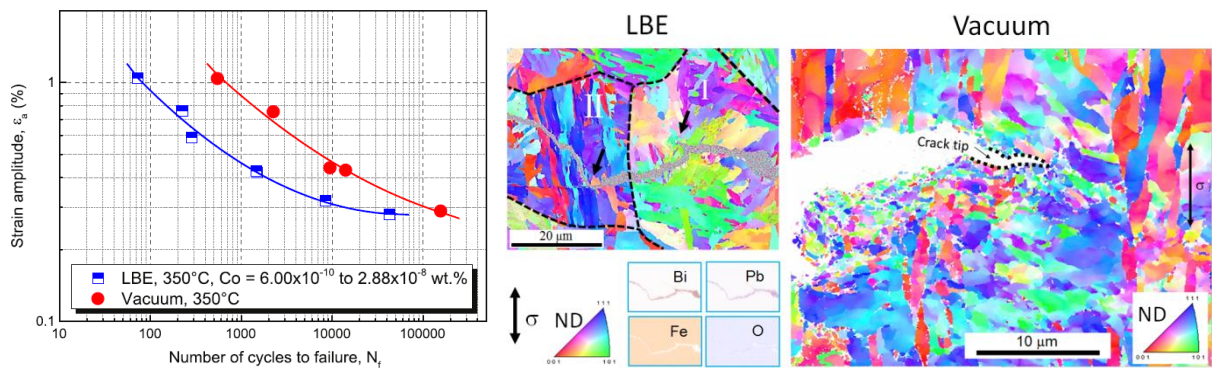
Introduction: The modified 9Cr-1Mo ferritic-martensitic steel (T91) is a promising material for liquid metal cooled Generation IV nuclear reactors. It has been selected as a candidate material to construct the proton beam window of the accelerator driven system (ADS) based MYRRHA reactor, which will use liquid lead-bismuth eutectic (LBE) as a coolant and a spallation target, and is currently being developed at SCK•CEN, Belgium. To secure the operation of the reactor, a detailed assessment on the compatibility of the material with the liquid metal environment is crucial. It has been demonstrated that liquid metal embrittlement (LME), a phenomenon resulting in premature brittle failure of a metallic material, can occur in T91 steel when stressed in LBE over a wide range of experimental conditions. For instance, Auger and Lorang found that the susceptibility of T91 steel to LME was markedly increased after the removal of native oxides from the steel surface. Plane strain fracture toughness tests on T91 steel in LBE at 200 and 300°C showed a decrease of 16 to 30% in fracture toughness compared to air. Dai et al discovered that microcracks on the surface of T91 steel increased the LME susceptibility and the embrittlement usually occurred after necking. They finally concluded that the requirements to involve the LME effect are surface cracks or flaws, wetting and stress concentrators at crack tips. More recently, using a Small Punch Test (SPT) technique, Ye et al investigated the influence of loading rate and oxygen content in LBE on the LME susceptibility of T91 steel at 200 to 400°C. They found that LME appeared even in oxygen-saturated LBE when low strain rates were applied. Moreover, low oxygen content in LBE and an increase in temperature intensified the LME effect. They also stated that strain rate was a critical parameter to observe LME in the T91/LBE system. The main prerequisites for the occurrence of LME are wetting, tensile stress, stress concentrators and significant plastic deformation. However, the underlying LME mechanism for the T91/LBE system is still not clear, limiting a quantitative prediction of LME risks. One of the barriers to a clear understanding of the mechanism is the complexity of the microstructure of T91 steel. For instance, it has even been debated whether the typical fracture occurring in the presence of LBE is cleavage but with some ductile features, or just pure boundary cracking. Most investigators described such ambiguous fracture features as being a kind of quasi-cleavage failure but without showing reliable evidence. Nevertheless, M.L. Martin and S. Hemery and their co-workers obtained interesting results based on transmission electron microscopy (TEM) observations of some secondary cracks of T91 steel embrittled by LBE, liquid indium and liquid sodium under monotonic loading. They concluded that intergranular cracking at martensite lath boundaries and prior-austenite grain boundaries is the main LME mechanism in T91 steel. This conclusion contradicts the traditional opinion that LME-induced cracking in T91 steel should be transgranular quasi-cleavage, but their experimental results enlighten that the identification of the crack propagation modes might be a necessary step to understand the LME phenomenon occurring in the T91/LBE system under low cycle fatigue.

In general, environmentally-assisted fatigue is one of the most important origins of mechanical damage of structural materials. Sufficient attention should be paid to this issue. Previous

investigations on low cycle fatigue properties of T91 steel and another ferritic martensitic steel (10.5Cr-steel Manet-II) in an oxygen-saturated LBE respectively at 300°C and 260°C showed that LME severely shortened the fatigue lives of the two steels by a factor of 3 to 7 at high strain amplitudes compared to those in air. A mechanism about the effect of LME on nucleation and propagation of surface cracks was proposed. It was stated that due to liquid metal wetting, the resistance of grain boundaries to crack propagation is substantially diminished. As a result, once the first crack is initiated at the specimen surface, it can propagate fast into the bulk and the stress loading to the remaining sample is reduced. This leads to little chance for other surface cracks to nucleate and grow. However, these two studies didn't explicitly describe how fatigue cracks propagate and the underlying LME mechanism still remains contentious. In addition, it has been reported that oxide films on the steel surface inhibit both liquid metal wettability and susceptibility to LME. In this regard, it is of great interest to study the fatigue properties of T91 steel in a low oxygen or even an oxygen-depleted LBE environment in order to maximize the LME effect. Indeed, this issue has not been extensively investigated due to a lack of reliable oxygen sensors to measure the oxygen concentration in LBE. The effect of LME on the morphology of secondary cracks formed at the fracture surface under cyclic loading was not studied in the literature as well, although it might bring some useful information for a better understanding of the LME mechanism.

The present study investigated the fatigue properties of T91 steel in a low oxygen concentration or oxygen-depleted LBE environment at 350°C and compared them with a vacuum environment at the same temperature. The effect of LME on the fatigue crack propagation and secondary cracking behavior was explored. Particular attention was paid to reveal the fatigue crack propagation modes in LBE and to examine the modifications of the bulk microstructure along the crack path in vacuum, by means of scanning electron microscopy (SEM) and the EBSD technique. A qualitative LME mechanism, in terms of a moderate weakening in atomic cohesion of a solid metal by adsorption of liquid metal atoms, is proposed to account for the LME phenomenon in the T91/LBE system. The different secondary cracking behaviors observed in LBE and in vacuum are also explained by the effect of LME on the behavior of the main fatigue crack tip.

Main results: The fatigue lives of T91 steel in a low oxygen concentration LBE are drastically reduced compared to those in vacuum due to the presence of LME. The microstructural observations on the fatigue crack propagation modes show that fatigue cracks in LBE mainly propagate across prior-austenite grain boundaries and then cut through martensitic lath boundaries. Intergranular and interlath cracking occur occasionally and their occurrence depends on the orientation of the boundaries relative to the stress axis. The complexity of the LME-induced fracture features can be attributed to a mixture of the multiple failure modes. Using a high resolution electron backscatter diffraction (EBSD) technique, highly localized plastic shear strain was observed in the vicinity of the crack tips in vacuum, manifested by the presence of very fine subgrains along the crack walls. This grain refinement phenomenon is not observed in the specimens tested in LBE.



Fatigue data of T91 steel in LBE and vacuum at 350°C; comparison of microstructure near the cracks after testing in LBE and in vacuum.

Conclusions: T91 steel is susceptible to LBE embrittlement under low cycle fatigue, evidenced by a drastic reduction of the fatigue endurance in the presence of LBE, compared to vacuum. Martensitic lath boundaries do not necessarily act as the preferred paths for the LME cracks to propagate along and the boundary decohesion depends on the orientation of the boundaries with respect to the loading axis. The crack tip plasticity is reduced by LME, since there is no grain refinement near the crack after testing in LBE, contrary to the case tested in vacuum where substantial grain refinement is visible.

Acknowledgments: The work is financially supported by the MYRRHA project, SCK•CEN, Belgium, and partly funded by the European Atomic Energy Community's (Euratom) Seventh Framework Programme FP7/2007-2013 under grant agreement No. 604862 (MatisSE project) and in the framework of the EERA (European Energy Research Alliance) Joint Programme on Nuclear Materials. Mr. Tom Van der Donck (MTM, KU Leuven) is acknowledged for the EBSD measurements. Dr. Serguei Gavrilov and Dr. Erich Stergar (SCK•CEN) are greatly thanked for valuable discussion.

Published in: Xing Gong, Pierre Marma, Ling Qin, Bert Verlinden, Martine Wevers, Marc Seefeldt /Materials Science and Engineering A, 618(2014)406–415.

Corrosion scales on various steels after exposure to liquid lead–bismuth eutectic

K. Lambrinou, V. Koch, G. Coen, J. Van den Bosch, C. Schroer

¹*SCK•CEN, Nuclear Materials Science Institute, Boeretang 200, B-2400 Mol, Belgium.*

Introduction

Recently, significant progress beyond the state-of-the-art understanding of the dissolution corrosion behaviour of austenitic stainless steels was achieved at SCK-CEN. This progress started with a well-designed series of corrosion tests in oxygen-poor static LBE on specimens of the 316L austenitic stainless steel, which is the candidate MYRRHA structural steel. The aim of these tests was to understand the 316L steel dissolution corrosion behaviour as a function of the exposure conditions (temperature, time, and amount of dissolved oxygen in the liquid LBE)

and the steel microstructure. For this purpose, five different 316L austenitic stainless steel heats were exposed to oxygen-poor static LBE in the 350-550°C temperature range, for different exposure times (253-5862 h). Testing was followed by a detailed characterisation of the corroded steel specimens by means of light optical microscopy (LOM), scanning electron microscopy (SEM), energy-dispersive X-ray spectrometry (EDS), electron backscatter diffraction (EBSD), focused ion beam (FIB), transmission-EBSD (t-EBSD) and transmission electron microscopy (TEM).

Main results

This study showed that the time dependence of dissolution damages was linear, while the temperature dependence of the same damages was governed by a power law. Knowing the time and temperature dependence of dissolution damages in 316L austenitic stainless steels allows for a rather confident prediction of the long-term corrosion behaviour of these steels in service. Another finding of high practical importance was that the steel corrosion response is strongly affected by the steel microstructure, which is in turn associated with the steel thermo-mechanical history. This finding must be taken into account when defining the specifications of the structural steels that are suitable for use in LBE-cooled nuclear systems, as it should be possible to limit the inherent steel susceptibility to LBE dissolution attack by controlling the steel manufacturing process. Steel microstructural features that affect the steel corrosion response include the grain size distribution, the density of deformation twin boundaries (formed during steel cold drawing) and various steel precipitates (oxides, sulphides, δ -ferrite).

Published in: Journal of Nuclear Materials, Volume 450, Issues 1–3, July p. 244-255 (2014).

Interatomic potential to study aging under irradiation in stainless steels: the FeNiCr model alloy

G. Bonny¹, N. Castin¹ and D. Terentyev¹

¹*SCK•CEN, Nuclear Materials Science Institute, Boeretang 200, B-2400 Mol, Belgium.*

Introduction:

The degradation of austenitic stainless steels in a radiation environment is a known problem for the in-core components of nuclear light water reactors. For a better understanding of the prevailing mechanisms responsible for the materials degradation, large-scale atomistic simulations are desirable. In this framework we developed an embedded atom method type interatomic potential for the ternary FeNiCr system to model the production and evolution of radiation defects. Special attention has been drawn to the Fe₁₀Ni₂₀Cr alloy, whose properties were ensured to be close to those of 316L austenitic stainless steels. The potential is extensively benchmarked against density functional theory calculations and the potential developed in our earlier work. As a first validation, the potential is used in AKMC simulations to simulate thermal annealing experiments to determine the self-diffusion coefficients of the components in FeNiCr alloys around the Fe₁₀Ni₂₀Cr composition.

Main results:

We have developed an EAM type interatomic potential (EAM-13) for the ternary FeNiCr system to model the microstructural evolution of radiation defects. Special attention has been drawn to the Fe10Ni20Cr alloy, whose properties were ensured to be close to those of 316L austenitic stainless steels. In particular, the stacking fault energy and vacancy formation energy are well reproduced while the values for the elastic constants are acceptable. The potential predicts a stable fcc phase in the complete concentration range and provides excellent agreement of point-defect solute interaction in the fcc Ni matrix. In addition, stable glide of edge and screw dislocation and stability of Frank loops in the Fe10Ni20Cr alloy were verified.

Compared to EAM-11, a significant improvement was realized with respect to point defect properties at the cost of the elastic constants that are less consistent with experimental observations. With respect to interstitial loops and dislocations, the present potential provides qualitatively similar results to EAM-11.

Thus, for the study of interactions between dislocations and radiation defects EAM-11 is a priori more suitable, even though the present potential is also capable of tackling such type of simulations. For the study of formation and evolution of point-defects, e.g., collision cascades, AKMC simulations, etc., the present potential is recommended, as EAM-11 has some essential shortcomings related to vacancy/interstitial solute interactions.

Conclusions:

As a first validation, the potential is used in AKMC simulations to simulate thermal annealing experiments to determine the self-diffusion coefficients of the components in FeNiCr alloys around the Fe10Ni20Cr alloy. The results from these simulations are consistent with experiments, i.e., $D_{Cr} > D_{Ni} > D_{Fe}$ and the self-diffusion coefficient increases with Ni and decreases with Cr content. The present results suggest that the developed potential is suitable to study the defect production (i.e. collision cascades) and evolution in an alloy with properties close to 316L steels.

Future work:

The developed potential is used to model AKMC and MD simulations within the SMM group.

Acknowledgment:

PERFORM60 / HELIOS HPC Japan

Published as: G. Bonny et al., Modelling and Simulation in Materials Science and Engineering 21 (2013) 085004

Energetics of radiation defects in Fe-based austenitic alloys: Atomic scale study

A. Bakaev^{abd}, D. Terentyev^{ad}, X. He^c, E.E. Zhurkin^d

^a SCK•CEN, Boeretang 200, Mol, B2400, Belgium

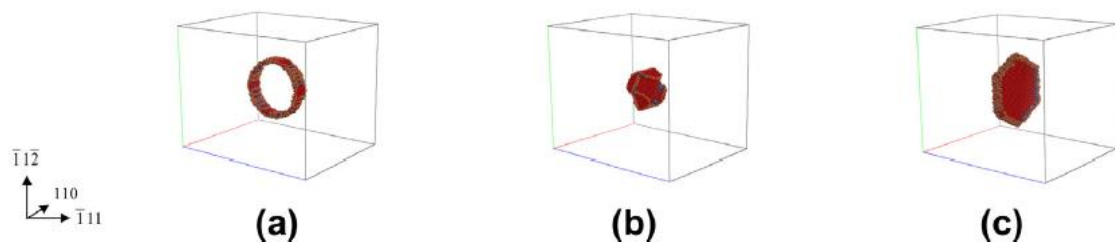
^b Center for Molecular Modeling, Department of Physics and Astronomy, Ghent University, Technologiepark 903, 9052 Zwijnaarde, Belgium

^c China Institute of Atomic Energy, 275-51 Xinzhen, Fangshan, Beijing, 102413, China

^d Department of Experimental Nuclear Physics K-89, Faculty of Physics and Mechanics, St.Petersburg State Polytechnical University, 29 Polytekhnicheskaya str., 195251, St.Petersburg, Russia

Introduction: Iron-based materials such as austenitic steels are important for many structural applications requiring high strength and good ductility, such as components in nuclear and fusion setups. With this respect, a good resistance against irradiation is another important requirement for such kind of materials. Neutron irradiation causes a certain degradation of the mechanical properties in these steels due to the production of radiation defects that are mainly dislocation Frank loops of self-interstitial (SIA) kind. Free energy of lattice defects depends on its size, morphology and ambient temperature. Thus, the knowledge of the defect formation energy vs. its size allows one to predict the morphology and structure of the defects generated under neutron irradiation.

Main results: The aim of the present work is to perform atomistic numerical calculations to compute the formation energy of different radiation defects (such as SIA and vacancy Frank loops, perfect dislocation loops, stacking fault tetrahedron (SFT) and voids) with size up to 12 nm (i.e. well resolvable in transmission electron microscopy) at zero temperature ($T=0$ K) in the random $\text{FeNi}_{10}\text{Cr}_{20}$ FCC alloy, which is used as a model for austenitic steel of 304L type. To do that, we employ a classical molecular dynamics (MD) and static (MS) simulations. The latter are performed using a set of recently developed interatomic potentials specifically derived to reproduce main features of 304L steel. A comparison of the obtained formation energy with the prediction according to the elasticity theory for vacancy type defects in FCC materials is also performed. In addition, we also study thermal stability of the examined defects by means of annealing modelled using MD simulations in the temperature range 300-1200 K.



Visualizations of final configurations of the defects: (a) interstitial circular perfect loop $d = 9.8$ nm; (b) vacancy hexagonal Frank loop $d = 5.0$ nm with the sides along $\langle 110 \rangle$ directions; (c) vacancy hexagonal Frank loop $d = 12.1$ nm with the sides along $h112i$ directions. The orientation of the crystal is the same in all figures

]

Conclusions: The formation energy of these defects has been calculated at 0 K and the obtained results have been compared with the prediction of the elasticity theory. A good agreement has been found in all the cases except for the hexagonal Frank loop, whose sides have splitted into $1/6\langle 112 \rangle$ partial dislocations, thus lowering the total formation energy. High temperature annealing, performed using molecular dynamics simulations, has proven that the considered defects are thermally stable in the temperature range 300-1200 K.

Acknowledgment: The author thanks FWO-Vlaanderen for their financial support. The research was partially supported by the European seventh Framework Program, under “PERFORM 60” project.

Published in: A. Bakaev, D. Terentyev, X. He, E.E. Zhurkin / Nuclear Instruments and Methods in Physics Research B 303 (2013) 33–36

Interaction of a screw dislocation with Frank loops in Fe-10Ni-20Cr alloy

D. Terentyev^a and A. Bakaev^{abc}

^a SCK•CEN, Boeretang 200, Mol, B2400, Belgium

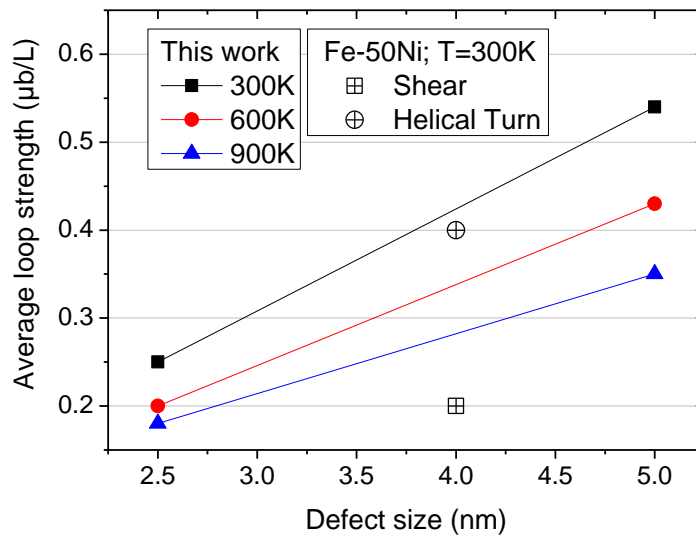
^b Center for Molecular Modeling, Department of Physics and Astronomy, Ghent University, Technologiepark 903, 9052 Zwijnaarde, Belgium

^c Department of Experimental Nuclear Physics K-89, Faculty of Physics and Mechanics, St.Petersburg State Polytechnical University, 29 Polytekhnicheskaya str., 195251, St.Petersburg, Russia

Introduction: Irradiation of structural steels for nuclear applications by neutrons throughout the lifecycle causes modification of the crystal microstructure resulting in the formation of black dots, dislocation loops and voids. These defects act as obstacles to dislocation glide, thereby causing hardening and consequently embrittlement, thus limiting the functional lifespan of a setup. Frank loops-dislocation interaction in pure FCC metals (in Cu and Ni) has been studied by MD simulations already. A systematic study performed by Nogaret et al. has revealed several mechanisms depending on the interaction geometry and an impinging dislocation character, namely: (i) loop shear; (ii) unfault into glissile configuration; (iii) absorption into a glissile superjog (on edge dislocation) or into a sessile helical turn (on a screw dislocation). Absorption into a helical turn results in especially high unpinning stress and thus is expected to be the main source of hardening. For both screw and edge dislocations the unfauling mechanism is controlled by the cross-slip process. In general, the number of geometrical configurations leading to loop unfauling is higher for a screw dislocation. Hence, the interaction with screw dislocations most likely determines both the hardening and the formation free channels.

An important drawback of the recently applied model on the basis of Fe-Ni was a strong variation of stacking fault energy (SFE) depending on local atomic arrangement. Even though the average SFE value in Fe-50Ni is 19 mJ/m² the width of the distribution is about ± 50 mJ/m². It is therefore possible that the strong local variation of SFE does not allow for the formation of extended constrictions even at relatively high level of applied shear stress while the FL is in contact with dislocation during the interaction process. The origin of the strong SFE variation is related to a tiny balance in the stability of FCC relative to BCC phase. To overcome this problem, a new Fe-Ni-Cr potential has been developed by utilizing FCC phase as a ground state for Fe, Ni and Cr. By doing that the full stability of FCC phase and smooth evolution of SFE, in a close agreement with the CALPHAD database, were ensured in the whole composition range. In addition, the potential was specifically developed to mimic elastic properties of 316 austenitic steels for 'target composition' i.e. Fe-10Ni-20Cr and was parameterized using a wide range of data including some obtained by *ab initio* calculations and from experiments.

Main results: The results reveal a number of interaction mechanisms depending on loop orientation and ambient temperature. Half of the observed reactions lead to loop unfauling despite a low SFE of the alloy. The unfauling reactions are enhanced with temperature and the critical stress for the unfauling is regularly higher in comparison with the loop shear interaction.



Average τ_c measured for FLs in this work compared with average τ_c for loop shear and emission of a helical turn measured in Fe-50Ni at 300K.

Conclusions: By comparing present results with a recent study done in a low SFE Fe-50Ni alloy, the study has revealed that a magnitude of local variation of SFE is an important factor controlling the formation of dislocation constrictions. In the Fe-50Ni alloy, characterized by strong variations of local SFE, the constrictions are almost never observed so that the loop shear interaction prevails, while absorption is rare. In the Fe-10Ni-20Cr alloy, characterized by small variations of local SFE, the constrictions are regularly formed resulting in frequent loop unfaulting.

Acknowledgment This work was performed in the framework of the EC-funded FP7/PERFORM60 project, under grant agreement 232612. Part of calculations has been performed at HPC Julich within the 'SORT' project. The research was partly supported by the FWO grant.

Published in: D. Terentyev, A. Bakaev / Journal of Nuclear Materials 442 (2013) 208–217

Interaction of dislocations with Frank loops in Fe-Ni alloys and pure Ni: An MD study

D. Terentyev¹, A. Bakaev^{1,2} and Yu.N. Osetsky³

¹ SCK-CEN, Nuclear Material Science Institute, Boeretang 200, B-2400 Mol, Belgium

² Center for Molecular Modeling, Department of Physics and Astronomy, Ghent University, Technologiepark 903, 9052 Zwijnaarde, Belgium

³ Materials Science and Technology Division, ORNL, Oak Ridge, TN 37831, USA

Introduction: Plasticity of metals and metallic alloys is known to be controlled by the movement of dislocations. Irradiation of metals, metallic alloys and steels by energetic particles causes modification of the crystal microstructure resulting in the formation of new lattice defects such as precipitates, dislocation loops and voids. These defects act as obstacles to

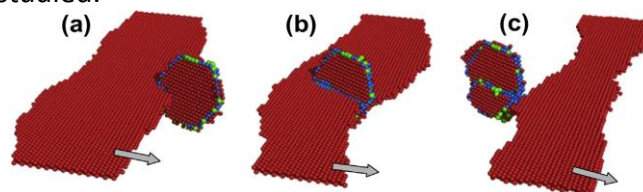
dislocation glide, thereby causing hardening and consequently embrittlement. In the case of neutron irradiation (of structural and in-core reactor components at temperature below $0.3T_M$), the matrix damage created is composed mainly of dislocation loops. Interaction of moving dislocations with loops is therefore an important contribution to plastic deformation mechanisms in irradiated crystalline materials, as was directly revealed by transmission electron microscopy studies.

In FCC metals, alloys and austenitic stainless steels, which are subject of the present work, both faulted Frank loops (FLs) with Burgers vector (BV) $1/3\langle 111 \rangle$ and perfect unfaulted loops with BV $1/2\langle 110 \rangle$ form under irradiation. Due to the low stacking fault energy (SFE) of austenitic alloys, FLs are a major component of the microstructure formed under neutron irradiation. The interaction of FLs with dislocations has already been studied by Molecular Dynamics (MD) simulations in pure FCC Ni and Cu. A systematic study performed by Nogaret et al. has revealed several mechanisms depending on the interaction geometry and impinging dislocation character. The following three mechanisms have been identified: (i) loop shearing; (ii) loop unfauling into glissile configuration; (iii) loop absorption into glissile superjogs (on edge dislocations) or helical turns (on screw dislocations). For both screw and edge dislocations the unfauling mechanism is controlled by a cross-slip process. In general, the number of geometrical configurations leading to loop unfauling is higher for a screw dislocation.

In the case of a screw dislocation two distinct unfauling mechanisms have been revealed: (i) the formation of a D-Shockley partial dislocation segment, which sweeps the fault. The sweeping is accommodated by cross-slip of the dislocation around the loop. (ii) Cross-slip of the dislocation, formation of a constriction and its re-dissociation in the loop habit plane. Then, two partials remove the fault. Both of these mechanisms require the formation of constrictions and propagation of dislocations in the secondary glide planes. Note that cross-slip dislocation movement, also occurring by means of the constriction formation and being directly related to SFE of a material, plays a crucial role in the process of work hardening.

The previous studies were performed for pure Ni and Cu, due to the lack of reliable interatomic potentials for austenitic steels (i.e. Cu has relatively low SFE but also too low shear modulus, while Ni has comparable shear modulus but very high SFE). Recently, however, an Fe–Ni interatomic potential set has been developed specifically to reproduce both shear modulus and SFE comparable to those of austenitic stainless steels.

Main results: The Fe–Ni potential was applied to study the interaction of FLs with dislocations in Fe–Ni solid solutions containing 50 at.% and 70 at.% Ni. The choice of these two compositions was governed by the desired value of SFE (i.e. to be in the range of that relevant for austenitic steels) and full stability of FCC phase. The simulations of pure Ni using two different potentials predicting low and high SFE were performed. In this way, it was made a step further towards understanding the effect of low SFE on dislocation-loop interaction. The effect of alloying (i.e. variation of SFE, shear modulus and dislocation friction stress) on dislocation-FL interaction mechanisms was also studied.



Interaction of a $1/2[110]$ SD with a $1/3[111]$ FL in Fe–50Ni at 300 K. Initially, the dislocation is attracted to the loop and moves to interact with the nearest side (a). However, due to the large spacing between the partials, loop shear by the leading partial starts before a constriction can

form (b). The two partials consequently shear the loop sequentially, leaving a $1/2[110]$ step on its surface (c).

Conclusions: It was concluded that by decreasing stacking fault energy below a certain value the formation of constrictions on dislocations is suppressed so that loop unfaulting becomes a less favorable mechanism in comparison with loop shear. Additional effect of solid-solution alloying, causing a non-negligible friction stress, is expressed in the impedance of the propagation of dislocations in the secondary glide planes, which is another factor limiting the unfaulting process.

Future work: Further research can be performed on the study of the possible influence of a combination of the enhanced friction stress and variation of SFE, relevant for alloys, on critical stress and interaction mechanism.

Acknowledgment: This work was performed in the framework of the EC-funded FP7/PERFORM60 project, under grant agreement 232612. Part of calculations has been performed at HPC Julich within the 'SORT' project. Research was partly supported by the Office of Fusion Energy Sciences, US Department of Energy (YNO).

Published in: D. Terentyev, A. Bakaev and Yu.N. Osetsky / Journal of Nuclear Materials 442 (2013) S628-S632

Tungsten

High temperature strain hardening behavior in double forged and potassium doped tungsten

Hua Sheng^{a,b}, Guido Van Oost^b, Evgeny Zhurkin^{a,c}, Dmitry Terentyev^a, Vladimir I. Dubinko^d, Inge Uytdenhouwen^a, Jozef Vleugels^e

a Structural Material Group, Institute of Nuclear Materials Science, SCKCEN, Mol, Belgium

b Department of Applied Physics, Ghent University, St. Pietersnieuwstraat 41, 9000 Ghent, Belgium

c Experimental Nuclear Physics Department, K-89, Faculty of Physics and Mechanics, Saint-Petersburg State Polytechnical University, 29

Polytekhnicheskaya Str., 195251 St. Petersburg, Russia

d NSC Kharkov Institute of Physics and Technology, Kharkov 61108, Ukraine

e Department of Metallurgy and Materials Engineering, KU Leuven, Kasteelpark Arenberg 44, 3001 Leuven, Belgium

Introduction:

In the present study, we continue to analyze the mechanical properties of two recently developed double forged and K-doped Tungsten grades, fabricated by PLANSEE AG, which were characterized earlier [8–10]. The mechanical and microstructural properties of the as-received and annealed double forged and K-doped W grades were analyzed in the 300–2000 C range [10]. The initial microstructure and loading rates played an important role in the high temperature deformation. In particular, a high strain rate deformation resulted in a larger ductility than at lower strain rate, which was not straightforward to explain [9].

Main results:

The strain-hardening behavior of two recently developed double forged and K-doped tungsten grades in the 300–2000 C range was analyzed applying a phenomenological model describing the evolution of the flow stress as a function of the dislocation density. The applied model allowed establishing a correlation between the strain hardening curvature and the size of microstructural features controlling the dislocation multiplication. The obtained results demonstrated that plastic deformation was controlled by the resistance of the low angle grain boundaries below 1000 C and the high angle grain boundaries at 1500 C and above. The experimental results obtained at different loading rates showed that thermal activation was essential for the passage of dislocations through grain boundary interfaces at 1000 C and above. The limitations of the applied model and need for further development of the physical model accounting for stress- and temperature-induced grain growth are discussed..

Conclusions:

The characteristic pinning distance L , obtained at 1000C in the ‘as received’ double forged grades, showed a strong dependence on the loading rate, namely: a decrease with rising strain rate. This, in turn, implies that thermal activation essentially contributes to the passage of dislocations through grain boundary interfaces.

Future work: Not foreseen.

Acknowledgment: EZ acknowledges the visiting scientist fellowship from the EU Erasmus Mundus master programme FUSION-EP. The work was partially supported by European Fusion Development Agreement under the contract with the Belgian Fusion Association.

Published in: Hua Sheng, Guido Van Oost, Evgeny Zhurkin, Dmitry Terentyev, Vladimir I. Dubinko, Inge Uytdenhouwen, Jozef Vleugelse / Journal of Nuclear Materials 444 (2014) 214–219

Dislocations mediate hydrogen retention in tungsten

D. Terentyev¹, V. Dubinko², A. Bakaev^{1,3}, Y. Zayachuk¹, W. Van Renterghem¹ and P. Grigorev^{1,4}

¹ *SCK·CEN, Nuclear Materials Science Institute, Boeretang 200, Mol, 2400, Belgium*

² *National Science Center, Kharkov Institute of Physics and Technology, Kharkov 61108, Ukraine*

³ *Center for Molecular Modeling, Department of Physics and Astronomy, Ghent University, Technologiepark 903, 9052 Zwijnaarde, Belgium*

⁴ *Department of Applied Physics, Ghent University, St. Pietersnieuwstraat 41, 9000 Ghent, Belgium*

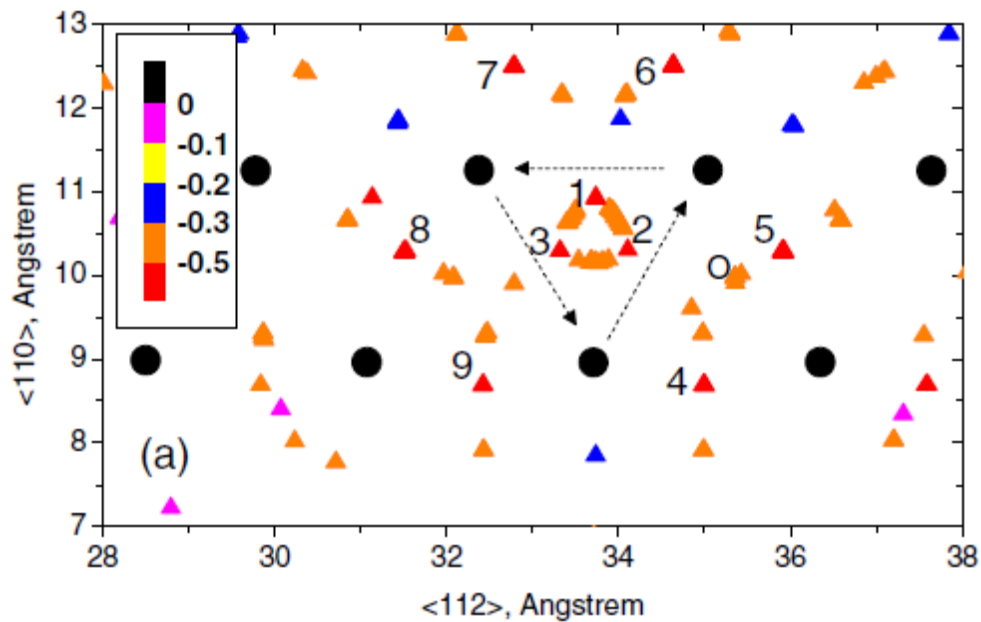
Introduction: Development of fusion technology for electrical power production is one of the biggest challenges faced in 21th century. Its realization must overcome a number of challenges, one of which is the selection of appropriate plasma facing materials (PFM). High flux plasma exposure degrades properties of materials and leads to permeation and trapping of plasma components including highly toxic tritium (phenomenon known as retention). Low erosion/sputtering, high melting point and controlled retention are typical prerequisites of PFM, among which tungsten (W) is the main candidate.

The retention of hydrogen (H) isotopes is attributed to their trapping at lattice defects resulting in the formation of bubbles and their subsequent growth into sub-surfaces blisters. The conventional analysis of the retention under high energy ion implantation is based on the premise that vacancies, generated in collision cascades, are responsible for the nucleation of stable H-vacancy clusters. In International Thermonuclear Experimental Reactor (ITER), the energy of impinging ions (<100 eV) is well below the displacement threshold, and the implantation range is limited to several nanometers. Nevertheless, samples exposed at linear plasma generators, demonstrate that the H permeation extends up to several micrometers (μm). At such depths, deep permeation of H cannot be assigned to the vacancy trapping as their equilibrium concentration is negligible at typical temperatures accessible to existing plasma generators, i.e. 300–800 K.

Grain boundaries were suggested as nucleation sites for bubbles, however, the retention also takes place in the recrystallized W and even in single crystal W. The self-trapping and nucleation of stable H clusters in W bulk is ruled out as a pair and triplet of H atoms exhibit negligible binding energy (~ 0.01 eV). Moreover, different impurity concentrations do not result in any significant difference in the H depth profiles. Hence, the mechanisms of H retention provoking intensive blistering and bubble formation under sub-threshold plasma exposure are still to be identified.

Main results: It is explored the interaction of H with screw dislocations (SDs), the main microstructural features of metals including W. Using density functional theory (DFT) calculations, we demonstrate that H atoms are strongly bound to the SD core and exhibit fast one-dimensional (1D) migration along the dislocation line. An elementary dislocation segment accepts up to six H atoms practically without losing the interaction strength. Once the cluster of eight H atoms is formed, it spontaneously transforms into an immobile configuration by punching out a jog on a dislocation line. The DFT data are incorporated in continuum rate theory model to evaluate the nucleation rate of H bubbles on a dislocation network as a function of depth. A good agreement with the experimental profiles suggests that dislocation microstructure is primarily responsible for the trapping of H isotopes under high flux plasma exposure. The TEM analysis performed on the W samples, exposed to plasma in our previous

work in conditions not yet featuring the blisters, reveals the presence of numerous nanometric cavities decorating dislocations with a linear density matching the predictions of our calculations.



H–SD binding energy map. Color code denotes the binding energy value in eV, note that H exhibits negative binding energy (i.e. attracted) in all positions near the dislocation core. Filled triangles display all metastable H positions, black circles display W atoms. Three dashed arrows show the $\langle 111 \rangle$ atomic rows forming the SD core.

Conclusions: It is proposed and defended a comprehensive mechanism for the nucleation and growth of hydrogen bubbles on dislocation lines under high flux plasma exposure of tungsten. The mechanism comprises the following stages: interstitial H atom trapping at dislocation lines, its fast 1D migration, growth of multiple H_N clusters eventually resulting in the punching of a jog.

Acknowledgment: The work was supported by the European Fusion Programme. V. Dubinko acknowledges the support of the Erasmus Mundus Fusion EP fellowship.

Published in: D. Terentyev, V. Dubinko, A. Bakaev, Y. Zayachuk, W. Van Renterghem and P. Grigorev / Nuclear Fusion 54 (2014) 042004

Review of many-body central force potentials for tungsten

G. Bonny¹, D. Terentyev¹, A. Bakaev^{1,2,3}, P. Grigorev^{1,2,4} and D. Van Neck²

¹ SCK•CEN, Nuclear Materials Science Institute, Boeretang 200, B-2400 Mol, Belgium.

² Ghent University, Center for Molecular Modeling, Department of Physics and Astronomy, Technologiepark 903, B-9052 Zwijnaarde, Belgium.

³ St. Petersburg State Polytechnical University, Department of Experimental Nuclear Physics K-89, Faculty of Physics and Mechanics, 29 Polytekhnicheskaya str., 195251 St. Petersburg, Russia.

Introduction:

Tungsten and tungsten based alloys are the primary candidate materials for plasma facing components in fusion reactors. The exposure to high-energy radiation, however, severely degrades the performance and lifetime limits of the in-vessel components. In an effort to better understand the mechanisms driving the materials' degradation at the atomic level, large-scale atomistic simulations are performed to complement experimental investigations. At the core of such simulations lays the interatomic potential, on which all subsequent results hinge. In this work we review 19 central force many-body potentials and benchmark their performance against experiments and density functional theory (DFT) calculations.

Main results:

As basic features we consider the relative lattice stability, elastic constants and point-defect properties. In addition, we also investigate extended lattice defects, namely: free surfaces, symmetric tilt grain boundaries, the $\frac{1}{2}\langle 111 \rangle \{110\}$ and $\frac{1}{2}\langle 111 \rangle \{112\}$ stacking fault energy profiles and $\frac{1}{2}\langle 111 \rangle$ screw dislocation core. We also provide the Peierls stress for $\frac{1}{2}\langle 111 \rangle$ edge and screw dislocations as well as the glide path of the latter at zero Kelvin. The presented results serve as an initial guide and reference list for both: modelling of atomically-driven phenomena in; and further development of potentials for bcc tungsten.

Conclusions:

Schematic summary of the performance of the potentials for different physical properties.

Property	FS	JO	FOI	ZWJ	KLL	ZSG	DLK	DND	MVG1	MVG2	MVG3	WZL
Elastic Constants	C	C	C	C	IC	C	C	C	C	C	C	C
$E_f(\text{Vac})$	C	C	C	C	C	C	C	C	C	C	C	C
$E_m(\text{Vac})$	UE	C	IC	C	C	IC	C	C	C	UE	C	UE
$E_b(\text{Di-Vac})$	IC	IC	IC	IC	IC	IC	IC	UE	UE	IC	UE	UE
$E_f(\text{SIA})$	UE*	IC	IC	IC	IC	IC	IC	C	C	C	C	C
$\langle 111 \rangle$ row potential	C	OE	IC	OE	OE	IC	OE	IC	OE	C	OE	C
Screw dislocation core	IC	IC	C	C	IC	C	C	IC	C	C	C	IC
Screw dislocation glide	IC	IC	IC	C	IC	IC	IC	IC	C	C	C	IC
Edge dislocation glide	C	C	IC	C	C	IC	C	IC	C	C	C	C

Free surface	UE	UE	UE	UE	UE	UE	UE	UE	UE	C	UE	UE
Grain boundary	UE	C	C	C	C	C	C	UE	C	UE	C	UE
Gamma surface cuts	UE	C	IC	C	C	IC	UE	IC	C	UE	C	UE
R_{cut}	2nn	2nn	2nn	2nn	2nn	2nn	6nn	2nn	5nn	4nn	5nn	2nn

IC – Inconsistent with experimental or DFT data.

C – Consistent with experimental or DFT data.

OE – Overestimation compared to experimental or DFT data.

UE – Underestimation compared to experimental or DFT data.

* Both AT and JW are consistent with the DFT data.

Future work:

This work helped to select the appropriate W potential to develop a WHHe potential.

Acknowledgment:

EFDA / HELIOS HPC Japan

Published as: G. Bonny et al., Modelling and Simulation in Materials Science and Engineering 22 (2014) 053001

Dislocation mechanism of deuterium retention in tungsten under plasma implantation

*V I Dubinko¹, P Grigorev^{2,3}, A Bakaev^{2,5}, D Terentyev², G van Oost⁴, F Gao⁵,
D Van Neck⁶ and E E Zhurkin⁷*

¹ National Science Center 'Kharkov Institute of Physics and Technology', Kharkov 61108, Ukraine

² SCK•CEN, Boeretang 200, 2400 Mol, Belgium

³ Ghent University, Applied Physics EA17 FUSION-DC, St. Pietersnieuwstraat 41 B4, B-9000 Ghent, Belgium

⁴ Department of Applied Physics, Ghent University, 9000 Ghent, Belgium

⁵ Pacific Northwest National Laboratory, Richland, WA 99352, USA

⁶ Center for Molecular Modeling, Department of Physics and Astronomy, Ghent University, Technologiepark 903, 9052 Zwijnaarde, Belgium

⁷ Department of Experimental Nuclear Physics, Institute of Physics, Nanotechnologies and Telecommunications, St. Petersburg State Polytechnical University, 29 Polytekhnicheskaya street, 195251, St. Petersburg, Russia

Introduction: The practical use of W is hindered by its high ductile-to-brittle transition temperature, and therefore risk of brittleness between plasma pulses in the course of operation. In order to improve the mechanical properties, tungsten alloys are considered. One of the issues still to be clarified is the retention of hydrogen (H) isotopes (including deuterium and radioactive tritium) in tungsten alloys, as the plasma-facing components are supposed to sustain highflux plasma. As hydrogen isotope ions are neutralized and thermalized following the implantation, further evolution depends on hydrogen solubility in W – i.e. the energy of H solution in W, which is positive. Above this solubility limit (e.g. under plasma exposure that implants H ions into material), H does not form hydrides with W, but precipitates in the bubbles filled with H₂ molecules. However, the thermodynamic diagram does not indicate the ways of the bubble formation, which occurs via diffusion, trapping, nucleation and growth. The critical issue here is to determine the mechanisms of trapping and nucleation of H bubbles, which basically define the retention of hydrogen in material. Experimental investigations of trapping and release of D in pure tungsten (W) and tungsten-tantalum (W-Ta) alloys show that there is a considerable amount of trapped D in the bulk within a depth of several microns, which is similar to the case of He trapping in W. However, the essential difference between hydrogen and helium agglomeration in tungsten is that the binding energy between two hydrogen atoms is an order of magnitude lower than that for helium. It means that, in a marked contrast to He, a homogeneous nucleation of D clusters is highly improbable. Accordingly, nucleation of hydrogen clusters requires binding sites. In current models dealing with deuterium (D) retention in tungsten, it is argued that the nucleation of D-complexes is determined crucially by the concentration of radiation-produced vacancies, which act as traps for fast-migrating D atoms. One vacancy has been argued to trap up to 5–6 hydrogen atoms [3–5]. At sufficiently low temperatures considered in ref. [2], vacancies are immobile while self-interstitial atoms (SIAs) diffuse and become trapped with impurity atoms (mainly carbon, C) or are absorbed by dislocations. Thus, the result strongly depends on the dislocation density and C-SIA trapping energy, which have to be high enough to trap SIAs so that the remaining vacancies can trap D atoms and act as nucleation sites for D-clusters. This model was developed to describe ion implantation with energies of 5–30 keV, but cannot be applied (even qualitatively) to nucleation of D-clusters at sub-threshold implantation conditions, i.e. when the ion energy is too low to produce stable vacancy-SIA pairs in the crystal bulk, and the operating temperature range is too low (<500 K) to induce any significant concentration of thermal vacancies. The sub-threshold implantation conditions are important, however, since they correspond to the plasma-wall interaction regime expected to occur in the ITER and experiments involving highflux, high-temperature deuterium plasmas with ion energies of up to several tens of eV. Hence, the description of the trapping of D at these irradiation conditions requires alternative mechanisms to those considered in the current models. In this work, we analyze the trapping of hydrogen on typical microstructural features such as dislocations and compare the efficiency of this mechanism with the homogeneous selftrapping mechanism (conventionally considered for helium retention). Based on the available ab initio results, we construct a theoretical model to evaluate the retention of D on dislocation lines. The model is then applied to describe thermal desorption spectroscopy (TDS) results, which are used to verify activation energies of deuterium detrapping.

Main results: Figure 1 shows that desorption temperature ranges from 450 to 700 K, with depth increasing from 1 nm to 1 micron, taking $E_m = 1$ eV. The profile of retained deuterium steeply decreases with depth, so the maximum of released deuterium comes from subsurface layers, which explains the position of the first TDS peak near 460 K. The second peak lies near

750 K, which corresponds to the release of deuterium from clusters via bulk diffusion. Activation energy for this process is given by the sum of detrapping and bulk migration energies, and is equal to 2 eV in order to fit the second peak at 750 K (figure 1). It does not depend on the depth since the limiting process in this case is detrapping deuterium from clusters rather than facilitating its diffusion to the surface. So, taking the D migration energy in bulk $E_m = 0.4$ eV, the detrapping activation energy is estimated as 1.6 eV. This value corresponds well to the H absorption barrier (from vacuum to W bulk) found by DFT to be 1.7 and 2.0 eV for the (100) and (110) surface [5]. Note that the second peak increases with rising implantation time, which implies that large bubbles formed at high fluence cannot be emptied by deuterium release via dislocation channels at the imposed heating rate. Apparently the second mechanism (i.e. emission directly to bulk) comes into play at sufficiently high temperature and competes with the emission via dislocation lines.

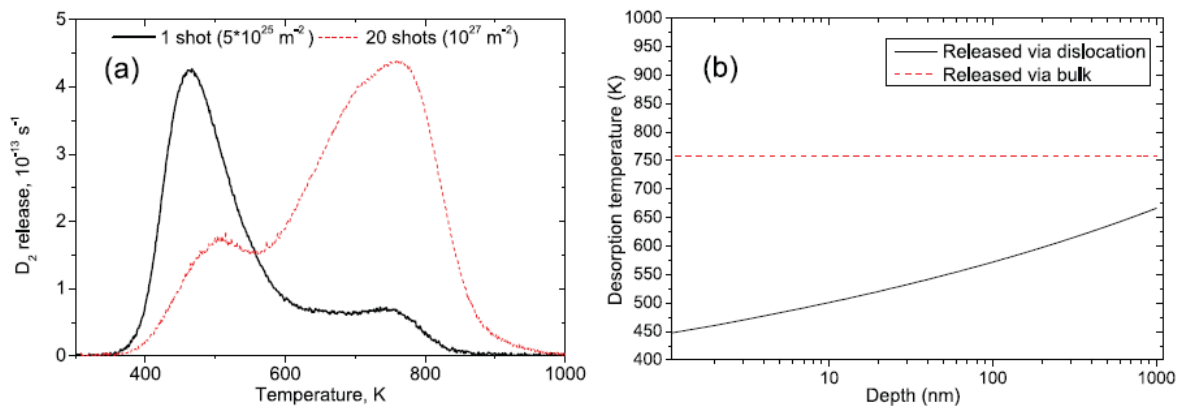


Figure 1(a) TDS spectra of the W sample after exposures to 1 plasma shot (70 s) and 20 shots at high deuterium flux $FD = 1020 \text{ m}^{-2}\text{s}^{-1}$ [(b) Calculated dependence of the temperature of desorption via dislocations on the depth, assuming $E = 1$ eV, versus the temperature of desorption via bulk, assuming the activation energy of 2 eV

Conclusions: We developed a model for D retention in W-based alloys under sub-threshold plasma implantation conditions, assuming the trapping of D at dislocation network. The latter serves not only as the source of trapping, but also as a means for D transport deeper in the bulk. The formulation of the present model was realized with the aid of ab initio calculations and experimental estimates deduced from TDS measurements. The model explains the observed saturation of D retention with implantation dose and effects due to alloying of tungsten by tantalum (which essentially changes grain size distribution). Hence, this work provides a link between the kinetics of D retention and microstructural features of the exposed W samples. Further experimental tests may include verification of a strong dependence of the D-penetration depth on the dislocation density. The prediction of the presently developed model for the effect of cold work/deformation on the dislocation-mediated retention is presented in figure 11. The validation of the prediction can be realized by exposure and subsequent nuclear reaction analysis (NRA) measurements, which offers excellent resolution up to a depth of several microns.

Future work: As an outlook regarding further development of the microstructure-mediated retention models, we consider that mobility and ‘loop-punching’ processes on edge dislocations, dislocation junctions and grain boundaries are the primary issues to be assessed. This information will provide a much more accurate description of the nucleation and growth kinetics of D-clusters in a wide range of exposure conditions.

Acknowledgment: V Dubinko acknowledges financial support from Erasmus Mundus (FUSION-EP_0). The work is partially supported by the EUROfusion programme. P Grigorev acknowledges the support from the Erasmus Mundus International Doctoral College in Fusion Science and Engineering (FUSION-DC).

Published in: V I Dubinko, P Grigorev, A Bakaev, D Terentyev, G van Oost, F Gao, D Van Neck and E E Zhurkin/ J. Phys.: Condens. Matter 26 (2014) 395001 (10pp)

On the binding of nanometric hydrogen-helium clusters in Tungsten

G. Bonny¹, P. Grigorev^{1,2,3}, D. Terentyev¹

¹ *SCK•CEN, Nuclear Materials Science Institute, Boeretang 200, B-2400 Mol, Belgium.*

² *Ghent University, Center for Molecular Modeling, Department of Physics and Astronomy, Technologiepark 903, B-9052 Zwijnaarde, Belgium.*

³ *St. Petersburg State Polytechnical University, Department of Experimental Nuclear Physics K-89, Faculty of Physics and Mechanics, 29 Polytekhnicheskaya str., 195251 St. Petersburg, Russia.*

Introduction:

In this work we develop an embedded atom method potential for large scale atomistic simulations in the ternary Tungsten-Hydrogen-Helium (W-H-He) system, focusing on applications in the fusion research domain. Following available ab initio data, the potential reproduces key interactions between H, He and point defects in W and utilizes the most recent potential for matrix W. The potential is applied to assess the thermal stability of various H-He complexes of sizes too large for ab initio techniques.

Main results:

We have developed two versions of a EAM potential for large scale atomistic simulations in the ternary W-H-He system. Both potentials reproduce key interactions between H, He and point defects calculated by DFT. We applied the potentials to compute the dissociation energy of various VHHe clusters of nano-metric size and parameterize a simple liquid-tear drop model applicable to up-scale mean field or kinetic Monte Carlo simulations. The obtained results show that the dissociation of mixed VHHe clusters primarily takes place by emission of H, whose trapping energy is not essentially changed by the presence He in the clusters. Hence, the H-He interaction does not affect the thermal stability of H in the vacancy-stabilized H-He clusters. Therefore we conclude that the origin of the H-He synergy expressed by the enhanced H uptake should be investigated at the stage of the nucleation of H-He defects.

Conclusions:

The results show that the dissociation of H-He clusters stabilized by vacancies will occur primarily by emission of hydrogen atoms and then by break-up of V-He complexes, indicating that H-He interaction does influence the release of hydrogen.

Future work:

The present potential will be used in MD simulations within the SMM group.

Acknowledgment: EFDA

Published as: G. Bonny et al., *Journal of Physics Condensed Matter* 26 (2014) 485001.

Temperature and deformation effect on the low and high angle grain boundary structure of double forged pure tungsten

Hua Sheng^{1, 2}, Zhi Sun³, Inge Uytendhouwen¹, Guido van Oost², Jozef Vleugels³

¹*SCKCEN, The Belgian Nuclear Energy Research Centre, Institute for Nuclear Materials Science, Structural Materials Group, Boeretang 200, B-2400 Mol, Belgium*

²*Department of Applied Physics, Ghent University, J.Plataustraet 22, B-9000 Ghent, Belgium*

³*Department of Metallurgy and Materials Engineering, K.U.Leuven, Kasteelpark Arenberg 44, B- 3001 Leuven, Belgium*

Introduction: Tungsten and tungsten alloys are proposed for plasma facing materials for future fusion reactors because of their high melting point, high thermal conductivity, low thermal expansion, high resistance against erosion and sputtering and the low tritium retention. The main drawback is its brittleness. Low temperature limit is restricted by the high DBTT (ductile to brittle transition temperature) and the high temperature limit by the low recrystallization temperature of tungsten. To explain the high temperature tensile behavior of tensile testing bars machined out of the double forged material in different directions, as reported elsewhere, a deeper understanding of the inhomogeneity of the material at micro-meter level was essential. All material properties and microstructural evolution processes depend on the nature of the grain boundaries, such as their energy, mobility, and chemistry. Therefore, the grain size and orientation as well as the sub-grain size and misorientation of the double forged tungsten are studied by electron backscatter diffraction (EBSD) in the present paper. Both the effect of temperature and structural changes caused by deformation were investigated by tensile testing of specimens at various temperatures in the 300–2000 °C range and subsequent analysis.

Main results: A significant amount of sub-grains (Low angle grain boundaries LAGB) were observed inside the larger grains (high angle grain boundaries HAGB) in both the longitudinal (L) as transverse (T) orientation, most probably formed during hot forging. In both orientations about 80-90% of the grain boundaries are LAGBs. A 5-10% higher fraction of LAGBs was found in T, thus decreasing the average grain size of T compared to L. The majority of the grains, including a huge amount of sub-grains, are smaller than 10µm. The sub-grains usually form during hot forging wherein the dislocation activity is being contained within the main grain and upon their continued interaction the dislocation cell walls are refined and divide the main grain into several sub-grains. The measured average grain size, including both HAGB and LAGB grains, is 5.1 µm in the L orientation and 4.3 µm in the T orientation.

Temperature effect: no difference in the averaged HAGB grain size up to 1500 °C. Only recovery (changes in the dislocation structure) or the onset to recrystallization. At 2000 °C, a LAGB to HAGB fractional shift of 40% is measured, due to sub-grain coarsening by the recovery action. During the thermal treatment, the sub-grain misorientation increased, which is caused by the sub-grain growth. The limited grain growth observed in the material heated at 2000 °C can be attributed to Ostwald ripening rather than high angle grain boundary migration, which would result in a substantially larger grain growth.

Deformation and temperature: for the specimens deformed at 1500 and 2000 °C, the average grain size increased rapidly due to recrystallization when the material was deformed at the same time. At 2000 °C, a higher strain rate resulted in a lower final average grain size.

Grain orientation spread due to deformation speed: As shown on the GBCD map in Fig. 1, the slowly deformed tungsten has less subgrains but a larger (sub-) grain size compared to the quickly deformed material. For the slow deformed specimen, some of the sub-grains (LAGB) can grow large enough to effectively become grains (HAGB), i.e., they may serve as nuclei for recrystallization of the deformed material. As a result, the average grain size is bigger compared to the fast deformed specimen. Therefore, one may draw the conclusion that the sub-grain misorientation increases with the strain rate.

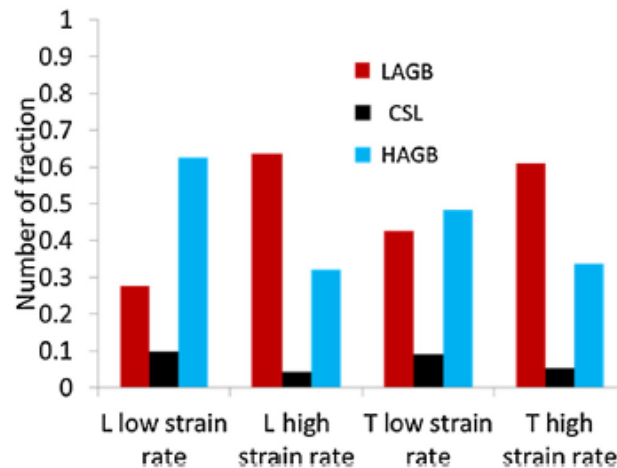


Fig. 1. Grain boundary character distributions (GBCD) in L and T directions of tungsten deformed at low and high strain rates at 2000 °C.

Conclusions: A large amount of sub-grains with a typical size below 5 μm were observed in the as-received double-forged tungsten. After thermally treating the double forged tungsten up to 2000 °C in vacuum, microstructural recovery was observed with the onset of recrystallization. Meanwhile, the sub-grain misorientation angle increases accompanied with limited sub-grain growth (LAGB) not enough to become grains (HAGB). Moreover, there is an observation of grain elongation in the direction perpendicular to the second hot forging direction, in the as-received double forged tungsten. The deformation temperature and the strain rate have a considerable influence on the final microstructure. The higher the temperature, the lower the amount of sub-grain boundaries due to sub-grain coarsening and the clearer the grain boundaries. The higher the deformation strain rate during tensile testing, the higher the grain orientation spread and the larger the sub-grain misorientation, but the smaller the grain size due to a lower extent of crystallization. These findings match well with the mechanical testing data, i.e., the higher strain rate, the bigger the elongation, the more ductile the material, as reported elsewhere.

Future work: More detailed analysis on the effect of time should be carried out in future experiments to make more definite conclusions related to the effect of high deformation and strain assisted recrystallization.

Acknowledgment: The authors greatly appreciate the scholarship awarded to Hua Sheng and financial support from SCK•CEN (Belgium).

Published in: H. Sheng, Zhi Sun, I. Uytendhouwen, G. Van Oost, J. Vleugels, International journal of refractory metals and hard materials 50 (2015) 184-190

Global erosion and deposition patterns in JET with the ITER-like wall

A. Baron-Wiechec^{a,1}, A. Widdowson^a, E. Alves^b, C.F. Ayres^a, N.P. Barradas^b, S. Brezinsek^c, J.P. Coad^a, N. Catarino^b, K. Heinola^e, J. Likonen^d, G.F. Matthews^a, M. Mayer^f, P. Petersson^g, M. Rubel^g, W. van Renterghem^h, I. Uytendhouwen^h, JET-EFDA contributors²

^a CCFE, Culham Science Centre, Abingdon OX14 3DB, UK

^b Instituto Superior Técnico, Instituto de Plasmas e Fusão Nuclear, Universidade de Lisboa, Lisboa, Portugal

^c Association EURATOM-Forschungszentrum Jülich, IPP, D-52425 Jülich, Germany

^d Association EURATOM-TEKES, VTT, PO Box 1000, 02044 VTT, Espoo, Finland

^e Association EURATOM-TEKES, University of Helsinki, PO Box 64, 00014 University of Helsinki, Finland

^f Max-Planck-Institut für Plasmaphysik, 85748 Garching, Germany

^g Royal Institute of Technology, Assoc. EURATOM-VR, 100 44 Stockholm, Sweden

^h SCKCEN, The Belgian Nuclear Energy Research Centre, Institute for Nuclear Materials Science, Structural Materials Group, Boeretang 200, B-2400 Mol, Belgium

Introduction: Plasma wall interactions create some of the greatest challenges for the realization of a fusion reactor. This is also true for ITER where tritium trapping due to implantation and co-deposition and plasma pollution due to impurities migrating from PFCs to the plasma are major concerns. After over two decades of JET operation with a carbon wall, the ITER-like wall project at JET (JET-ILW) was initiated to explore plasma performance and plasma-wall interaction processes with a full metal wall: bulk beryllium (Be), Be-coated Inconel in the main chamber and bulk tungsten (W) or W-coated carbon fibre composites (CFC) in the divertor. The transition to all metal PFC was an essential step to minimize hydrogen fuel retention. The first period of operation after installation of the new wall ran from September 2011 to July 2012. An extensive post-mortem surface analysis program on PFC has been carried out after the ILW campaign and initial results were published elsewhere. In this paper a more complete accounting of erosion and deposition regions is presented, with data from fifteen locations in the JET chamber cross-section, and more detailed characterization of the divertor deposition.

Main results: A set of Be and W tiles removed after the first ITER-like wall campaigns (JET-ILW) from 2011 to 2012 has been analysed. The results indicate that the primary erosion site is in the main chamber (Be) as in previous carbon campaigns (JET-C). In particular the limiters tiles near the mid-plane are eroded probably during the limiter phases of discharges. W is found at low concentrations on all plasma-facing surfaces of the vessel indicating deposition via plasma transport initially from the W divertor and from main chamber W-coated tiles; there are also traces of Mo (used as an interlayer for these coatings). Deposited films in the inner divertor have a layered structure, and every layer is dominated by Be with some W and O content.

Conclusions: The rate of erosion at the inner wall guard limiters (IWGL) during the limiter phases of ILW operations has been calculated to be similar to that during the previous carbon campaign. It is expected that erosion during the limiter phases will be balanced by re-deposition on limiter surfaces deeper into the scrape-off layer (SOL), but despite more measurements this balance has not been demonstrated due to the limited number of tile samples, surface roughness and/or flaking of coating in deposition areas. During the divertor phase of each discharge, erosion is probably dominated by charge exchange neutral (CXN) bombardment of the main chamber wall, and is followed by migration along the SOL to the inner divertor. This is evidenced by erosion measurements at the Inner Wall Cladding (IWC)

tiles that line the vessel wall between the IWGL which suggest that the IWC may account for a significant fraction of the Be deposition found in the divertor. Some contribution may also be expected from re-erosion of the deposits on the IWGL, which may have a higher erosion yield than the bulk material.

Future work: no

Acknowledgment: This work was partly funded by the RCUK Energy Programme [Grant number EP/I501045] and by the European Union Horizon 2020 research and innovation programme. The work was also part-funded by the European Communities under the contract of Association between EURATOM/CCFE within the framework of the European Fusion Development Agreement. The views and opinions expressed herein do not necessarily reflect those of the European Commission.

Published in: A. Baron-Wiechec, A. Widdowson, E. Alves, C.F. Ayres, N.P. Barradas, S. Brezinsek, J.P. Coad, N. Catarino, K. Heinola, J. Likonen, G.F. Matthews, M. Mayer, P. Petersson, M. Rubel, W. van Renterghem, I. Uytendhouwen, JET-EFDA contributors, "Global erosion and deposition patterns in JET with the ITER-like wall", *Journal of Nuclear Materials*, In Press, Corrected Proof, Available online 27 January 2015

Microscopically non-uniform deposition and deuterium retention in the divertor in JET with ITER-like wall

H. Bergsåker^{b2}, I. Bykov^b, P. Petersson^b, G. Possnert^c, J. Likonen^d, S. Koivuranta^d, J.P. Coad^d, W. Van Renterghem^e, I. Uytendhouwen^e, A.M. Widdowson^a, JET EFDA Contributors¹
a JET-EFDA, Culham Science Centre, Abingdon, OX14 3DB, UK

b Department of Fusion Plasma Physics, Association EURATOM-VR, School of Electrical Engineering, KTH Royal Institute of Technology, S-10044 Stockholm, Sweden

c Uppsala Universitet, Tandem Laboratory, Association EURATOM-VR, S-75105 Uppsala, Sweden

d VTT, Association Euratom-Tekes, PO Box 1000, FI-02044 VTT, Finland

e SCKCEN, The Belgian Nuclear Energy Research Centre, Institute for Nuclear Materials Science, Structural Materials Group, Boeretang 200, B-2400 Mol, Belgium

Introduction: The migration of materials in large fusion devices is of concern particularly in view of the trapping of fuel at surfaces through co-deposition with wall material. Where more than one plasma facing material is used, the mixing of materials due to migration is likewise an issue. It is essential to investigate the microscopic distribution of impurity deposition and fuel retention and its relation to surface roughness from the points of view of understanding where and how fuel is trapped, to interpret surface analysis results correctly and to make reliable extrapolations, e.g. from JET with ITER-like wall (JET-ILW) to ITER (with initially smooth, although castellated) W surfaces in the divertor. It is also relevant to the assessment of fuel removal methods. This report shows how deuterium and impurities are distributed microscopically at the surfaces of the JET divertor following the first operations with ITER-like wall and the relation to surface topography.

Main results: The divertor surfaces in JET with ITER-like wall (ILW) have been studied using micro ion beam analysis (I-IBA) methods and scanning electron microscopy (SEM). Deposited layers with beryllium as main constituent had been formed during plasma operations through 2011–2012. The deuterium trapping and impurity deposition were non-uniform, frequently

enhanced within pits, cracks and valleys, regions reaching in size from 10 μm to 200 μm . The impurity deposition and fuel retention were correlated with the surface slope with respect to the direction of ion incidence. Typically more than 70% of the total measured areal density of trapped D was found in less than 30% of the surface area. This is of consequence for the interpretation of other surface analyses and in extrapolation from fuel retention in JET with ITER-like wall and rough divertor surfaces to ITER with smoother surfaces.

Conclusions: Microscopically non uniform impurity deposition and deuterium retention has been found at the divertor surfaces in JET-ILW. In particular, impurities and deuterium have accumulated preferentially in pits, cracks and depressed regions on the surfaces exposed to ion flux. Typically more than 70% of the total measured areal density of trapped D at representative surfaces is found in less than 30% of the surface area. The asymmetric deposition at the edge sides of larger pits, as well as the consistent orientation of elongated surface structures shows that the predominant direction of ion incidence plays an important role for the layer growth.

Future work: no

Acknowledgment: This work was supported by EURATOM and carried out within the framework of the European Fusion Development Agreement. The views and opinions expressed herein do not necessarily reflect those of the European Commission.

Published in: H. Bergsåker, I. Bykov, P. Petersson, G. Possnert, J. Likonen, S. Koivuranta, J.P. Coad, W. Van Renterghem, I. Uytendhouwen, A.M. Widdowson, JET EFDA Contributors, "Microscopically non-uniform deposition and deuterium retention in the divertor in JET with ITER-like wall", Journal of Nuclear Materials, In Press, Corrected Proof, Available online 11 December 2014

Romanelli, F.; Abel, I.; Afanesyev, V.; et al., Group Author(s): JET EFDA Contributors "Overview of the JET results with the ITER-like wall ", NUCLEAR FUSION Volume: 53 Issue: 10, special issue SI, article number: 104002

Effect of thermal heat loads on the microstructure of recrystallized double forged tungsten

W. Van Renterghem, I. Uytendhouwen

SCKCEN, The Belgian Nuclear Energy Research Centre, Institute for Nuclear Materials Science, Structural Materials Group, Boeretang 200, B-2400 Mol, Belgium

Introduction: Tungsten is considered as a material for first wall components in future tokamaks. During the operation in a tokamak, the first wall components will be exposed to heat loads due to the interaction of the plasma with the material. One of the interactions are edge localized modes (ELMs) which occur with a high repetition rate of more than 1 Hz and during which a significant amount of energy is deposited in a short time (<1 ms). Due to these thermal heat loads, the microstructure of the materials will be affected and the surface of the components may be damaged [1]. To guarantee the integrity of the plasma facing material, the effect of these thermal heat loads on the microstructure of the material needs to be investigated and understood. However, until now, very few studies were performed to determine the effect of the exposure of W to the plasma. In particular, the effect on the microstructure is not known. In this paper, a first experiment is described. A recrystallized tungsten material was exposed to electrons to reveal the effects of the thermal heat load only. The changes in microstructure are revealed by a combination of scanning electron microscopy (SEM) and transmission electron microscopy (TEM).

Main results: A TEM specimen preparation method was developed to investigate specimens about 10 μ m below the surface. This technique was applied to investigate the change in the microstructure after thermal heat loading. Tungsten was exposed to electrons of 120 keV during 100 pulses of 1 ms giving an absorbed power density of 1.26 GW/m². The only effect of the thermal heat load was a deformation of the matrix. The surface became rough with a series of parallel ridges of a few μ m high, but no cracking was observed in the exposed area.

On a microstructural level, the deformation was expressed by an increased number of line dislocations and the reappearance of tilt boundaries. A typical example of the microstructure in the electron beam exposed part is given in fig 1. A low density of interacting line dislocations was observed. The dislocation density of $2.8 \pm 0.5 \times 10^{13} \text{m}^{-2}$ was measured, which is a significant increase compared to the reference material, but still a moderate amount. As a result of the stress, the dislocations were mobile and the interaction of the moving dislocations resulted in dislocation tangles, dislocations with a <100> type Burgers vectors and dislocation loops (arrows fig 1b).

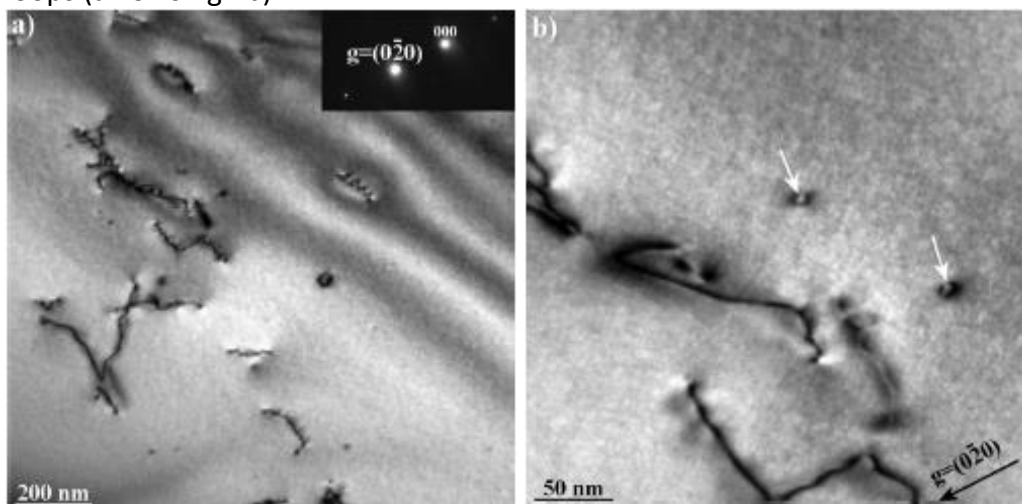


Fig 1: Microstructure of the electron beam exposed area: (a) bright field image of the line dislocations. The inset shows the diffraction pattern in which the diffraction vector is indicated and (b) Higher magnification bright field image. The white arrows point at small dislocation loops.

The second effect of the deformation is the reappearance of small angle tilt boundaries. These tilt boundaries create a subgrain structure with an average size of $7 \pm 1 \mu\text{m}$. Dislocation networks are formed at the tilt boundary to accommodate the lattice mismatch. However, dislocation bands have been found, which are not associated to a tilt boundary. Based on this observation, it is suggested that these dislocation bands assisted the formation of small angle tilt boundaries.

Conclusions: Two recrystallized double forged W materials, one which was pre-heated up to 400°C and exposed to 120 keV electrons during 100 pulses of 1 ms giving a total power of 1.26 GW/m² and one as reference which was only pre-heated to 400°C, were investigated with SEM and TEM to reveal the effect of the exposure on the microstructure. The reference material revealed that the selected material contains only some large angle grain boundaries and occasionally a few isolated dislocations. The e-beam exposure of the material resulted only in a deformation of the matrix. The surface has roughened and series of parallel ridges were observed in the SEM images. However, no cracks or other signs of material rupture were found. On a microscopic level the deformation manifested as an increased number of tangled dislocations and the reappearance of small angle tilt boundaries.

Future work: Determination of which kind of defects are introduced during e-beam exposure and how they can lead to the small angle grain boundaries observed. Comparison of exposure conditions on the resulting defect structure.

Acknowledgment: The authors would like to acknowledge G. Pintsuk and the JUDITH facility for the material exposure in the frame of the TEC agreement.

Published in: Van Renterghem, W.; Uytendhouwen, I., "Effect of thermal heat loads on the microstructure of recrystallized double forged tungsten", FUSION ENGINEERING AND DESIGN Volume: 88 Issue: 9-10 Pages: 1650-1654

Thermal shock response of deformed and recrystallised tungsten

Wirtz, M.^a; Cempura, G.^b; Linke, J.^a; Pintsuk G.^a and Uytendhouwen I.^c,

*a*Forschungszentrum Jülich, EURATOM Association, 52425 Jülich, Germany

*b*AGH University of Science and Technology, Al. A. Mickiewicza 30, 30-059 Krakow, Poland

c SCKCEN, The Belgian Nuclear Energy Research Centre, Institute for Nuclear Materials Science, Structural Materials Group, Boeretang 200, B-2400 Mol, Belgium

Introduction: The response of plasma facing materials (PFMs) to thermal shock loads is a major issue for future fusion devices like ITER and DEMO. Especially in the divertor region, the chosen materials have to with-stand severe environmental conditions in terms of steady state (upto 10 MW m⁻²), slow transient (up to 20 MW.m⁻²) and transient heat loads (up to 1 GW m⁻² and above). Beside these thermal loads PFMs are also exposed to high particle fluxes of hydrogen, helium and neutron, which will deteriorate the material properties and therefore have an impact on the thermal shock response. Under these conditions, tungsten is one of the most promising materials for application as PFM especially in the divertor region. Its main advantages are a high melting point, high thermal conductivity, low sputtering yield and low tritium retention. But tungsten has also some drawbacks such as the high atomic number and the brittleness at low temperatures. Thermal shock damages induced by ELM like events simulated in the electron beam facility JUDITH 1 (Juelich Divertor Test Facility in Hot Cells) comprise surface modifications and crack formation. How pronounced these damages are, depends not only on the test conditions such as absorbed power density and base temperature but also on the material's thermal and mechanical properties as well as on its microstructure. Both are strongly influenced by the manufacturing process of the material in terms of deformation and heat treatment.

In order to characterize the influence of a strongly elongated grain structure on the thermal shock response as well as the mechanical properties, deformed, so-called single forged, tungsten was exposed to 100 ELM like cyclic thermal shocks at various base temperatures to address the influence of the brittleness of the material. Additionally, the material was recrystallized and also exposed to the same cyclic thermal shocks to study the influence of recrystallization, which will take place during the operation of ITER or DEMO.

Main results: The material parameters of tungsten do not only depend on the material composition but also on the production process and hence on the microstructure. Especially the mechanical properties (see fig 1) are strongly influenced by the grain orientation and structure. In order to investigate the impact of these differences on the thermal shock response of tungsten as a PFM, heavily deformed and recrystallized W-UHP samples were exposed to 100 ELM like thermal shock events. The results show that both, the strongly elongated grain structure and the recrystallization, influence the thermal shock response of tungsten. Not only threshold values such as damage and cracking thresholds vary with microstructure but also the induced thermal shock damages and surface modifications depend on it. For the recrystallized state surface roughening due to plastic deformation is more pronounced. Crack parameters as well as crack propagation is strongly influenced by grain orientation due to preferential crack formation along grain boundaries. These changes can be traced back to microstructural and grain structure effects such as the "texture strengthening" in case of the longitudinal/transversal grain orientation or the thermally activated agglomeration of lattice defects at the grain boundaries of the recrystallized material. Based on these results it can be stated that for none of the tested grain structures severe damage formation, namely cracking and roughening, can be avoided under these very high power densities. Longitudinal

samples have the highest damage threshold (valid for 100 pulses) but show cracking parallel to the surface, which may lead to overheating and enhanced erosion. In contrast to that, transversal samples show no parallel cracks but have worse threshold values and very high crack densities, which could also lead to enhanced erosion especially for very high pulse numbers. Recrystallization of the material, which will take place during the steady state loading, will increase the erosion of complete grains and could therefore lead to an intolerable contamination of the plasma.

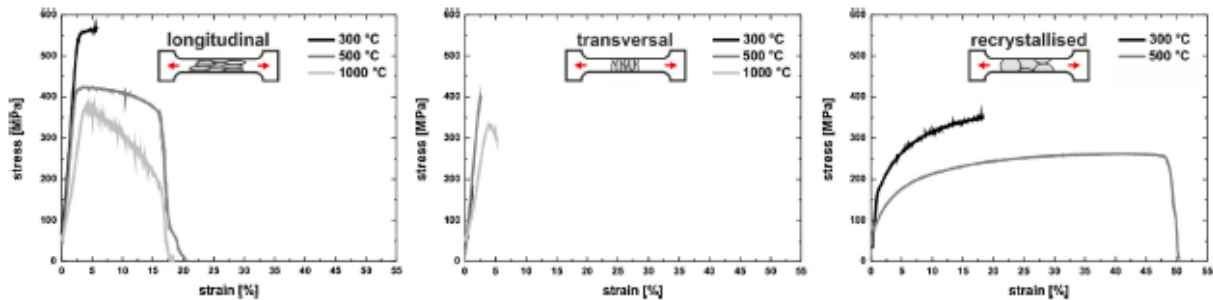


Fig 1: Stress–strain diagrams for W-UHP at 300°C, 500°C and 1000°C for longitudinal (left), transversal (middle) and recrystallized (right) specimens.

Conclusions: The thermal shock response of a ultra high purity (UHP) tungsten as a plasma facing material (PFM) strongly depends on its mechanical properties and consequently on its microstructure. Tensile tests at different temperatures show that the mechanical properties such as fracture strength and strain depend on the grain orientation and microstructure. Transmission electron microscope images of the as received and the recrystallized material show that the defect density of the recrystallized samples is decreased. Threshold values such as damage and cracking threshold vary with microstructure by a factor of 2. Also the induced thermal shock damages and surface modifications are strongly depend on the microstructure. Surface roughening due to plastic deformation is more pronounced in the recrystallized state and crack parameters as well as crack propagation is influenced by grain orientation due to preferential crack formation along grain boundaries.

Future work: Combined effect of hydrogen and plasma exposure on the changes of the damage thresholds under thermal shock loading. Correlation of heat flux loading damages with microstructural and mechanical properties.

Acknowledgment: The authors would like to thank Dr. E. Wessel and V. Gutzeit for their kind assistance with the SEM/LM pictures. This work, supported by the European Communities under the contract of Association between EURATOM/Forschungszentrum Jülich, was carried out within the framework of the European Fusion Development Agreement. The views and opinions expressed herein do not necessarily reflect those of the European Commission.

Published in: Wirtz, M.; Cempura, G.; Linke, J.; Pintsuk G. and Uytendhouwen I., “Thermal shock response of deformed and recrystallised tungsten “, FUSION ENGINEERING AND DESIGN Volume: 88 Issue: 9-10 Pages: 1768-1772

Analytical and experimental determination of the multipole cusp magnetic field in the VISIONI plasmatron

Van Hoe, O.^{a,b}; Schuurmans J.^a; Uytendhouwen I.^a; Van Oost G.^b

*a*SCKCEN, The Belgian Nuclear Energy Research Centre, Institute for Nuclear Materials Science, Structural Materials Group, Boeretang 200, B-2400 Mol, Belgium

*b*Ghent University, Rozier 44, 9000 Ghent, Belgium

Introduction: The VISIONI plasmatron is a plasma simulator located at the Belgian Nuclear Research Centre SCK•CEN. It is dedicated to thermonuclear fusion material studies. The plasma in VISIONI is created by means of a DC arc. The anode is formed by the bottom and the side of the plasma chamber. The cathode is formed by two 1 mm V-shaped tungsten filaments. These filaments are heated ohmically with a heating power of up to 2 kW. This causes thermionic electron emission. Hence, the filaments also serve as primary electron source. The target plate at the top of the plasma chamber is put at a negative voltage with respect to the anode. This is done to accelerate the ions towards the sample which is mounted centrally on the target plate. The plasma conditions in VISIONI to which the sample is exposed are very similar to the conditions expected at the first wall of the next-generation fusion reactor ITER. While presently most experiments are performed with a deuterium plasma, in the future it will be possible to work with tritium. This makes VISIONI the ideal test bed for candidate ITER first wall materials. The plasma in VISIONI is confined by means of a strong multi-pole cusp magnetic field produced by permanent samarium–cobalt magnets positioned at the bottom and the side of the plasma chamber. The magnetic field also enhances the ionization efficiency and leads to a very homogeneous plasma in the central field-free region. Sm₂Co₁₇ magnets were chosen because of their very high coercivity and high temperature ratings. The magnetic field as a function of the location in the plasma chamber is an important input for the ongoing plasma and material migration computer simulations for VISIONI. The magnetic field strongly determines the path of the charged particles in the plasma chamber. In this work, therefore, the aim was to derive an analytical formula to calculate the magnetic field as a function of the location in the plasma chamber.

Main results: The VISIONI plasmatron is a plasma simulator dedicated to thermonuclear fusion material studies. The plasma is confined by means of a strong multipole cusp magnetic field produced by rectangular permanent samarium–cobalt magnets positioned just outside of the plasma chamber. The magnitude of this field as a function of the location in the plasma chamber is an important input for the ongoing plasma and material migration computer simulations for VISIONI. In this work the magnetic field in the VISIONI plasma chamber was calculated analytically. The calculations are based on the electric current point of view and based on the concept of magnetic charges. The calculated results were benchmarked and verified experimentally by Hall probe measurements. By fitting the calculation to the measurements a value of $\mu_0 J = 1.12 \text{ T}$ was obtained for the initially unknown equivalent current density J . The order of magnitude is in agreement with typical tabulated values for the remanence of Sm₂Co₁₇ magnets. Fig 1 shows a horizontal cross section of the magnetic field lines through the centre of the plasma chamber. The pictures were made with the JAVA tool based on the Line Integral Convolution technique. One can clearly distinguish the typical arcs of a multipole cusp magnetic field. These are also visible in the light emission of the plasma shown partly in Fig. 1. Close to the side magnet the magnetic field was calculated to be about 0.2 T, which is in perfect agreement with the measurements performed earlier. Towards the centre of the plasma chamber the field drops rapidly over about two orders of magnitude. The central

part of the chamber, especially around the sample, can be considered as a field-free region. The analytical formulas are very convenient for use indifferent simulation codes.

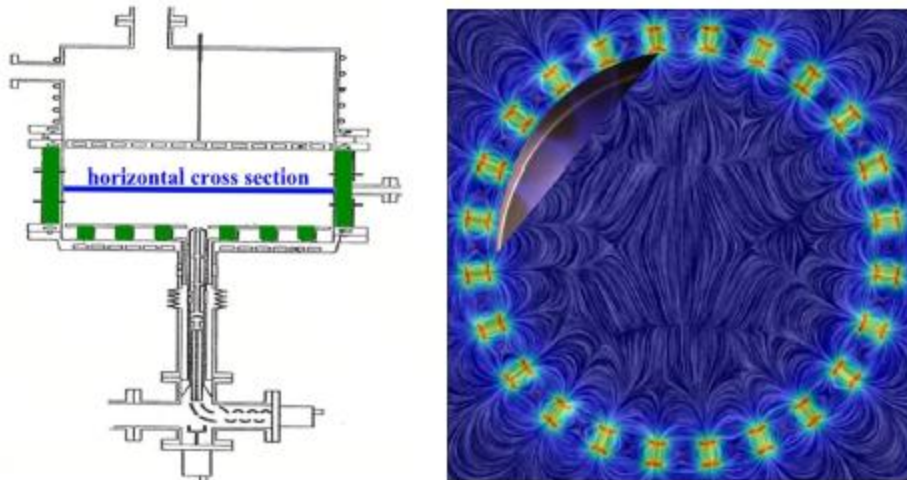


Fig 1: The horizontal cross section of the magnetic field lines in VISIONI through the centre of the device exhibits the typical pattern of a multicusp magnetic field.

Conclusions: The VISIONI plasma is confined by means of a strong multipole cusp magnetic field created by multiple rectangular samarium–cobalt magnets at the side and bottom of the plasma chamber. This magnetic field was calculated analytically from Biot–Savart’s law. A value of $\mu_0 J = 1.12\text{T}$ was found for the initially unknown equivalent surface current density J in these analytical equations by means of Hall probe measurements. These measurements also showed that the analytical equations nicely reproduce the measured spatial variation of the magnetic field in VISIONI. The analytical formulas are very convenient for use in ongoing plasma and material migration computer simulations for VISIONI.

Future work: no

Acknowledgment: The presented study was made possible by an Aspirant grant from FWO (Fonds voor Wetenschappelijk Onderzoek) and additional working budgets from Ghent University and SCK•CEN.

Published in: Van Hoey, Olivier; Schuurmans, Johan; Uytendhouwen, Inge; Van Oost Guido, “Analytical and experimental determination of the multipole cusp magnetic field in the VISIONI plasmatron”, FUSION ENGINEERING AND DESIGN Volume: 88 (2013) Issue: 6-8 Pages: 661-665

Improved carbon migration modelling with the ERO code

Olivier Van Hoey^{a,b}, Andreas Kirschner^c, Carolina Björkas^c, Dmitry Borodin^c, Dmitry Matvee^{a, c},
Inge Uytendhouwen^b, Guido Van Oost^a

a Department of Applied Physics, Ghent University, Rozier 44, 9000 Ghent, Belgium

*b SCKCEN, The Belgian Nuclear Energy Research Centre, Institute for Nuclear Materials Science,
Structural Materials Group, Boeretang 200, B-2400 Mol, Belgium*

*c Institute for Energy and Climate Research – Plasma Physics, Forschungszentrum Jülich,
Wilhelm-Johnen-Strasse, 52425 Jülich, Germany*

Introduction: Material migration is a crucial issue in thermonuclear fusion devices. Plasma-facing materials are continuously being eroded by particle bombardment. Part of the eroded species is pumped out, but the majority gets deposited. This gives rise to net erosion and net deposition zones. Reactor lifetime and safety strongly depend on these processes. Therefore, predictions based on a combination of experiments and modelling are indispensable for next step fusion devices like ITER and DEMO. To study carbon migration, $^{13}\text{CH}_4$ has been injected through a polished graphite roof-like test limiter in the TEXTOR scrape-off layer. Interpretation of the deposition patterns on the roof limiter surface requires modelling, which has been done with the ERO code. Previous studies showed ^{13}C deposition efficiencies predicted by ERO that are two orders of magnitude higher than the experimental values. An enhanced re-erosion mechanism for re-deposited carbon had to be assumed to reproduce the very low experimental deposition efficiencies. However, the erosion of carbon by hydrogenic species produced during dissociation of injected $^{13}\text{CH}_4$ was not taken into account in these studies. It was thought that this additional erosion could maybe explain the very low experimental ^{13}C deposition efficiencies. Therefore, the tracing of hydrogenic species from $^{13}\text{CH}_4$ dissociation was implemented in ERO to take into account this additional erosion. Also more realistic physical sputtering yields and hydrocarbon reflection probabilities were implemented. The effect of these improvements on the modelling of the roof limiter experiment is discussed in detail in this paper.

Main results: Hydrogen tracing, Eckstein physical sputtering yields and Tichmann hydrocarbon reflection probabilities were implemented in ERO. The effects of these improvements on the modelling of $^{13}\text{CH}_4$ injection through a roof limiter in TEXTOR were studied in detail. The ^{13}C deposition profiles simulated by ERO with the three improvements included are significantly narrower than the experimental profiles. It was found already before that it is possible to obtain broader profiles with ERO only by using much higher reflection probabilities for the hydrocarbons. So, the disagreement can be due to the uncertainty in reflection probabilities of carbon and hydrocarbons or due to uncertainty of the SIMS measurement. Traced hydrogen causes significant chemical erosion of the roof limiter and decreases the ^{13}C deposition efficiency by 3%. The Eckstein sputtering yields are on average somewhat smaller than the old Bohdanský-Yamamura yields and increase the ^{13}C deposition efficiency by 3%. The effect of the Tichmann hydrocarbon reflection probabilities is negligible. If all improvements are included, one gets a deposition efficiency around 53.4%. This result is only about 0.5% lower than the result without the improvements implemented in this work. This contrasts sharply with the much lower experimentally observed values around 0.3% and, therefore, confirms the need for enhanced re-erosion of re-deposited carbon in ERO. An enhancement factor of about 50 for both physical and chemical erosion had to be assumed to get agreement with experiments. In previous studies the agreement was obtained with an enhancement factor of about 10 for chemical erosion only, but zero sticking for all hydrocarbons (neutrals and ions).

The spatial distribution of the deposited ^{13}C was studied. On the left hand side in Fig. 1 the direction of the considered ^{13}C deposition profile along the centre of the deposition pattern is shown. On the right hand side a comparison is given between the normalised profiles from a SIMS measurement and an ERO run with all improvements included, without and with enhancement 50. The agreement of the shapes is reasonable, though not perfect. Both profiles are strongly peaked around the puffing hole, but the peak of the SIMS profile is somewhat broader.

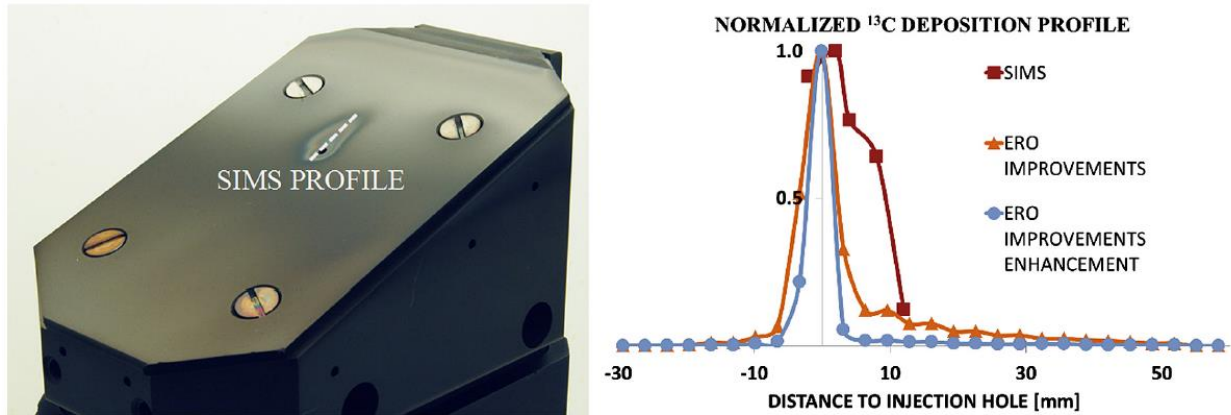


Fig 1: Graphite roof limiter with the location of the SIMS profile along the amorphous hydrocarbon deposit (left). Comparison of the SIMS profile with the profiles from the ERO simulations with all improvements included, with and without the needed enhanced factor of 50 for physical and chemical re-erosion (right).

Conclusions: As main conclusion of this work one can say that implementing the most recent insights concerning particle reflection and physical sputtering in ERO, led only to a very small modification of the resulting ^{13}C deposition efficiencies. To get agreement with the very low experimentally observed ^{13}C deposition efficiencies one needs a much bigger effect such as the enhanced re-erosion of re-deposited carbon. This observation supports the idea that enhanced re-erosion of re-deposited carbon really is an important phenomenon that has to be taken into account in predictions of erosion/deposition for future fusion devices.

Future work: no

Acknowledgment: The presented study was made possible by an Aspirant Grant from FWO (Fonds voor Wetenschappelijk Onderzoek) and additional working budgets from Ghent University and SCKCEN. The work was mainly performed in the Institute of Energy and Climate Research – Plasma Physics at Forschungszentrum Jülich under the TEC (Trilateral Euregio Cluster) agreement.

Published in: Olivier Van Hoey, Andreas Kirschner, Carolina Björkas, Dmitry Borodin, Dmitry Matveev, Inge Uytendhouwen, Guido Van Oost, "Improved carbon migration modelling with the ERO code ", JOURNAL OF NUCLEAR MATERIALS Volume: 438 Supplement: S Pages: S891- S894

Other topics

LEXUR-II-LBE an irradiation program in lead–bismuth to high dose

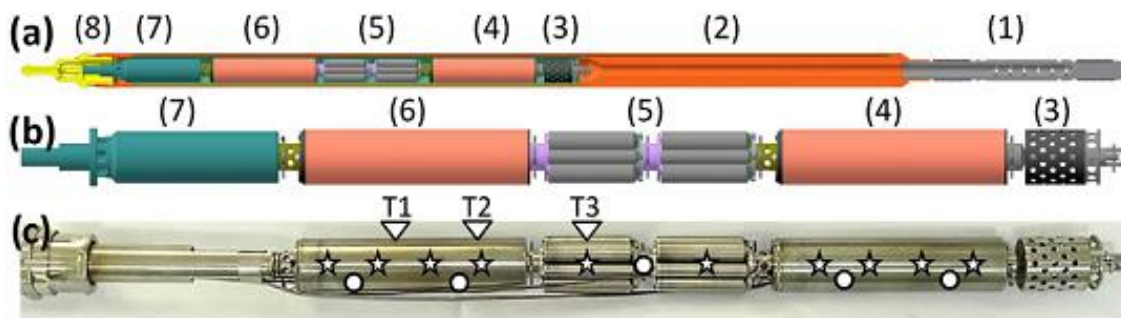
E. Stergar^a, S. Eremin^b, S. Gavrilov^a, M. Lambrecht^a, N. Poglyad^b, I. Zhemkov^b

^aSCK-CEN, BE-2400, Mol, Belgium

^bRIAR, Research Institute of Atomic Reactors, Dimitrovgrad, Russia

Introduction: The core and near core components of MYRRHA will be irradiated by fast neutrons while simultaneously being in contact with the lead–bismuth eutectic coolant. To ensure the integrity of the components, the behavior of steels has to be investigated under these conditions. The LEXUR-II-LBE experiment is aimed at studying the effects of fast neutron spectrum irradiation on the materials of interest for Generation IV fast reactors (such as MYRRHA). In particular, the combined effects of fast spectrum irradiation and exposure to lead–bismuth environment have to be evaluated at high neutron doses.

Main results: This publication documents the design and execution of the LEXUR-II-LBE experiment. It describes construction of the irradiation rig intended for irradiation of steel specimens in lead–bismuth eutectic, compartments with the specimens to be tested, neutronics and temperature simulations. Results of the temperature monitoring during the first irradiation cycle in the BOR-60 reactor are described and an in parallel conducted furnace test without irradiation for parameterization is highlighted.



The LEXUR-II irradiation rig. a) overview, b) detailed view on the test assembly, c) photograph of the actual irradiation rig before irradiation. The stars and dots mark positions of radiation monitors and thermocouples.

Conclusions: This experiment will deliver important data for the understanding of the combined influence of LBE and irradiation on mechanical properties and corrosion of potential candidate materials for future reactors. The combination with a furnace test which simulates the influence of temperature will help to parameterize different occurring effects

Published in: E. Stergar, S.G. Eremin, S. Gavrilov, M. Lambrecht, N.S. Poglyad, I.Yu. Zhemkov, J. Nucl. Mater. 450 (2014) 262-269

Sink strength calculations of dislocations and loops using OKMC

Ville Jansson⁴ and Lorenzo Malerba, SCK-CEN, The Belgian Nuclear Energy Research Centre, Institute for Nuclear Materials Science, Structural Materials Group, Boeretang 200, B-2400 Mol, Belgium

Andrée DeBacker and Charlotte Becquart, Unité Matériaux Et Transformations (UMET), UMR CNRS 8207, Université de Lille 1, ENSCL, F-59655 Villeneuve d'Ascq Cedex, France

Christophe Domain, EDF-R&D, Département Matériaux et Mécanique des Composants (MMC), Les Renardières, F-77818 Moret sur Loing Cedex, France

Introduction: Object kinetic Monte Carlo (OKMC) techniques are stochastic numerical methods suitable to simulate the nanostructural evolution of materials under irradiation in terms of density, size and type of defect populations. The creation, migration, and disappearance of defects is tracked inside a small simulation volume of material, with periodic boundary conditions to simulate a much bigger crystal. The OKMC technique is in fact a stochastic numerical way to solve the master rate equation system that refers to defect populations of interest, with the advantage of being able to take naturally into account inhomogeneities and in general geometry dependent features of defect evolution. It is important to verify that, under the same conditions, equations and simulation provide the same result. This is especially of importance for what concerns the so-called sink strengths, which is the coefficient that governs the in the equations the absorption of defects by sinks and physically corresponds to the inverse of the mean square distance covered by defects before being absorbed. In previous work it was verified that OKMC simulations provide naturally the correct sink strength in the case of spherical absorbers and grain boundaries, both for defects that migrate three-dimensionally and one-dimensionally, including the correct reproduction of the transition between the two regimes in terms of theoretical master curve [1]. Here we calculate the sink strength of dislocation lines and loops (toroidal absorbers) and compare the results with the corresponding theoretical expressions.

Main results: We get good agreement with theory for both dislocations and loop-shaped absorbers in the case of 3D migrating defects, provided that the volume fraction is low, and fair agreement for dislocations absorbing 1D migrating defects. Specifically, in the case of 3D migrating defects absorbed by dislocation lines and loops we can clearly reveal the inadequacy of some theoretical expressions as soon as the volume fraction exceeds values of 0.1-1%: only one expression allows, for dislocation lines, correct calculations in a wide range of volume fractions. Moreover, the only expression available for dislocation loops (toroidal absorbers) fails not only for volume fractions above 0.1%, but also for small ratios between large and small radii of the torus. Although no theoretical expressions exist for the sink strengths of toroidal absorbers for 1D migrating defects, we show that the expression valid for dislocation lines in this case applies also for loops. Finally, the master curve for the 3D to 1D transition is well reproduced with loop-shaped absorbers and fairly well with dislocations: in fact the master curve fails slightly in the transition for dislocation lines, but overall it proves to be valid.

Conclusions: We conclude that, on the one hand, the master curve expressing the transition from 3D to 1D migration regime is correct for a wide range of sinks and that, on the other,

⁴ Currently at Accelerator Laboratory, [Helsinki Institute of Physics](#), P.O.Box 43 (Pietari Kalmink. 2) 00014 [University of Helsinki](#)

OKMC techniques inherently take correctly into account the strengths of sinks of any shape, provided that an effective way of appropriately inserting the sinks to be studied can be found.

Future work: The present work in fact concludes the validation of the OKMC technique as suitable for irradiation damage, by including naturally the correct reproduction of the theoretical sink strengths. Potentially, in the future this technique could be used to deduce the sink strength due to geometrically complex shapes or microstructures, for which theoretical expressions are not easily deduced.

Acknowledgment: This work was supported within by the 7th Framework Programme Project PERFORM60 under Grant Agreement No. FP7-232612.

Published in: V. Jansson, L. Malerba, A. DeBacker, C. Becquart, C. Domain, Journal of Nuclear Materials 442 (2013) 218-226.

[1] L. Malerba, C. Becquart, C. Domain, Journal of Nuclear Materials 360 (2007) 159.

Interstitial helium diffusion mechanisms in <110> tilt grain boundaries in BCC FeCr alloys: A atomistic study

X. He^a, D. Terentyev^b, Y. Lin^a, W. Yang^a
a China Institute of Atomic Energy, Beijing, China

b SCK-CEN, Structural Materials Group, Nuclear Materials Science Institute, B-2400 Mol, Belgium

Introduction:

In this work, we studied the migration of He in different h110i tilt grain boundaries (GBs) (R19{331}, R9{221}, R3{111}, R3{112}, R11{113}, R9{114}) in Fe–(5,10,14)Cr random alloys, with the misorientation angle varying in the range 26–141. We performed systematic molecular statics and molecular dynamics simulations to characterize the interaction of He with the core of the GBs and to estimate the diffusion coefficient, migration mechanism, and effective core migration energy.

Main results:

The simulations were performed in the 600–1400 K temperature range, applying a set of interatomic potentials for Fe–Cr–He system recently proposed by Juslin et al., specially fitted to the properties of He in bulk Fe. We found that the migration of an interstitial He near the core of the R3{112} GB is essentially three dimensional (3D) within the investigated temperature range. The transition of diffusion mode from one-dimensional (1D) to 3D was observed in other GBs in the studied alloys.

Conclusions:

The results clearly demonstrate, that the accommodation, migration mechanism, and diffusivity of He is extremely sensitive to variations in atomic structure of a particular GB. Alloying with Cr was found to enhance the mobility of a He interstitial in the GB region.

Future work: Not foreseen.

Acknowledgment: This work was supported by National Natural Science Foundation of China, Grant nos. 10975194 and 51201184; National Basic Research Program of China, Grant no. 2011CB610503.

Published in: X. He, D. Terentyev, Y. Lin, W. Yang / Journal of Nuclear Materials 442 (2013) S660–S666

Effect of low-temperature phase transition on mechanical behavior of Fe–Cu alloys

Boris Minov^a, Dmitry Terentyev^a, Wouter Van Renterghem^a, Yuri Osetsky^b,

Milan J. Konstantinović

^a Studiecentrum voor Kernenergie/Centred'Etude de l'Energie Nucléaire, SCKCEN, Boeretang 200, B-2400 Mol, Belgium

^b Materials Science and Technology Division, Oak Ridge National Laboratory, Oak Ridge, TN, USA

Introduction:

It has been surmised that this phase transition might be related to the low-temperature transition to the 9R structure of coherent Cu-precipitates, appearing as a consequence of complex cluster boundary conditions (9R is a twinned crystal structure, intermediate between bcc, which is fully coherent with the iron matrix, and the non-coherent fcc structure). Even though a number of atomistic studies already reported the presence of phase transformation, there is no quantitative assessment and precise analysis of the transformed value and structure depending on precipitate size and ambient temperature. While the observation of this transition in a low temperature range raises indeed questions related to the change of macroscopic mechanical behavior of these alloys in this same range. In this paper, we therefore investigate the low-temperature mechanical properties of Fe-1%Cu alloys, thermally aged at 773 K for 120 h.

Main results:

Mechanical tests of thermally aged Fe-Cu alloys were performed in the temperature range between 97 K and 297 K in order to investigate their low temperature mechanical behavior. Tests performed below 122 K have shown that the material breaks in a random fashion already in the elastic region, while above it a clearly pronounced yield point is observed. This sudden change of the mechanical behavior has been rationalized on the basis of atomistic simulations, addressing the interaction of dislocations with Cu precipitates. The latter study has revealed the presence of bcc to fcc transition induced by dislocations which is temperature dependent process. It is suppressed with increasing temperature and enhanced with increasing a precipitate size. This transition, efficient at low temperature, leads to the transformation of Cu precipitates into non-coherent particles, which act as stronger obstacles and cause the experimentally observed premature failure.

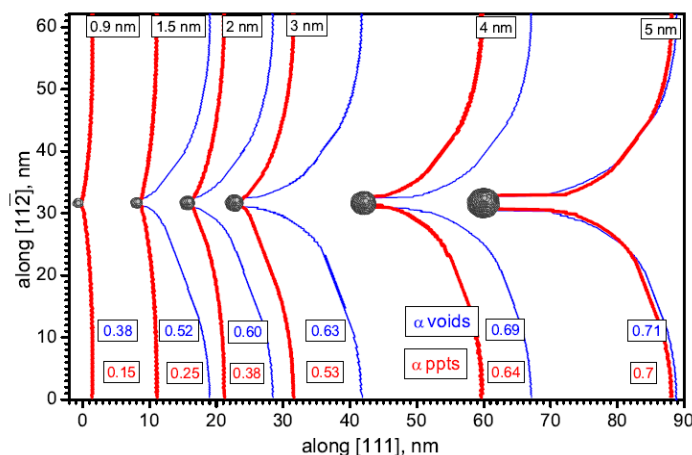


Fig.1. Configuration of the dislocation at break away modeled at 0 K when interacting with Cu precipitates and voids of different sizes. The size and the obstacle strength (α) are specified in

the figure. τ_C was determined as $\tau_C = \alpha Gb/L$, where G , b , and L are the shear modulus (65 GPa), Burgers vector and the free passage distance, respectively.

Conclusions:

The presence of small non-coherent Cu-precipitates, expected to form according to atomistic predictions, and not observed prior to deformation, was confirmed by means of transmission electron microscopy.

Future work: Not foreseen.

Acknowledgment: This research is carried out in the frame of FWO project No:G.0127.08

Published in: Boris Minov, Dmitry Terentyev, Wouter Van Renterghem, Yuri Osetsky and Milan J Konstantinovic / *Materials Science&EngineeringA*597(2014)46–51

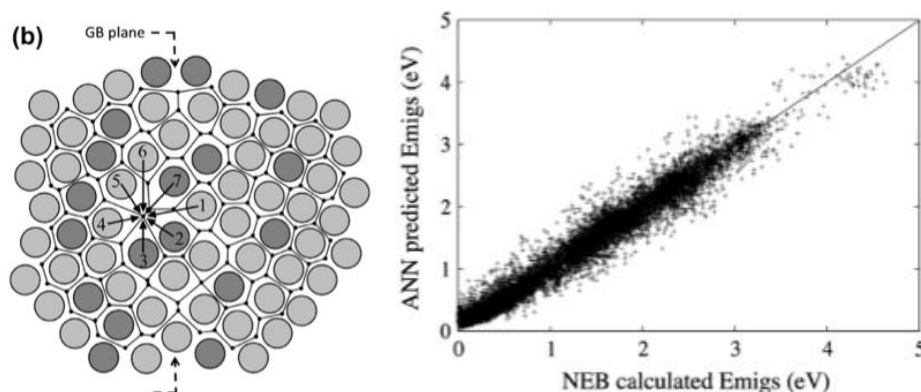
Predicting vacancy migration energies in lattice-free environments using artificial neural networks

N. Castin^{a,b,†}, J.R. Fernández^{a,c,d}, R.C. Pasianot^{a,c,d}

^a Consejo Nacional de Investigaciones Científicas y técnicas (CONICET), Av. Rivadavia 1917, C1033AAJ Buenos Aires, Argentina .^b Belgian Nuclear Research Centre, SCK•CEN, Nuclear Materials Science Institute, Boeretang 200, B-2400 Mol, Belgium ^c Comisión Nacional de energía atómica (CNEA), CAC, Gcia. Materiales, Av. Gral. Paz 1499 San Martin, Buenos Aires, Argentina ^d Instituto Sabato, UNSAM/CNEA, Avda. Gral. Paz 1499, 1650 San Martin, Argentina

Introduction: We proposed a methodology for predicting migration energies associated to the migration of single atoms towards vacant sites, using artificial neural networks (ANN). The proposed technique is designed in conjunction with a novel kind of lattice-free atomistic kinetic Monte Carlo (AKMC) model. The idea is to avoid as much as possible heavy atomistic simulations, e.g. static relaxation or general methods for finding transition paths. We demonstrate the feasibility of this new concept.

Main results: A detailed off-lattice AKMC model has been proposed (events definition as illustrated in left figure below), and a method for designing proper ANN predicting their associated migration energies (results illustrated in right figure below).



Conclusions: The proposed scheme is a promising starting point for the development of complex, fast and accurate lattice-free KMC models.

Future work: The application of the proposed model to realistic-scale problems is ongoing.

Acknowledgment: The authors acknowledge partial funding of this work by the PIP-CONICET 804/10 project.

Published in: N. Castin et al., Computational Materials Science 84 (2014) 217–225.

Reliability of electrochemical noise measurements: Results of round-robin testing on electrochemical noise

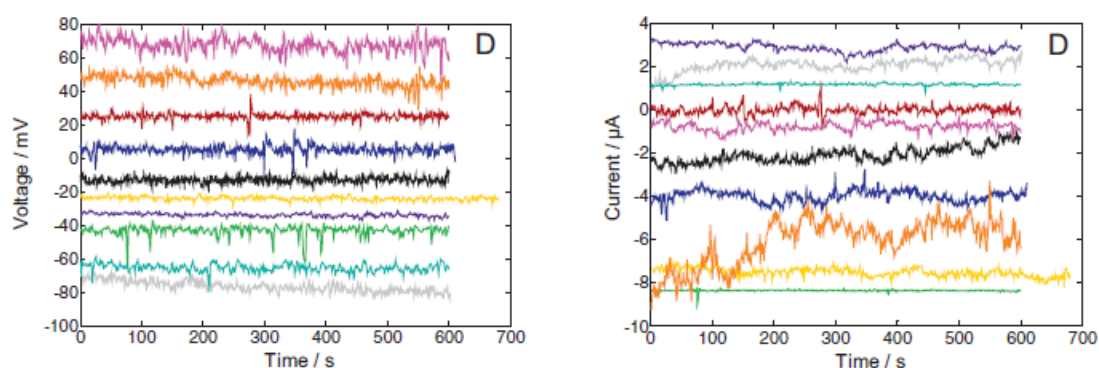
R.W. Bosch*, R.A. Cottis**, K. Csecs, T. Dorsch, L. Dunbar; A. Heyn, F. Huet, O. Hyokvirta, Z. Kerner, A. Kobzova, J. Macak, R. Novotny, J. Oijerholm, J. Piippo, R. Richner, S. Ritter, J.M. Sanchez-Amaya, A. Somogyi, S. Vaisanen, W.Z. Zhang

* SCK-CEN, Boeretang 200, Mol, Belgium

** Corresponding author, University of Manchester, Manchester, UK

Introduction: Electrochemical noise (EN) measurements are gradually becoming accepted for the study of corrosion processes, although much remains to be done in developing a complete understanding of the interpretation of EN. Furthermore, there is considerable evidence that many EN measurements are contaminated by extraneous noise and measurement artefacts of various sorts. For this reason a round-robin study has been performed to test the quality of EN measurement equipment and to test standard procedures for the validation of such equipment's.

Main results: Sixteen laboratories have performed electrochemical noise (EN) measurements based on two systems. The first uses a series of dummy cells consisting of a “star” arrangement of resistors in order to validate the EN measurement equipment and determine its baseline noise performance, while the second system, based on a previous round-robin in the literature, examines the corrosion of aluminium in three environments. All participants used the same measurement protocol and the data reporting and analysis were performed with automatic procedures to avoid errors. The measurement instruments used in the various laboratories include commercial general-purpose potentiostats and custom-built EN systems.



Potential and current noise time records on aluminium

The measurements on dummy cells have demonstrated that few systems are capable of achieving instrument noise levels comparable to the thermal noise of the resistors, because of its low level. However, it is of greater concern that some of the instruments exhibited significant artefacts in the measured data, mostly because of the absence of anti-aliasing filters in the equipment or because the way it is used. The measurements on the aluminium samples involve a much higher source noise level during pitting corrosion, and most (though not all) instruments were able to make reliable measurements. However, during passivation, the low level of noise could be measured by very few systems.

Conclusions: The round-robin testing has clearly shown that improvements are necessary in the choice of EN measurement equipment and settings and in the way to validate EN data

measured. The results emphasise the need to validate measurement systems by using dummy cells and the need to check systematically that the noise of the electrochemical cell to be measured is significantly higher than the instrument noise measured with dummy cells of similar impedance.

Future work: Round Robin testing has been continued with EIS (Electrochemical Impedance Spectroscopy). Data have been collected over the period 2010 – 2013 and will be made available for publication in due course.

Published in: R.W. Bosch, R.A. Cottis, K. Csecs, T. Dorsch, L. Dunbar; A. Heyn, F. Huet, O. Hyokvirta, Z. Kerner, A. Kobzova, J. Macak, R. Novotny, J. Oijerholm, J. Piippo, R. Richner, S. Ritter, J.M. Sanchez-Amaya, A. Somogyi, S. Vaisanen, W.Z. Zhang, ELECTROCHIMICA ACTA 120, 2014, p. 379-389.

LIMETS 3, a Novel System for High Strain Fatigue Testing in Lead-Bismuth Eutectic

Pierre Marmy¹, Xing Gong^{1,2}

¹ SCK•CEN (Belgian Nuclear Research Centre), Boeretang 200, B-2400 Mol, Belgium

² KU Leuven, Department of Materials Engineering (MTM), Kasteelpark Arenberg 44 Bus 2450, B-3001 Leuven, Belgium

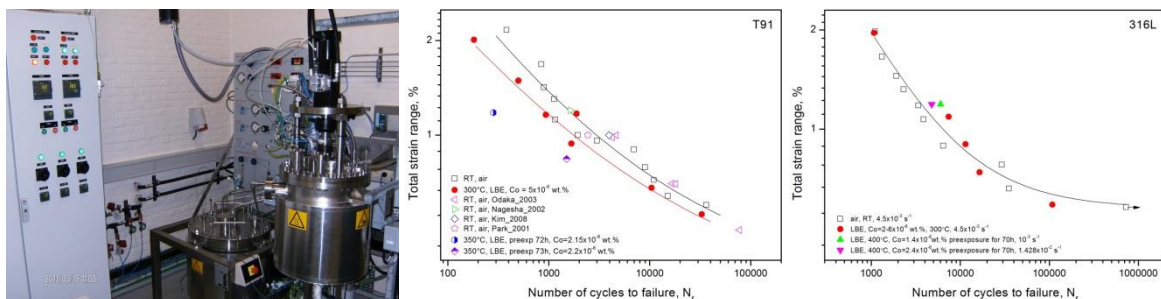
Introduction: Lead Bismuth Eutectic (LBE) is the coolant of the multi-purpose nuclear facility MYRRHA being developed at the nuclear research centre SCK•CEN in Belgium. The use of this new type of coolant requires an assessment of its compatibility with structural materials, in a defined dissolved oxygen concentration and temperature range, corresponding to the operating parameters of the reactor. According to the present status of the design, the reactor components and the internals and main vessel are at temperatures between 270 and 410 °C. At end of the operating cycle, the fuel cladding material will reach temperatures as high as 525°C. A stringent requirement of MYRRHA is that the reactor coolant should be kept in a very narrow oxygen concentration range, in order to operate the reactor in a regime where corrosion is under control. This O₂ concentration range is presently defined as going from 10⁻⁶ wt. % at 270°C, the LBE temperature at the outlet of the heat exchangers to 10⁻⁷ wt. % at 470°C, the LBE temperature at the core outlet. Three structural materials are foreseen: 316L will be used for the main vessel, for most of the structural and internal components of MYRRHA, T91 for the beam window and eventually the wrappers, and finally 1.4970 (15-15Ti) for the fuel cladding tubes. Due to the characteristics of the reactor design and operation, the structural materials of MYRRHA will be loaded with cyclic stresses and strains. The code RCC-MRx used for the mechanical design by the MYRRHA engineering team requires specific material's information about the basic fatigue endurance for a total imposed strain range between 0.6 and 2.0 % and the cyclic curves. The LIMETS 3 set up shall be able to produce reliable fatigue data in the listed alloys, under the influence of the liquid metal coolant, covering the parameter range defined above.

A large number of studies on the effects of LBE on the mechanical properties of metallic materials have already been published in the literature. The physical conditions and the mechanical parameters under which LME occurs have been described. The occurrence of Liquid metal embrittlement (LME) necessitates two primary conditions: first, an effective wetting of the solid metal by the liquid metal and second the presence of local plastic deformation and/or high residual stresses. The solid metal is said to be in intimate contact with the liquid metal. Oxide layers are recognized to impede wetting and to delay LME. The concentration of oxygen in the liquid metal is consequently an important parameter since Fe and Cr have a strong affinity with oxygen to form oxide layers. The techniques necessary to measure and control oxygen in LBE have not been available for most of the studies already published and therefore the results cannot be truly applied to engineering problems. The main reason is the difficulty of conditioning LBE to a target oxygen concentration in a small volume and the absence of sensors to measure oxygen. Another weakness of most of the published fatigue works is the fact that strain extensometers suitable for the hostile conditions of LBE were not available, at the exception of a work by Kalkhof in which a classical strain gage extensometer was attached to the gauge length and immersed in LBE. Nevertheless this extensometer was limited to temperatures below 300 °C . Other works were using calibrated extensometer placed outside the gauge length of the specimen. This technique can be tricky in strain controlled tests because the calibration depends directly from the applied force which will then be temperature and material behaviour dependent.

LIMETS 3 has been designed to achieve the following objectives: be equipped with a high temperature extensometer attached to the gauge length, use reliable oxygen sensors and have an LBE conditioning facility capable of achieving any required oxygen level between oxygen saturation and very low concentrations. The experiments should contribute to a better understanding of the role of LBE dissolved oxygen and its influence on the onset of LME.

The paper presents the first results obtained in LBE on T91 and 316 steels and their comparison with tests produced with LIMETS 3 in air as well as tests produced in the literature.

Main results: A first series of experiment has been conducted in 316L and T91 steels, at temperatures between 300 and 400°C. The main results are: the fatigue life of T91 steel is reduced when tested in LBE and the reduction of life seems to be larger at lower oxygen levels. The fatigue damage occurs by the propagation of a unique crack. The propagation of the macroscopic crack is accelerated under LBE; In 316L , under the tested conditions, the fatigue life does not seem to be influenced negatively.



Limets3 fatigue test system and the preliminary fatigue results of T91 and 316L steels in LBE

Conclusions: A new fatigue test system has been developed to test the mechanical properties of metallic samples under an LBE environment. The system allows to conduct fatigue experiments under controlled oxygen level, from saturation to very low oxygen contents. The

system incorporates a mechanical extensometer which allows the measurement of strain on the gauge length. Comparison of the first fatigue experiments with the literature has shown a very good agreement.

Acknowledgment: The engineering collaboration of Anja van Baelen (SCK-CEN) for the design of LIMETS 3 is gratefully acknowledged. The authors wish to thank Jef R Sannen (SCK-CEN) and his team for their contribution and assistance during the construction of LIMETS 3. Guido Engelen (SCK-CEN) and collaborators are thanked for the design and realisation of the LIMETS 3 electrical and control system.

Published in: P. Marmy and X. Gong/Journal of Nuclear Materials 450 (2014) 256–261.

Liquid Metal as a Heat Transport Fluid for Thermal Solar Power Applications

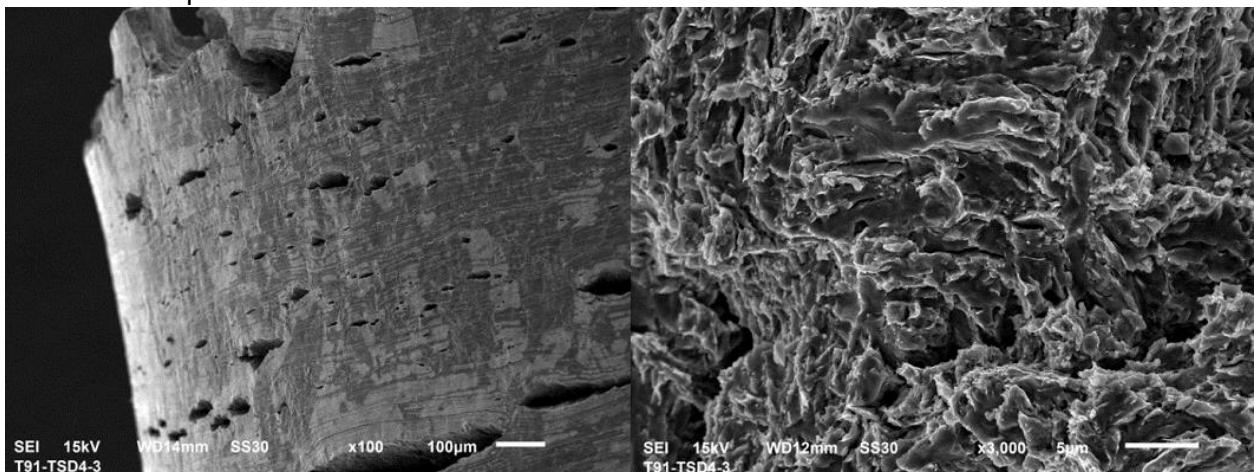
D. Frazer^a, E. Stergar^b, C. Cionea^a, P. Hosemann^a

^aUniversity of California at Berkeley, 3117 Etcheverry Hall, Berkeley, CA 94720, United States

^bSCK-CEN, BE-2400, Mol, Belgium

Introduction: In order to increase the thermal efficiency and produce process heat for hydrogen production, the operating temperature of the heat transfer fluid in thermal solar plants needs to increase. Current thermal solar heat transport fluids begin to disintegrate around 600 C. In general it can be stated that the goal of 900 °C is too high for any type of oil based fluid leaving only gases, liquid salts or liquid metals as potential heat transfer fluids. While gases have a low density and therefore less efficient heat transport, salts are known to have high melting points. For non-solar applications, low melting-temperature metals, such as sodium have been utilized in the past.

Main results: In this work the potential to use liquid metals as heat transfer medium for thermal solar power are discussed.



An overview of a tensile test done in LBE and a detail of the according fracture surface. A large number of cracks in the necking region can be observed.

Conclusions: While the subject of LBE based research is extensive and under consideration for the nuclear industry for a long time it is a novel concept for the solar community. And it is the intention of this paper to introduce in brief the associated materials science issues. Extensive

research is needed in order to utilize liquid metals as a heat transport fluid but one can build upon past experiences and knowledge in order to avoid mistakes made previously.

Published in: D. Frazer, E. Stergar, C. Cionea, P. Hosemann, Energy Procedia 49 (2014) 627-636

